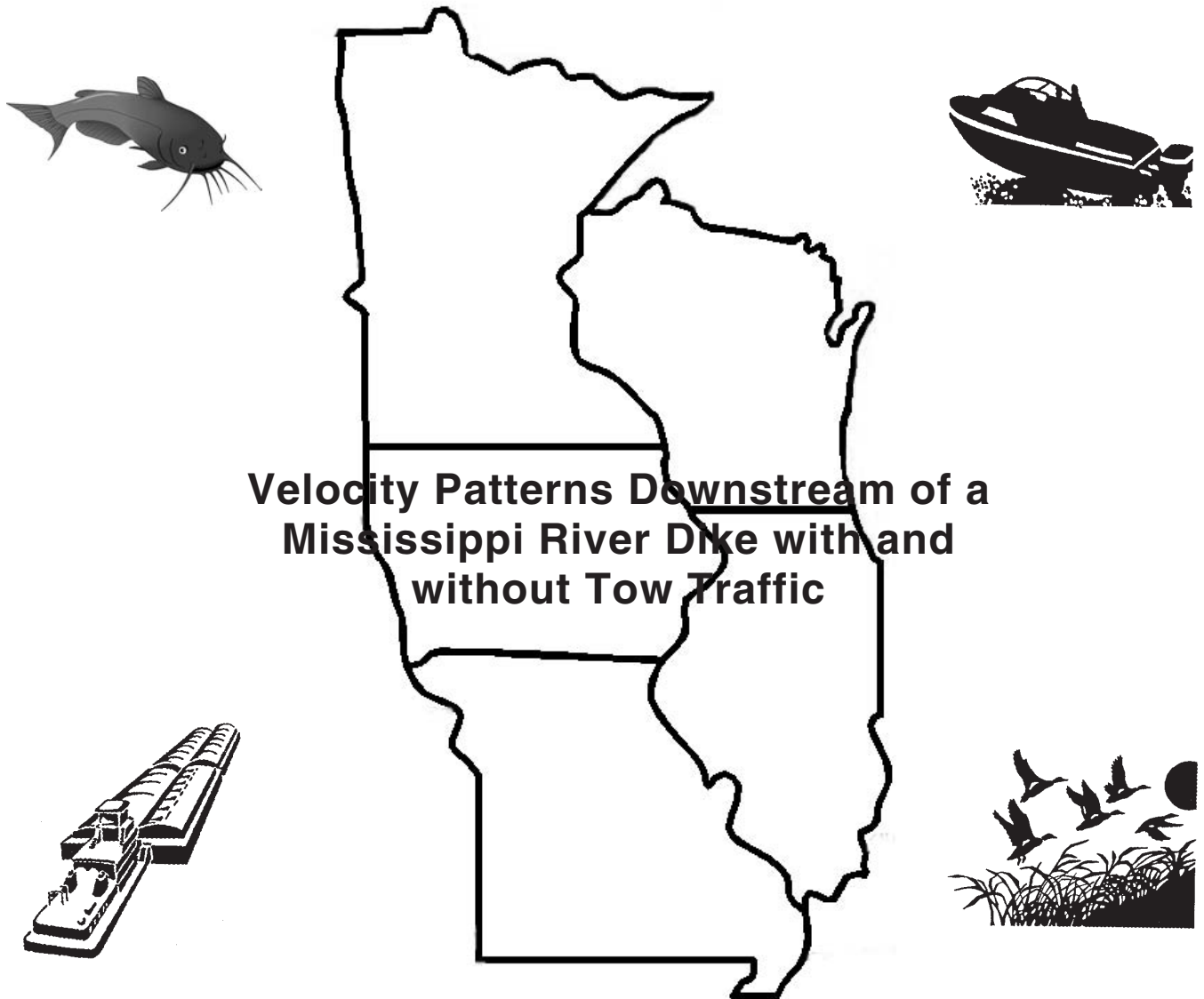


Interim Report For The Upper Mississippi River - Illinois Waterway System Navigation Study



US Army Corps
of Engineers

March 2000

Rock Island District
St. Louis District
St. Paul District

The contents of this report are not to be used for advertising, publication, or promotional purposes. Citation of trade names does not constitute an official endorsement or approval of the use of such commercial products.

The findings of this report are not to be construed as an official Department of the Army position, unless so designated by other authorized documents.



PRINTED ON RECYCLED PAPER

Velocity Patterns Downstream of a Mississippi River Dike with and without Tow Traffic

by Stephen T. Maynard

Coastal and Hydraulics Laboratory
U.S. Army Engineer Research and Development Center
3909 Halls Ferry Road
Vicksburg, MS 39180-6199

Interim report

Approved for public release; distribution is unlimited

Prepared for U.S. Army Engineer District, Rock Island
Rock Island, IL 61204-2004
U.S. Army Engineer District, St. Louis
St. Louis, MO 63103-2833
U.S. Army Engineer District, St. Paul
St. Paul, MN 55101-1638

9. (Concluded).

U.S. Army Engineer District, Rock Island, Clock Tower Building, P.O. Box 2004, Rock Island, IL 61204-2004

U.S. Army Engineer District, St. Louis, 1222 Spruce Street, St. Louis, MO 63103-2833

U.S. Army Engineer District, St. Paul, Army Corps of Engineers Centre, 190 5th Street East, St. Paul, MN 55101-1638

13. (Concluded).

Velocities were measured downstream of a typical Middle Mississippi River dike before and during passage of a model tow for typical winter flow conditions. Upbound versus downbound tows and tows near the dike as well as far from the dike were evaluated in the experiments. A limited set of experiments measured ambient velocities downstream of the dike when the dike is being overtopped and the effect of adding an "L-head" to the dike on velocities before and during tow passage.

Contents

Preface	iv
1—Introduction.....	1
Background.....	1
Objective.....	1
Previous Studies.....	2
Prototype Dike Description.....	2
2—Materials and Methods.....	5
Physical Model Description	5
Description of Experiments	8
3—Results.....	17
Flow Visualization	17
Computed Return Velocities.....	18
Existing Dike with Tow Passage.....	30
Flow Overtopping Existing Dike without Tow Passage	30
L-Head Dike with Tow Passage.....	31
4—Summary and Discussion	33
References.....	35
Appendix A: Time-Histories of Velocity for Existing Dike Experiments.....	A1
Appendix B: Time-Histories of Velocity for Vertical Velocity Profile Experiments	B1
Appendix C: Time-History of Velocity for Overtopping Dike Experiments.....	C1
Appendix D: Time-History of Velocity for L-head Dike Experiments	D1

SF 298

Preface

The work reported herein was conducted as part of the Upper Mississippi River-Illinois waterway (UMR-IWW) System Navigation Study. The information generated for this interim effort will be considered as part of the plan formulation process for the System Navigation Study.

The UMR-IWW System Navigation Study is being conducted by the U.S. Army Engineer Districts, Rock Island, St. Louis, and St. Paul, under the authority of Section 216 of the Flood Control Act of 1970. Commercial navigation traffic is increasing and, in consideration of existing system lock constraints, will result in traffic delays that will continue to grow into the future. The system navigation study scope is to examine the feasibility of navigation improvements to the Upper Mississippi River and Illinois Waterway to reduce delays to commercial navigation traffic. The study will determine the location and appropriate sequencing of potential navigation improvements to the system, prioritizing the improvements for the 50-year planning horizon from 2000 through 2050. The final product of the System Navigation Study is a Feasibility Report, which is the decision document for processing to Congress.

The work was performed by members of the staff of the U.S. Army Engineer Research and Development Center (ERDC), Coastal and Hydraulics Laboratory (CHL), during 1998-1999. The study was under the direction of Dr. James R. Houston, Director, CHL; Mr. Charles C. Calhoun, Jr., Assistant Director, CHL; and Mr. C. E. Chatham, Jr., Chief, Navigation and Harbors Division (NHD), CHL. The study was conducted by Dr. S. T. Maynard, Navigation Branch, NHD.

At the time of publication of this report, Acting Director of ERDC was Dr. Lewis E. Link, and Commander of ERDC was COL Robin R. Cababa, EN.

The contents of this report are not to be used for advertising, publication, or promotional purposes. Citation of trade names does not constitute an official endorsement or approval of the use of such commercial products.

1 Introduction

Background

The Upper Mississippi River-Illinois Waterway System (UMR-IWWS) Navigation Feasibility Study will evaluate the justification of providing additional lockage capacity at sites on the UMR-IWWS while maintaining the social and environmental qualities of the river system. The system navigation feasibility study will be accomplished by executing the Initial Project Management Plan (IPMP) outlined in USACE (1994). The IPMP outlines Engineering, Economic, Environmental, and Public Involvement Plans.

The Environmental Plan identifies the significant environmental resources on the UMR-IWWS and probable impacts in terms of threatened and endangered species; water quality; recreational resources; fisheries; mussels and other macroinvertebrates; waterfowl; aquatic and terrestrial macrophytes; and historic properties. It considers system-wide impacts of navigation capacity increases, while also assessing in preliminary fashion potential construction effects of improvement projects.

One element of the Environmental Plan addresses the impacts of navigation on larval and adult fish. Part of the fish study evaluates the impact of tow traffic on adult fish using the low-velocity habitat found during winter months downstream of dikes on the Mississippi River.

Objective

The objective of this study is to measure velocity downstream of a typical Middle Mississippi River dike before and during passage of a model tow for typical winter flow conditions. Upbound versus downbound tows and tows near the dike as well as far from the dike will be evaluated in the experiments. A limited set of experiments will determine ambient velocities downstream of the dike when the dike is being overtopped and the effect of adding an “L-head” to the dike on velocities before and during tow passage.

Previous Studies

Flow past a dike is analogous to flow past an abrupt channel expansion. Raudkivi (1967) found the maximum velocity in the eddy downstream of an abrupt expansion equal to about 0.25 times the velocity of the approach flow. Simons and Richardson (1971) reported on another analogous flow situation, velocities in the trough of a dune in a sand bed channel. Velocities in the eddy located in the dune trough (downstream of the face of the dune) were one-third to one-half of the average stream velocity and acting in an upstream direction. Copeland (1981) studied spur dikes as a means of providing bank protection and conducted flow visualization with spur dikes on the outer bank of a bendway for various dike angles with respect to the bank. Pilarczyk, Klassen, and Verhey (1989) described the flow field around nonovertopped dikes with and without passage of vessels. Under ambient flow conditions, Pilarczyk, Klassen, and Verhey reported “The current velocities in the groyne field (0.3 m/sec) are smaller than the velocities in the main current (1 m/sec).” Pilarczyk, Klassen, and Verhey also reported that “Three important stages can be distinguished during the passage of a pushtow unit sailing upstream. The return current is at a maximum immediately when the bow passes a groyne. The return current is furnished by water from the upstream groyne field and the groyne field alongside. An eddy develops at the groyne head and the small vortex at the downstream end of the groyne field apparently disappears entirely. As the pushtow passes by the supply flow refills the groyne field. When the stern of the pushtow passes the particular groyne field, the supply flow is forced to flow perpendicular to the axis of the fairway, out of the groyne field at the upstream groyne. The eddy immediately downstream of the groyne is transported downstream by the main current.” Pilarczyk presented plots of velocity vectors for various tow positions. In 1990, unpublished flow visualization with dye was conducted by this author using a slack water model channel and a dike field. Results were documented in video only. In the absence of ambient velocities, the eddy between the dikes set up by the tow extended well out into the main channel after passage of the tow. Tingsanchali and Maheswaran (1990) compared a two-dimensional depth averaged numerical model to measured velocities near a dike. These studies showed that the length of the recirculation zone (also called reattachment length) below a single dike (no dikes either upstream or downstream) is about nine times the dike length for the dike length/channel width ratios typically found on the Mississippi River. (The dikes studied herein have a spacing of about three times the dike length.) Several other studies, including Pande, Prakash, and Agarwal (1980), Gupta and Raju (1987), and Rajaratnam and Nwachukwu (1983), provide detailed velocity data for the single dike configuration which is not directly applicable to the Mississippi River dike configurations.

Prototype Dike Description

The dike selected for the simulation was the left bank dike (looking downstream) at River Mile (RM) 160.0 on the Mississippi River about 32 km (20 miles) downstream of St. Louis, MO). An aerial photograph from the hydrographic survey is shown in Figure 1 and the stage at the time of the

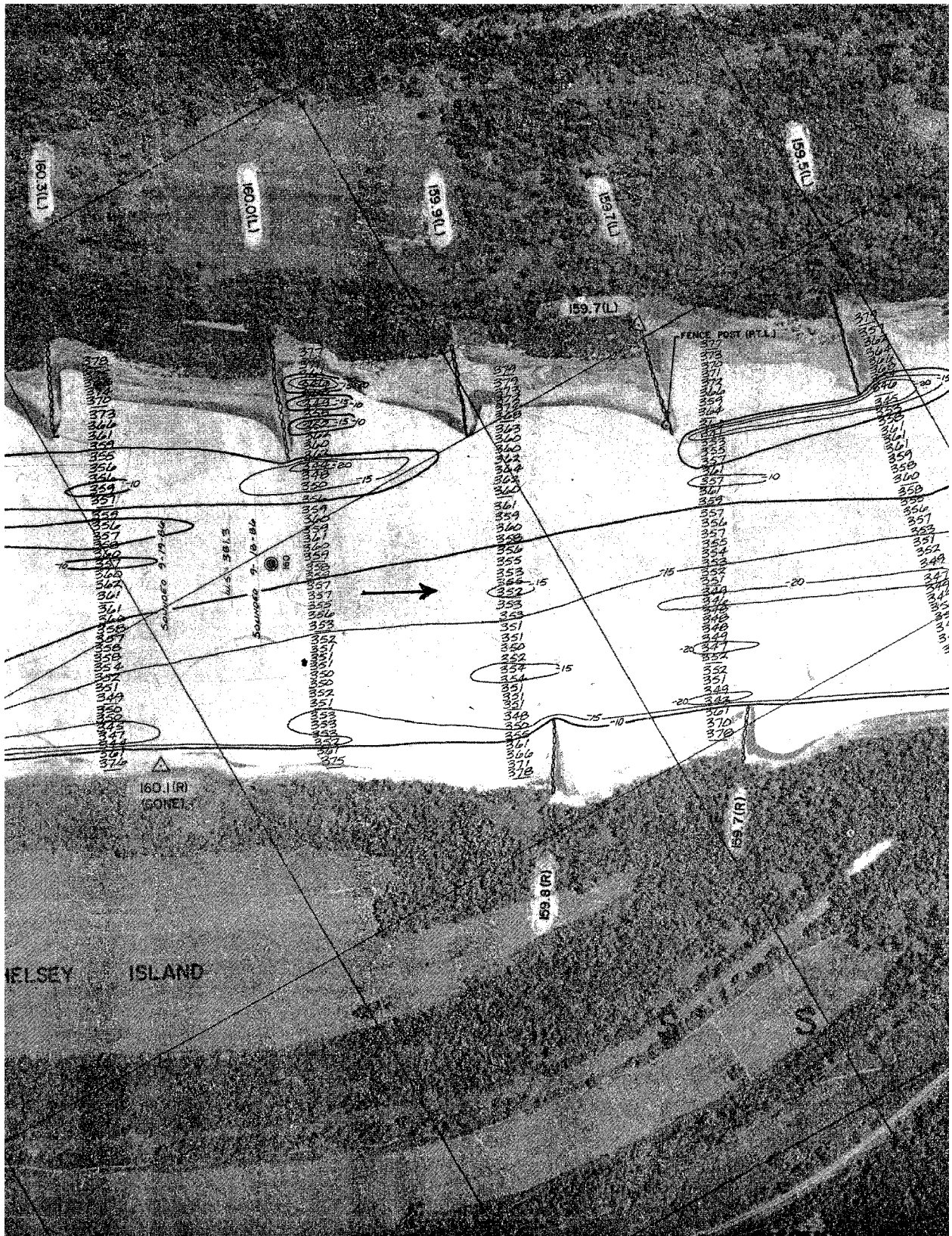


Figure 1. Aerial view from hydrographic survey of dike at RM 160.0, Mississippi River, downstream of St. Louis

photograph was el 114 m.* The bed topography was obtained in September 1986 when the stage was el 116. The first dike upstream of the selected experimental dike, located at RM 160.3 is about 110 m (360 ft) long and about 366 m (1,200 ft) upstream. The selected dike at RM 160.0 is about 152 m (500 ft) long. The next downstream dike, RM 159.9, is 274 m (900 ft) downstream and about 122 m (400 ft) long. Detailed bed topography was not available for the experimental dike and the model layout was based on the transect at RM 160.0 and the contours of the scour hole. The cross section using the transect at RM 160.0 is shown in Figure 2. The dike has a top elevation of 117 and the low-water reference plane at RM 160.0 is about 112. The water surface width of the cross section away from the dike is about 625 m (2,050 ft) at a stage of el 115. The flow rate used in the experiments for the nonovertopping flow was the mean stage in January, which is el 115 and corresponds to a discharge of 3,429 cms (121,000 cfs). January flows were used in the experiments to evaluate the impacts of tow traffic on adult fish using the low-velocity habitat found during winter months downstream of dikes on the Mississippi River. The average channel velocity for the mean January condition is $3,429/2,930 = 1.2$ m/sec using the channel area between the nose of the dike and the opposite bank. For the overtopping experiments, a stage el 118 or 0.6 m (2 ft) above the dike was used and corresponds to a discharge of 7,000 cms (247,000 cfs). The average channel velocity for the overtopping condition was $7,000/4,720 = 1.5$ m/sec. Historically, 9 percent of the days in January have a stage of 0.6 m (0.183 ft) or more above the top of the dike. In the 55 years of record, 13 years have at least 1 day in January where the stage is 0.6 m (0.183 ft) or more above the dike.

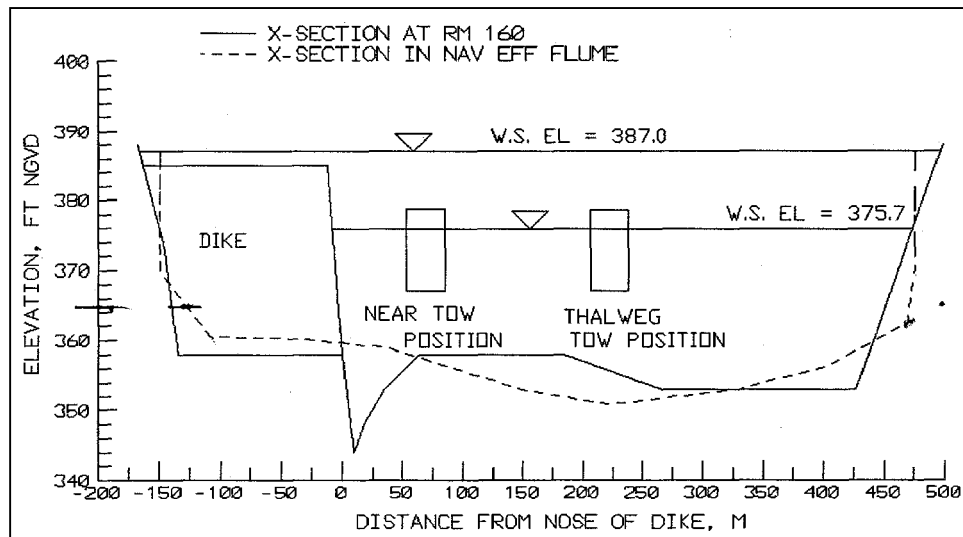


Figure 2. Cross section using transect at RM 160.0. (To obtain meters multiply feet by 0.3048)

* All elevations (el) cited herein are in meters, referenced to the National Geodetic Vertical Datum (NGVD).

2 Materials and Methods

Physical Model Description

The reach of the Mississippi River near RM 160.0 was modeled at a scale ratio of 1:30 using an existing cross section in the navigation effects flume. Similarity of model and prototype is best achieved in a navigation model by equality of the Froude number which is the ratio of inertial to gravity forces. Scaling relations used to convert from model to prototype are as follows:

<u>Quantity</u>	<u>Model value: Prototype value</u>
Length	1:30
Area	1:900
Time	1:5.48
Velocity	1:5.48
Discharge	1:4,930

Unless stated otherwise, all dimensions are converted to their equivalent value in the prototype.

The navigation effects flume is 122 m long by 21.3 m wide (both model dimensions). The center 61 m (model dimension) of the flume length uses marine plywood sheeting to form the cross section shown in Figure 2. A portion of the plywood floor of the flume was removed and filled with 0.6-cm (model dimension) gravel. A scour hole similar to the scour hole in Figures 1 and 2 was formed in the gravel as shown in Figure 3. Bed elevation contours away from the scour hole are shown in Figure 4. The proper width and maximum depth of the scour hole was simulated, but the length downstream was limited to about 152 m (500 ft) and the length upstream limited to 43 m (140 ft) to reduce model construction costs. The experimental dike had a triangular cross section with el 117 and a 22-m-wide base. The channel cross section in the navigation effects flume represents the section at Clark's Ferry on the Mississippi River at RM 468.2 and described by Maynard and Martin (1998). Both the prototype and physical model cross sections are shown in Figure 2. The total area from nose of dike to right bank at el 115 was 3,170 sq m in the navigation effects flume cross section as compared to 2,930 sq m at RM 160.0. The layout of the dike field in the flume



a. Overhead view looking downstream, experimental dike at bottom, downstream dike at top



b. Side view, experimental dike at left, downstream dike at right, scour hole in gravel

Figure 3. Model of dikes: 1:30 scale

is shown in Figure 5. A fourth dike was added upstream to better represent the system of dikes present in the river.

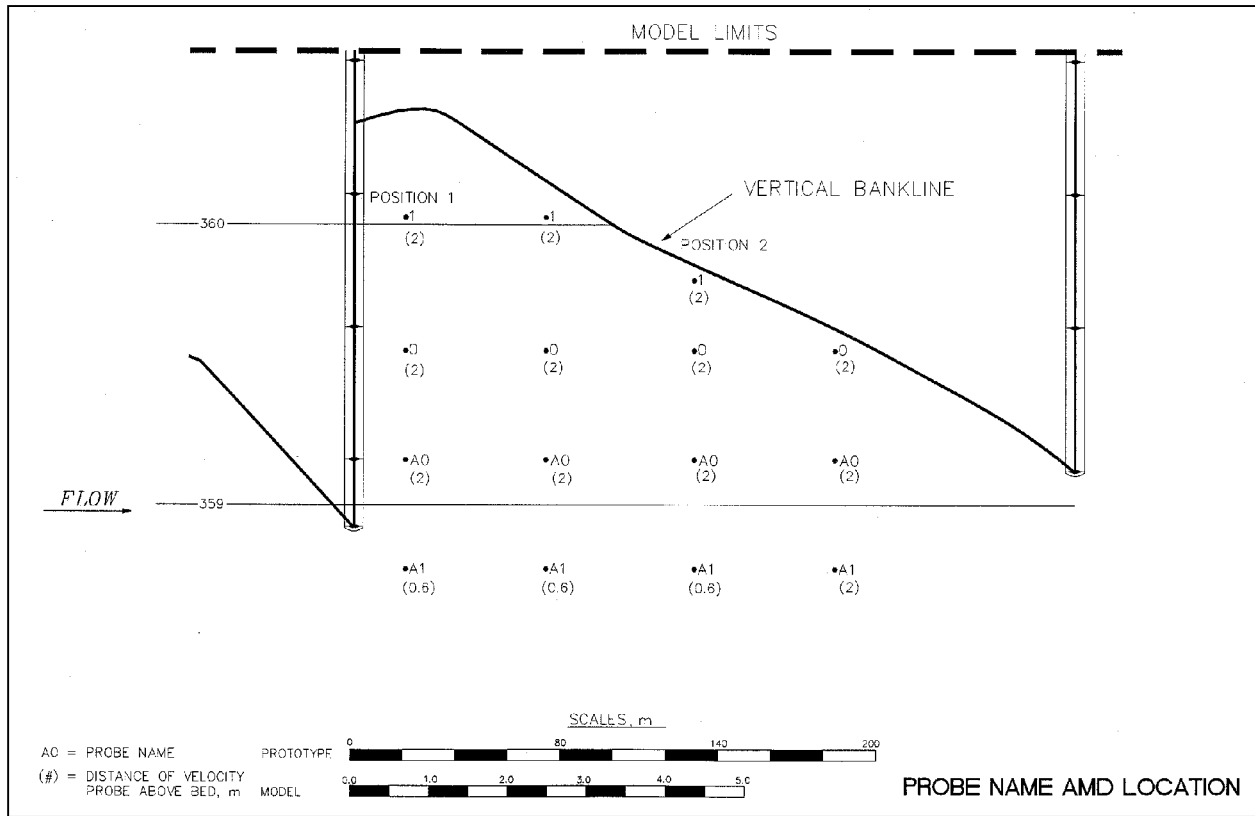


Figure 4. Bed elevation contours away from scour hole

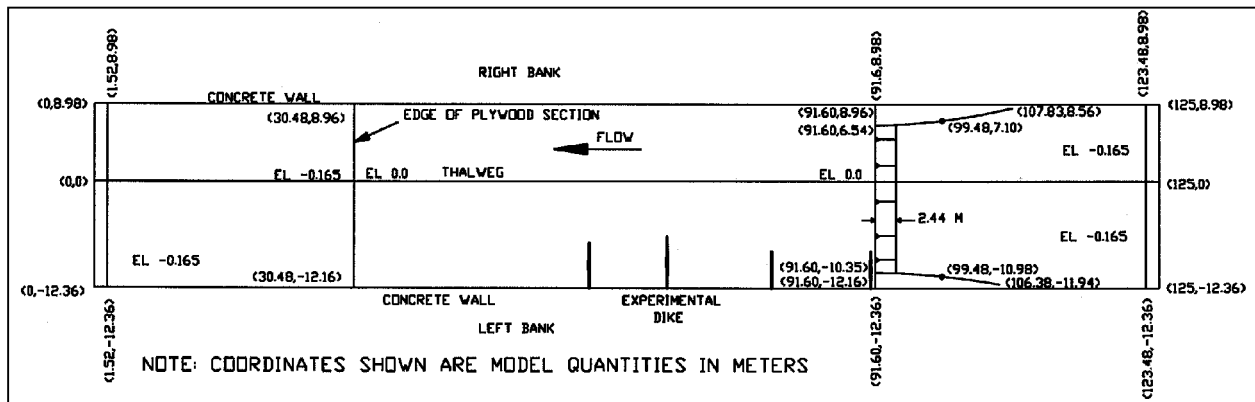


Figure 5. Layout of dike field in the navigation effects flume

Pumps recirculated flow through the navigation effects flume to simulate the desired discharge. A towing carriage was used to move the model tow through the flume at the desired speed and lateral location. The model tow was constructed of Plexiglas and was 311 m long by 32 m wide by actual draft of 2.44 m and an effective draft of 3.05 m. The effective draft is greater than the actual draft because of the scale effects discussed by Maynard and Martin (1998). No towboat was used in these experiments because the tow effects on flow downstream of the dike are caused by the return velocity and drawdown resulting from the displacement effects of the vessel and not the propeller jets, particularly for the

channel size in the open river portion of the Mississippi River and because the closest position of the tow was 77 m from the center line of the tow to the waterline on the dike. The only exceptions to no propeller jet effects below the dike field would be a tow highly skewed relative to the channel axis or a tow maneuvering with large rudder angles in the vicinity of the dikes. Both exceptions can occur but are not typical effects from a tow over a significant reach of the river.

One of the problems with tow experiments in the navigation effects flume is that the model acceleration must be larger than the acceleration used in the prototype, because the flume is short compared to the distance required for a tow to reach operating speeds. This larger acceleration in the model causes an exaggerated wave at the bow of the vessel that can be seen in the data. This same wave travels to the end of the flume, bounces off the far wall, and returns to the experimental section. Data taken after the wave returns are not valid.

Velocities were measured at the locations shown in Figure 4 using two- and three-dimensional acoustic doppler velocity (ADV) meters made by Sontek and described in Krauss, Lohrmann, and Cabrera (1994). In Figure 4, probe names 1, 0, and A0 were positioned at a scaled distance of 2 m above the bottom which was about 40 percent of the local depth. The 2-m position was chosen to ensure that the maximum velocities were measured that were induced by the tow. Probe A1 was positioned 0.6 m above the channel bottom at locations 1, 2, and 3 (to determine the velocities near the bed in the scour hole) and 2 m above the bed at location 4. For typical open-channel velocity profiles, the velocity at 0.3 m (1 ft) above the bottom in the 4.9-m depth downstream of the dike would be about 0.6 of the velocity at 2 m above the bed and about 0.8 of the value at 0.6 m. Also shown in Figure 4 are the distance of the velocity probes above the bed and the location of the vertical wall that simulates the shoreline position shown in Figure 1.

Description of Experiments

Experiments were conducted with upbound and downbound tows located either 77 m from the center line of the tow to the waterline on the dike (referred to as the near tow position) or with the tow centered on the thalweg of the navigation effects flume which was 230 m from the waterline on the dike. The area left of the tow (looking downstream) for the near tow position was 517 sq m and for the thalweg tow position was 1,564 sq m. Vessel speed over ground for the experiments was 2.4 m/sec upbound and 4.8 m/sec downbound, thereby resulting in a speed through the water of about 3.6 m/sec for both upbound and downbound tows.

For each experiment, three replicates were conducted and velocity time histories were plotted for each of the three replicates against the time relative to passage of the bow past the ADV meter shown in the plot. The three plots were analyzed and the replicate most representative of the three was selected and shown in Appendix A. The Appendix A plots show the velocity vector (magnitude and bearing) with 0 deg = 360 deg being upstream, 180 deg downstream, 90 deg

toward the dike bank, and 270 deg toward the far bank. The experiment and probe name description in the Appendix A plots are described as follows:

First position (letter): Blank or A- Blank refers to velocity probes 0 or 1, A refers to velocity probes A0 or A1

Second position (letter): Always U for Upper Mississippi River

Third position (letter): D or L—D refers to original dike, L refers to L-head dike experiments

Fourth position (letter): U or D—U for upbound, D for downbound

Fifth position (number): 1,2,3, or 4—refers to ADV meter position shown in Figure 4

Sixth position (letter): N or T—N refers to near tow position, T refers to thalweg tow position

Seventh position (letter): A, B, C, etc—refers to the replicate

Some of the plots show a rapid change in bearing with the bearing going from 0 to 360 and back to 0. This rapid change in bearing occurs under two conditions: (a) when the eddy downstream of the dike- or the tow-induced motion causes a bearing of close to 0 deg which is equal to 360 deg (velocity is upstream, parallel to channel axis and perpendicular to the dike axis), or (b) when the velocity magnitude is near zero, the bearing can show an erratic behavior. The data are valid, but the plots must be viewed with an understanding of these two factors. Other plots show a slow or cyclical change in bearing that is typical of flow below dikes, because the eddy strength often tends to increase up to a point where the eddy breaks down or weakens and then begins to reform and strengthen. This cyclical pattern makes the determination of tow influences difficult. The rapid fluctuations in velocity at all ADV meters are a result of typical variations in turbulent flow. At ADV meter A1, the variations may be larger than normal, because the ADV meter is positioned near the unstable interface between the high-velocity flow coming off the nose of the existing dike and the lower-velocity flow below the existing dike.

Based on all three replicates, an average ambient velocity magnitude and bearing was determined for each ADV meter from the time period before passage of the tow and plotted in Figures 6a through d for the four experimental conditions shown in Table 1. The average ambient velocity at the 11 ADV velocity locations in the shadow of the existing dike (does not include measurements riverward of dike nose at ADV meter A1) was 0.17 m/sec. The average ambient velocity in the low-velocity zone just below the existing dike (based on average of six upstream ADV meters excluding meter A1) was 0.12 m/sec.

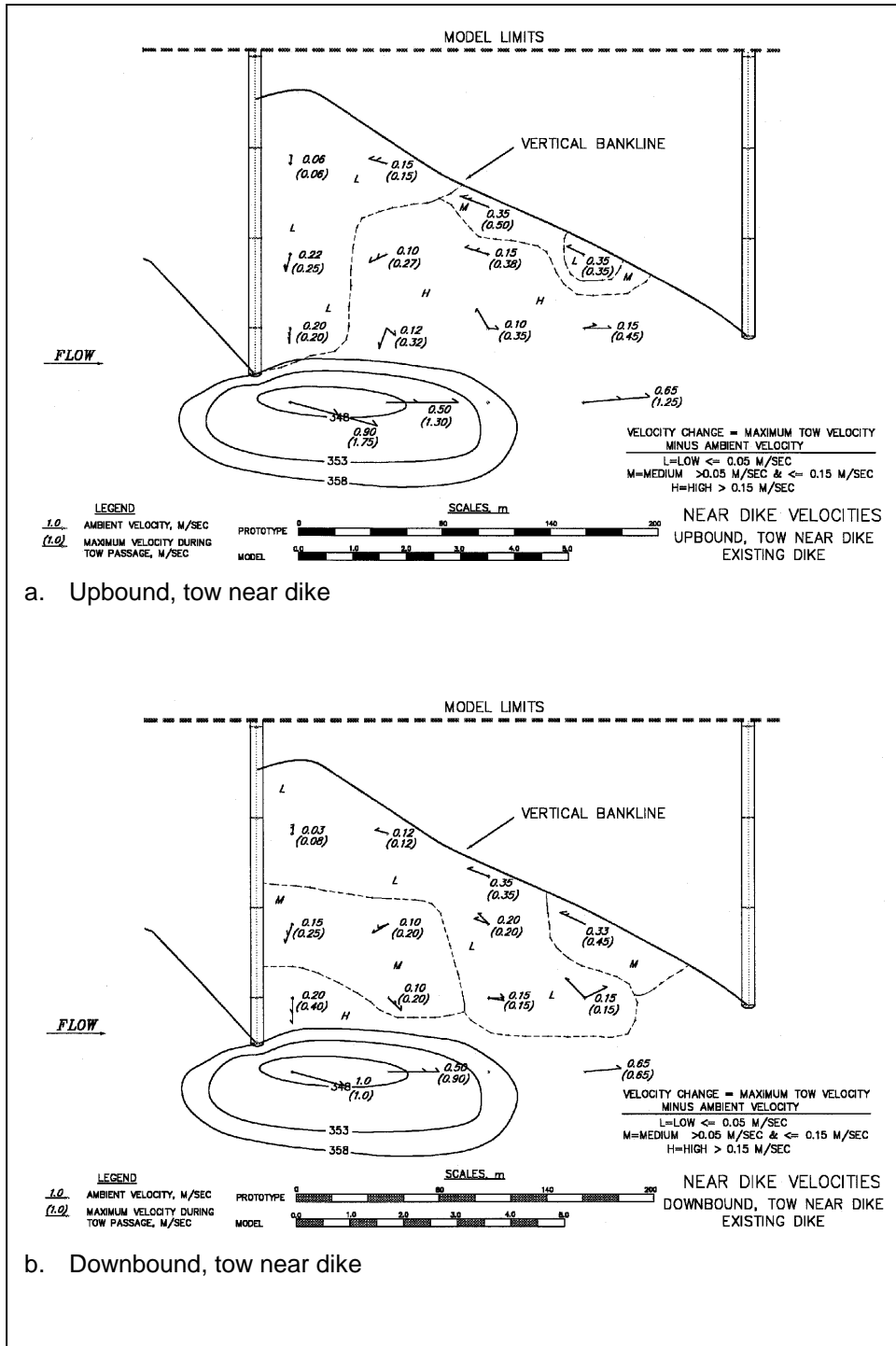


Figure 6. Near dike (existing dike) velocities for experimental condition (Continued)

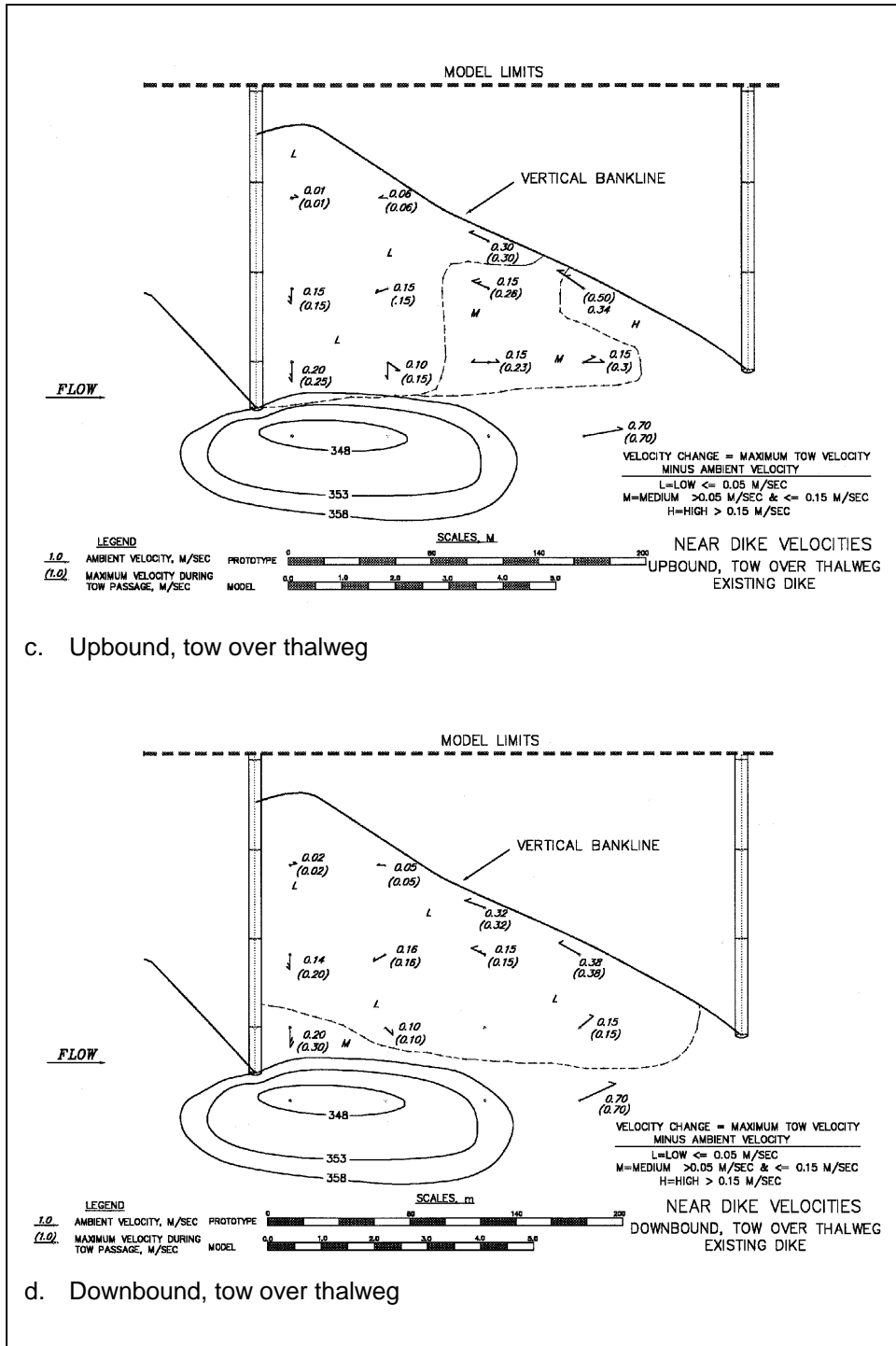


Figure 6. (Concluded)

Table 1 Return Velocity Computed from NAVEFF Model and Observed Velocity Changes				
Tow Direction	Tow Position	Computed maximum return velocity at nose of dike during tow passage, m/sec	Observed maximum velocity change*, m/sec	Observed average velocity change**, m/sec
Upbound	Near	0.226	0.30	0.12
Downbound	Near	0.197	0.20	0.06
Upbound	Thalweg	0.108	0.16	0.05
Downbound	Thalweg	0.094	0.10	0.02

* Maximum of 11 readings in shadow of existing dike (does not include measurements riverward of dike nose at ADV meter A1).
 ** Average of 11 readings in shadow of existing dike (does not include measurements riverward of dike nose at ADV meter A1).

Appendix A only shows the representative velocity plot chosen from the three replicates. Also shown in Figures 6a through d is the maximum velocity that occurred during or after passage of the tow. When the ambient and maximum velocity are the same, it does not mean that the tow had no influence since the tow can cause a decrease in velocity. The maximum velocity was chosen for this study because it was felt to be the appropriate measure of how the low-velocity habitat below the dike was affected. Two arrows are shown if the bearing changed from the ambient to the maximum tow velocity. One arrow with two arrow heads is shown if the magnitude changed but the bearing remained the same. Only velocities measured 300 secs or less after bow passage were used because of the influence of the bow wave reflection off the flume wall discussed previously.

Four experiments were conducted to measure the velocity in the scour hole (ADV meter A1 at most upstream ADV meter position 1) for various positions above the bed in addition to the measurement at 0.6 m presented above. One replicate was run and time-histories are shown in Appendix B for distances of 1.8-, 3.0-, 4.5-, and 6.0 m above the bed of the scour hole in experiments AUDU1NE, F, G, and H, respectively.

One experiment was conducted without tow passage and with 0.6 m of flow over the existing dike and the flow rate increased to 7,000 cms. Only ambient velocities were measured and the time-histories are shown in Appendix C. This experiment was conducted to see if higher flows, which can occur in January, cause velocity changes of a magnitude similar to the tow induced changes. Experiment names used in the overtopping experiments were as follows:

(blank or "a")(UD2)(ADV meter position)(TD)

with blank or “a” and ADV meter position as in the previous experiment names.

A summary plot in Figure 7 shows the average ambient velocity and bearing taken from the time-history plots.

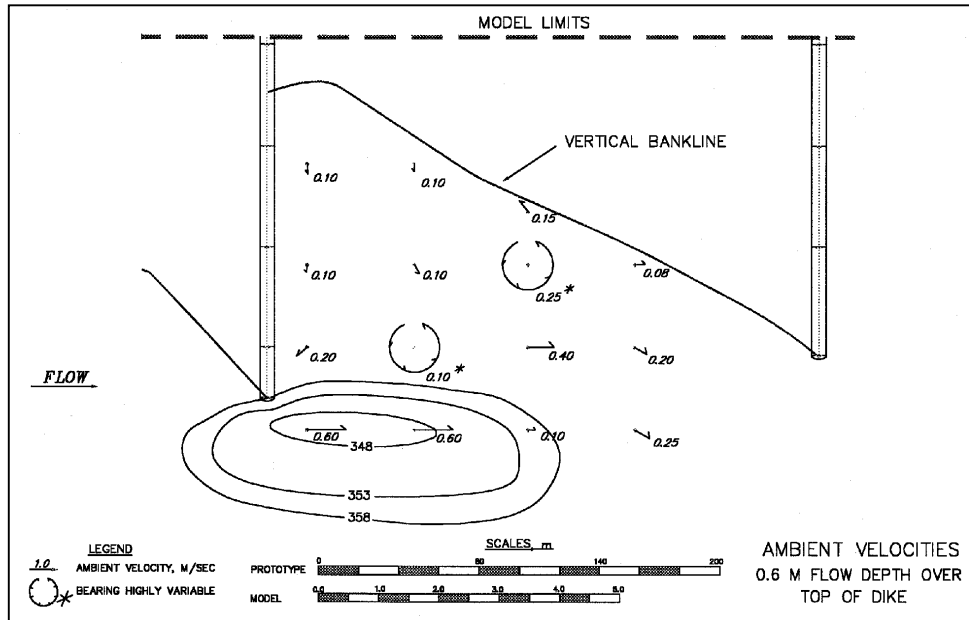


Figure 7. Average ambient velocity and bearing for flow over existing dike

A series of experiments were conducted with four configurations of an L-head dike for the upbound tow at a scaled distance of 77 m from the dike which simulated a worst-case scenario of an upbound tow passing close to a dike field. Except for addition of the L-head, all experimental conditions were identical to the experiments with the existing dike. The L-head dike was simulated using a vertical sheet metal wall. The initial L-head experiment was conducted with a 3.5-m-high L-head dike (top el 113, overtopped by 1.5 m) and extending from the nose of the existing dike 137 m downstream. This point was a distance halfway between the experimental dike and the next downstream dike. Three replicates were conducted and the representative replicate for each ADV meter is shown in Appendix D. A summary plot in Figure 8a shows the ambient and maximum velocity during tow passage for the upbound, near-tow passage. A second run of the 137-m-long by 3.5-m-high L-head dike was conducted with three replicates as before, and a summary plot of velocities is shown in Figure 8b. The next L-head dike was 137 m long by 1.7 m high (3.2 m of overtopping), and a summary plot of velocities based on three replicates is shown in Figure 9a. Figure 9b shows a summary plot of velocities for a 69-m-long by 3.5-m-high L-head dike. Figure 9c shows a summary plot of velocities for a 69-m-long by 1.7-m-high L-head dike. The individual velocity plots for Figures 8b through 9c are not included in Appendix D in an attempt to limit the size of this report.

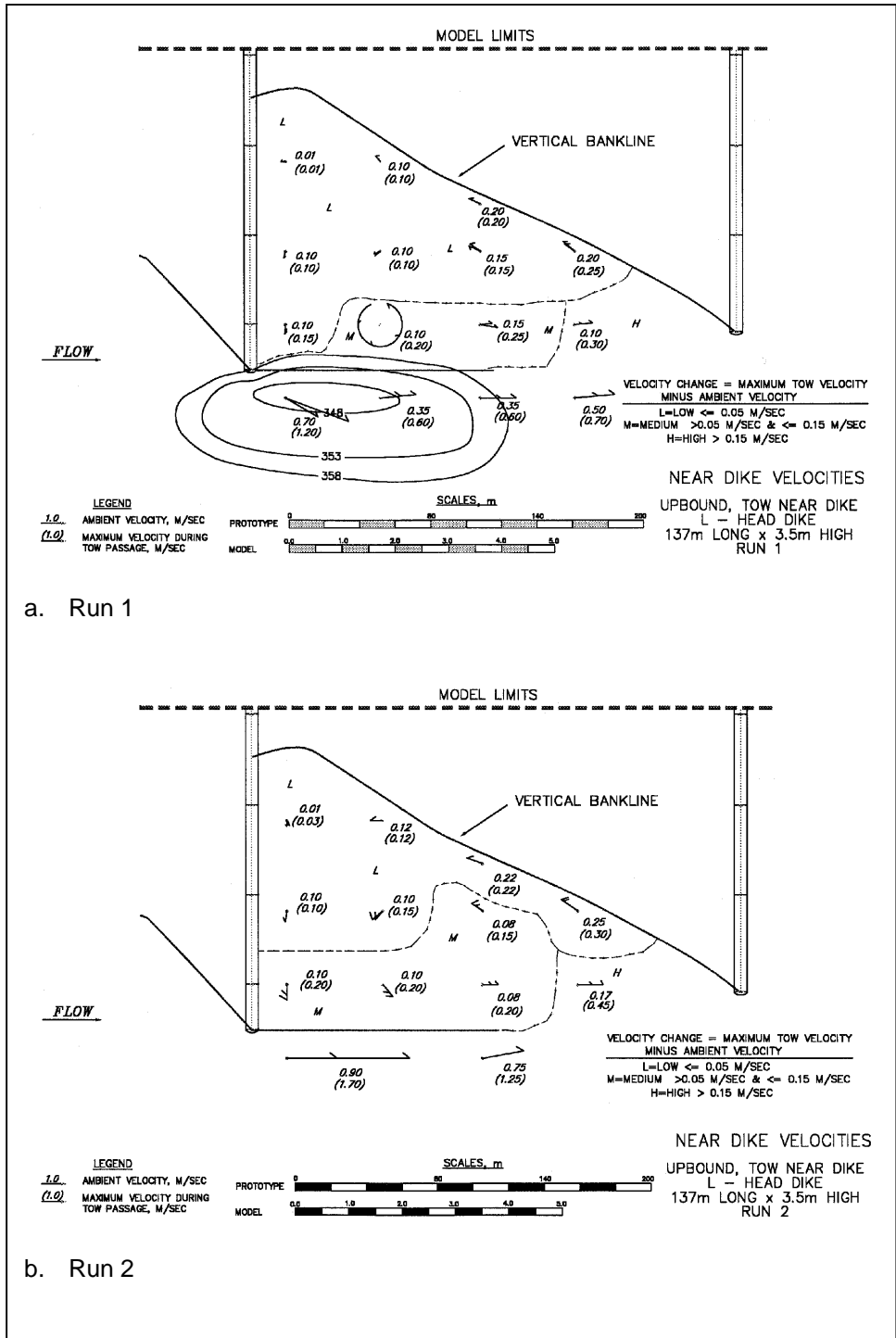


Figure 8. Near dike (existing) velocities for experimental conditions and dimension of L-head

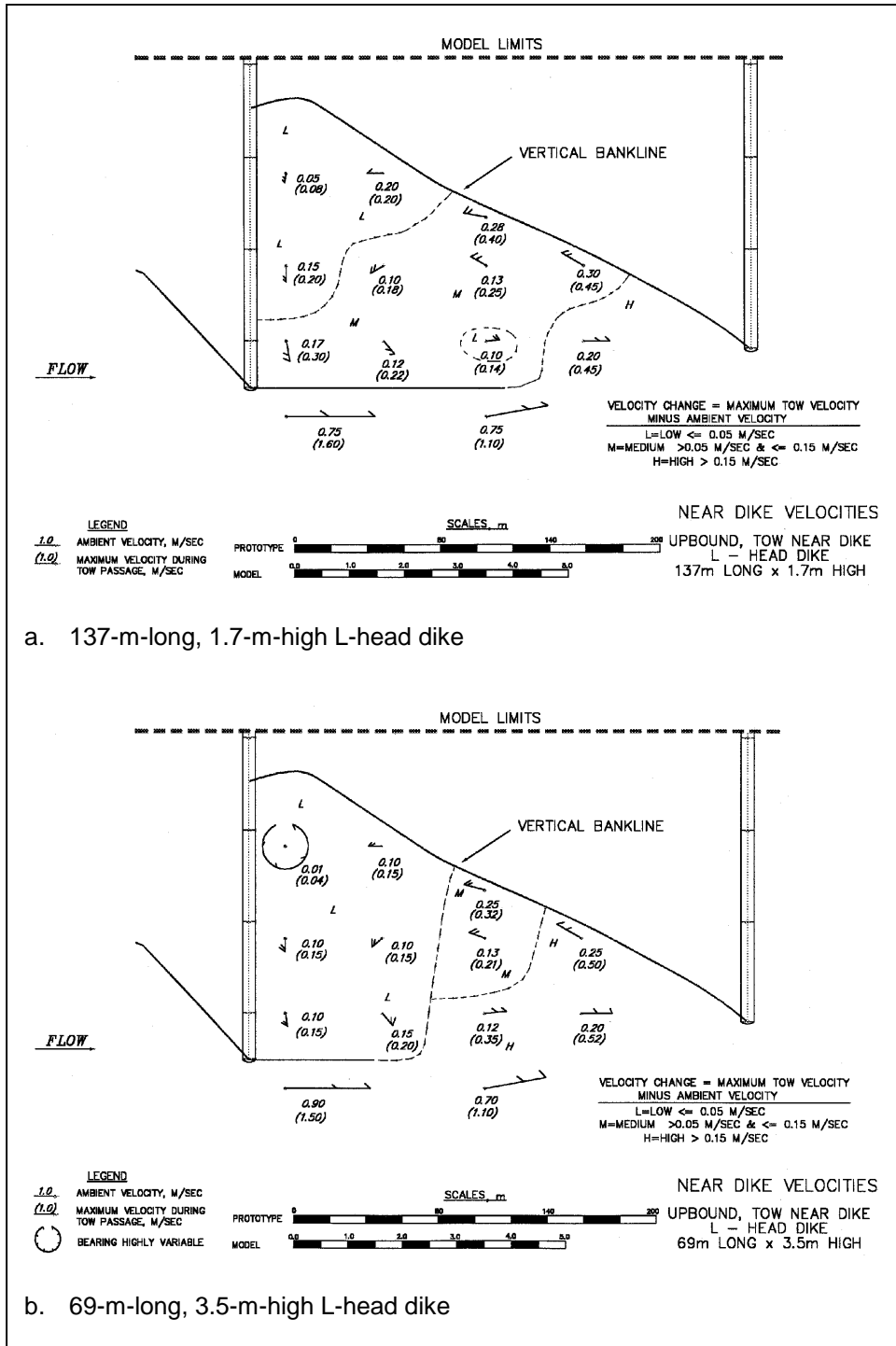
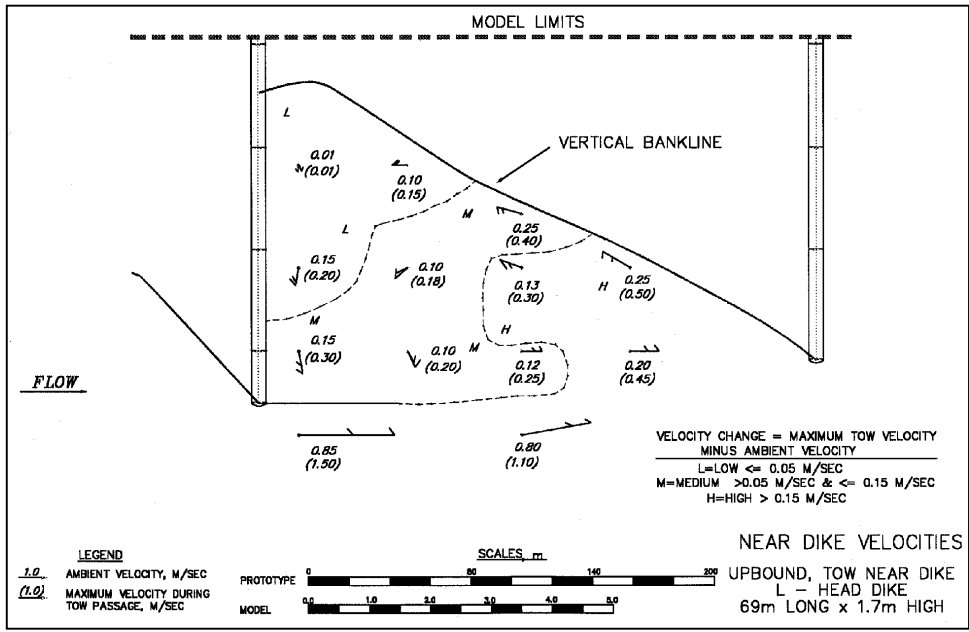


Figure 9. Near dike (existing) velocities for velocities for experimental conditions and dimensions of L-head (Continued)



c. 69-m-long, 1.7-m-high L-head dike

Figure 9. (Concluded)

3 Results

Flow Visualization

Photographs of confetti (1.9-cm by 1.9-cm pieces of paper) were used to document surface velocity patterns with and without tow passage. Short streaks indicate areas of low surface velocity and longer streaks indicate areas of higher surface velocity. Only the upbound tow near the dike was used because this tow causes the most noticeable change between with and without tow conditions. The shutter on the camera was left open for 10 secs (model) which is equivalent to 55 secs in the prototype for both with and without tows. This time was selected based providing a long enough streak on the photograph to indicate surface patterns. It was nearly impossible to get the same amount of confetti in each photograph which should be considered when analyzing the photographs. What appears to be more intense activity in the photograph may be the result of a greater amount of confetti in the model. The with-tow photographs were taken with the shutter opened when the stern of the tow passed the test dike and closed 10 secs later. Table 2 shows the experimental conditions and the corresponding photograph numbers.

Under ambient conditions, all dike configurations show the presence of a low-velocity zone just downstream of the existing dike. Further downstream is a large eddy. After passage of the tow, the large eddy moves upstream and away from the near bank, generally toward the nose of the existing dike. This causes an increase in velocity in the ambient low-velocity zone, particularly toward the end of the existing dike.

Table 2 Flow Visualization Photographs		
Photograph	Tow	Dike Configuration
1	without	Existing dike
2	with	A
3	without	L-Head Dike, 137 m long by 3.5 m high
4	with	A
5	without	L-Head Dike, 137 m long by 1.7 m high
6	with	A
7	without	L-Head Dike, 69 m long by 3.5 m high
8	with	A
9	without	L-Head Dike, 69 m long by 1.7 m high
10	with	A

Computed Return Velocities

Return velocities for the experiments were computed using the “NAVEFF” model (Maynard 1996) and are given in Table 1 along with the maximum observed velocity change during tow passage and the average observed velocity change during tow passage. The return velocity for an upbound tow acts opposite to the tow direction (in a downstream direction) and adds to the ambient current. The combined ambient and return current for the upbound tow causes the eddy rotation speed to increase. The speed increase is not instantaneous because the eddy is large and has a significant mass that must be accelerated. After the tow passes, the return current drops to zero but the eddy, because of its large mass, requires some time to decrease back to a speed consistent with the ambient current alone. Consequently, the higher eddy speed, in conjunction with the ambient current alone, allows the eddy to penetrate farther out into the main channel for a short period of time.

For a downbound tow, the return velocity acts in an upstream direction and decreases the ambient current. In some cases, the ambient current is low enough and the return current is high enough to cause the river to temporarily flow in an upstream direction. In most cases, the ambient current is reduced by the return velocity but is still directed downstream. This ambient current and return velocity tend to reduce the rotational speed of the eddy.

Because of the interaction of the eddy and the direction of return velocity movement, upbound tows will cause larger velocity increases in the eddy below dikes than downbound tows, all other conditions being equal. The velocities



Photo 1. Existing dike, without tow



Photo 2. Existing dike, with tow



Photo 3. L-head dike, 137 m long by 3.5 m high, without tow



Photo 4. L-head dike, 137 m long by 3.5 m high, with tow



Photo 5. L-head dike, 137 m long by 1.7 m high, without tow



Photo 6. L-head dike, 137 m long by 1.7 m high; with tow



Photo 7. L-head dike, 69 m long by 3.5 m high, without tow

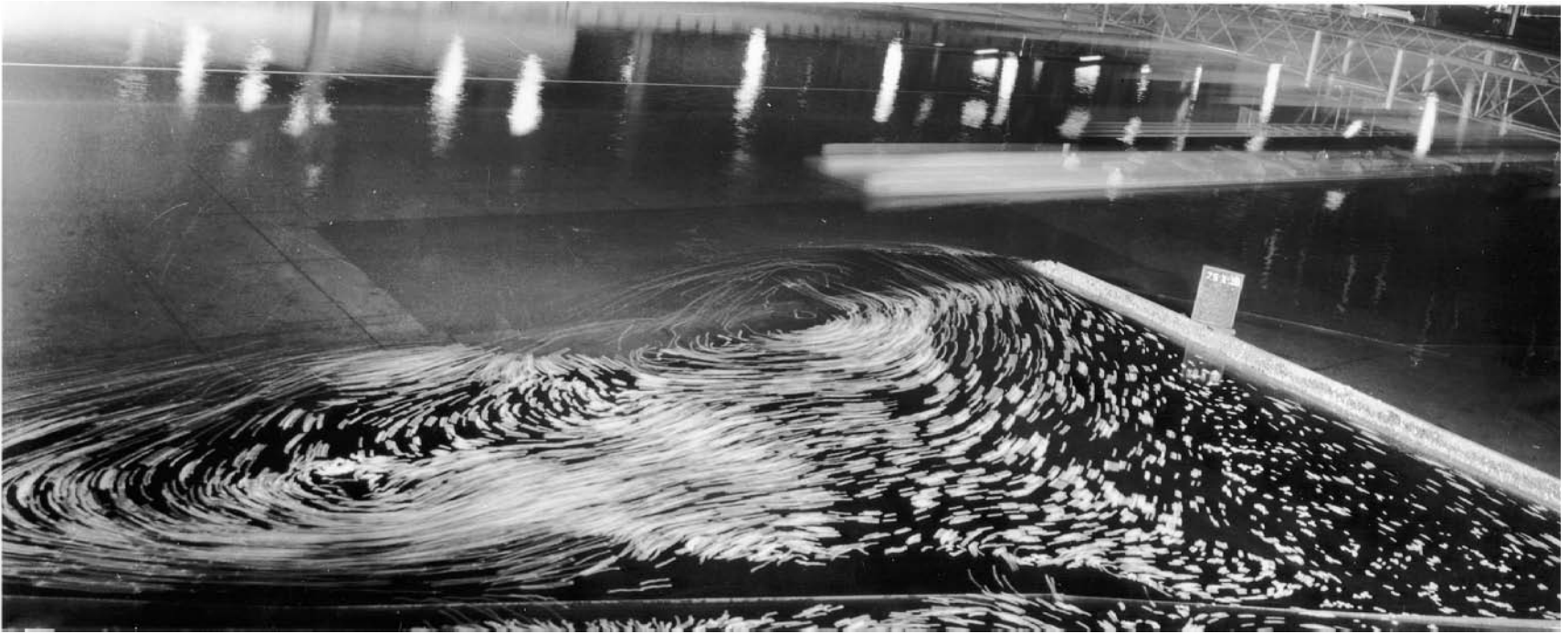


Photo 8. L-head dike, 69 m long by 3.5 m high, with tow



Photo 9. L-head dike, 69 m long by 1.7 m high, without tow

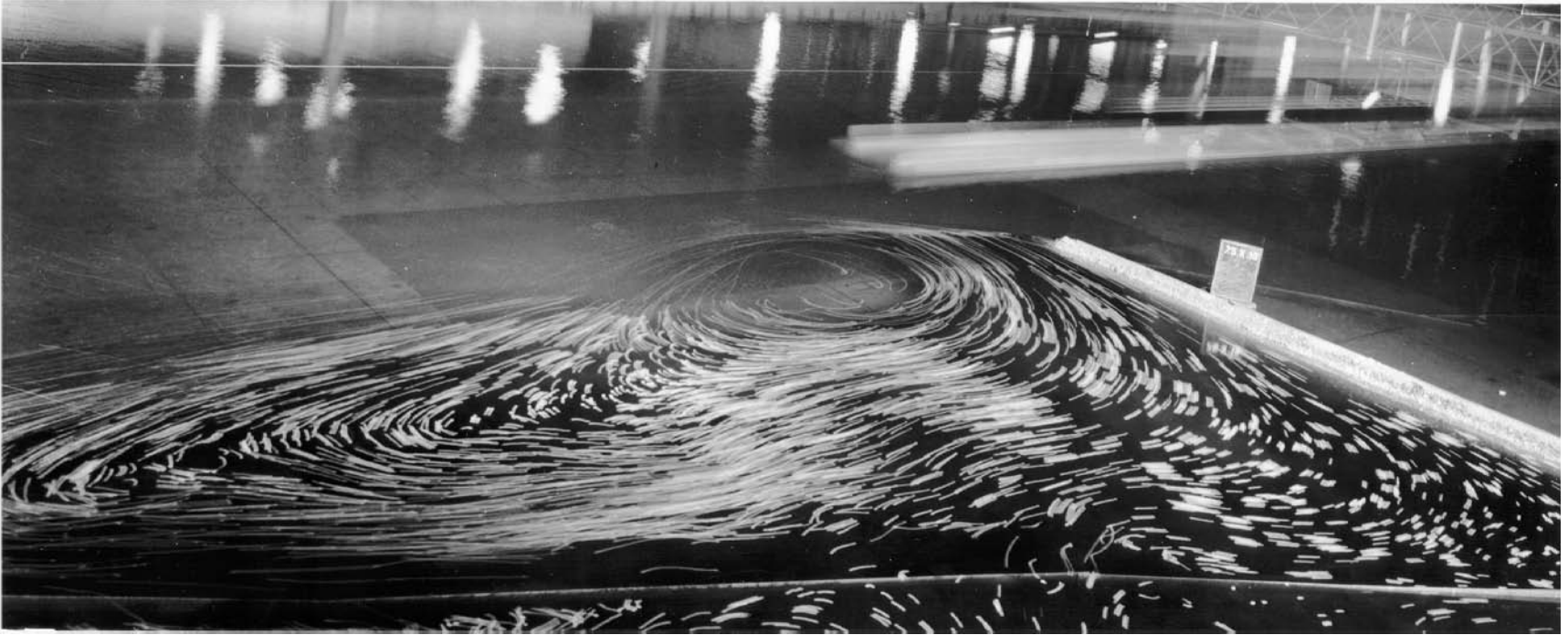


Photo 10. L-head dike, 69 m long by 1.7 m high, with tow

below the dike during tow passage are not only a function of return velocity/eddy speed interaction because the tow also creates drawdown of the water level. This drawdown of the water level also impacts the velocity field below the dike. The impacts of drawdown are a likely explanation of the relatively high-velocity changes for the downbound tow near the dike and for the movement of the large eddy toward the nose of the existing dike. Because return velocity and drawdown are directly linked since they are caused by the same phenomenon, only return velocity is used as a characteristic measure of tow effects below a dike. Another site-specific concern is that the eddy penetration out into the main channel, after tow passage at upstream dikes, could cause changes at the dikes downstream. Some of this may be happening in the dike arrangement used in the physical model conducted herein, but the magnitude of the effect is not known.

Since return velocity is a primary cause of changes below a dike, the computed return velocities are compared to the observed changes in the velocities below the dike. Relationships between the observed velocity changes below dikes and computed return velocity will allow application of these results to other river cross sections. Based on the plots of maximum velocity during tow passage, the upbound tow near the dike produced the greatest velocity change (up to 0.3 m/sec (based on location in Figure 6a where ambient velocity is 0.15 m/sec and maximum velocity during tow passage is 0.45 m/sec)) whereas the downbound tow over the thalweg produced the least change (less than or equal to 0.1 m/sec (based on location in Figure 6d where ambient velocity is 0.20 m/sec and maximum velocity during tow passage is 0.3 m/sec)). These values apply to the low-velocity habitat in the shadow of the dike and not to the values measured past the end of the original dike at ADV meter A1 where ambient velocities are large and consequently not potential winter habitat. Since the velocity changes below the dike are driven by the magnitude of the return velocity, these findings are consistent with the return velocity magnitude shown in Table 1. Both the upbound tow over the thalweg and the downbound tow near the dike produced intermediate changes (less than or equal 0.2 m/sec) downstream of the dike. For upbound tows near the dike, the maximum velocity change during tow passage below the dike was 1.3 times the computed return velocity from the NAVEFF model (based on 0.30 (from Figure 6a)/0.226 (from Table 1)) using the cross section between the nose of the dike and the far bank. For upbound tows on the thalweg, the maximum velocity change during tow passage below the dike was 1.5 times the computed return velocity from the NAVEFF model (based on 0.16 (from Figure 6c)/0.108 (from Table 1)). For downbound tows near the dike, the maximum velocity change during tow passage was 1.0 times the computed return velocity from the NAVEFF model (based on 0.20 (from Figure 6b)/0.197 (from Table 1)). For downbound tows on the thalweg, the maximum velocity change during tow passage was 1.1 times the computed return velocity from NAVEFF model (based on 0.10 (from Figure 6d)/0.094 (from Table 1)). In terms of the average velocity change below the existing dike during tow passage shown in Table 1, the upbound near-dike tow was 53 percent of the computed return velocity, the downbound near-dike tow was 30 percent, the upbound thalweg tow was 46 percent, and the downbound thalweg tow was 21 percent.

Existing Dike with Tow Passage

As discussed previously, surface confetti in the physical model prior to tow passage indicated an eddy typical of the region downstream of a dike that rotates counterclockwise on the left descending bank. Upon passage of an upbound tow, the eddy strength appeared to increase based on the observed greater movement of the dye and surface confetti toward the main channel. The center of the eddy was close to ADV meter A0, position 3 for the existing dike.

In the comparison of velocity in the scour hole, the peak velocity at about 70 secs during tow passage is similar for all four vertical positions. The drop in velocity that follows the peak at ADV meter A1, position 1, is the effect of the eddy, which has increased in speed, temporarily pushing the high-velocity flow from the nose of the dike toward the main channel and away from ADV meter A1.

The velocity changes at the ADV meter near the end of the dike (ADV meter A1 at position 1) were all greater than the computed return velocity shown in Table 1 because of the contracting effects of the dike. The NAVEFF model computations are based on a channel having a uniform width. The velocity change at ADV meter A1, position 1, is about two to three times the value from the NAVEFF model for the upbound tow.

Figures 6 through 9 delineate areas of velocity change in the shadow of the dike which does not include areas riverward of the nose of the dike. In Figures 6a through d and 7 through 9, velocity changes are mapped based on magnitude of velocity change defined as maximum velocity during tow passage minus ambient velocity. The low (L)-velocity change is less than or equal to 0.05 m/sec, moderate (M)-velocity change is greater than 0.05 m/sec up to less than or equal to 0.15 m/sec, and high (H)-velocity change greater than 0.15 m/sec. For an upbound tow near the dike (Figure 6a), the existing dike has a significant amount of the area below the dike that has a high-velocity change when compared to other tow directions and tow locations. For a downbound tow near the dike (Figure 6b), much of the area below the dike has a low or moderate change in velocity. For an upbound tow over thalweg (Figure 6c), the entire width of the existing dike has a low-velocity change for a distance of about 100 m. For a downbound tow over thalweg (Figure 6d), almost the entire area below the dike has a low-velocity change. Based on Figures 6a through d and the maximum and average observed velocity change below the existing dike in Table 1, the order of severity of velocity change over the entire area below the dike is as follows: (a) the upbound tow near dike is highest; (b) the downbound tow near the dike is second highest; (c) the upbound tow over the thalweg produces the third highest velocity change; and (d) the downbound tow over thalweg produces the lowest velocity change.

Flow Overtopping Existing Dike without Tow Passage

The flow over the dike tends to reduce the eddy action below the dike based on comparison of the ambient velocities shown on Figures 6a through d without overtopping and the ambient velocities shown in Figure 7 with overtopping.

Ambient velocity magnitude in the shadow of the dike was similar with (average = 0.16 m/sec) and without (average = 0.17 m/sec) overtopping, but channel velocities at ADV meter A1 were reduced during overtopping flow because of less flow contraction by the dike.

L-Head Dike with Tow Passage

Figures 8a and b show the largest L-head dike evaluated, 137 m long by 3.5 m high, for the upbound tow near the dike. Both runs can be compared to Figure 6a and show that the L-head results in lower ambient velocities and significantly larger areas of low- and moderate-velocity changes in the shadow of the dike. Based on dye injections and surface confetti, the center of the eddy for the 137-m-long by 3.5-m-high L-head dike was just upstream of ADV meter A0 at position 3. In Figure 9a, the L-head is 137 m long but reduced in height to 1.7 m above the bed. The 137-m-long by 1.7-m-high L-head dike shows increased areas of moderate-velocity change compared to the 3.5-m-high L-head dike. In Figure 9b, the L-head dike is shortened to 69 m in length but kept at the largest height evaluated, 3.5 m. The 69-m-long by 3.5-m-high L-head dike has lower ambient velocities in the shadow of the existing dike compared to the existing dike alone and an area of low-velocity change that extends downstream from the existing dike about equal to the length of the L-head. The smallest L-head dike evaluated (Figure 9c), 69 m by 1.7 m, has a reduced area of low-velocity change compared to the other L-head dikes. Average ambient velocity and maximum and average observed velocity changes with the existing and L-head dikes are shown in Table 3.

Table 3 Average Ambient Velocity and Maximum and Average Velocity Change for Existing and L-Head Dikes				
L-head length, m	L-head height, m	Average ambient velocity, m/sec	Maximum velocity change, m/sec	Average velocity change, m/sec
0(existing dike)	0	0.17	0.30	0.12
137	3.5	0.12	0.29*, 0.28**	0.05*, 0.07**
137	1.7	0.16	0.25	0.10
69	3.5	0.14	0.32	0.11
69	1.7	0.14	0.25	0.13
* Run 1. ** Run 2.				

Based on average ambient velocity and average velocity change below the existing dike, only the 137-m-long by 3.5-m-high L-head dike provides significant reduction in velocity change and ambient velocity compared to the existing dike.

4 Summary and Discussion

The maximum ambient velocities measured herein below the nonovertopped existing dike (up to 0.38 m/sec in 1.2 m/sec main channel velocity) are similar in magnitude to the Pilarczyk, Klaassen, and Verhey (1989) velocities (0.3 m/sec below dike in 1.0-m/sec main channel velocity) and to other analogous flow conditions such as in the trough of dunes (Simons and Richardson 1971) and below abrupt channel expansions (Raudkivi 1967).

Velocity changes below the existing dike during tow passage are largest with upbound tows near the dike and smallest with downbound tows on the channel thalweg. Upbound tows on the thalweg and downbound tows near the dike produced similar velocity changes which were about midway between the largest values from the upbound near dike tow and the downbound thalweg tow.

Return velocity can be used to estimate tow induced changes below the existing dike where ambient velocities are low. Maximum velocity changes were 1.3 and 1.5 times the computed return velocity for upbound tows and 1.0 and 1.1 times the computed return velocity for downbound tows. Average velocity changes were 0.46 and 0.53 times the computed return velocity for upbound tows and 0.21 and 0.30 times the computed return velocity for downbound tows.

Average ambient velocity below the existing dike during overtopping of 0.6 m (0.16 m/sec) (Figure 7) was comparable to average ambient velocity below the existing dike without overtopping (0.17 m/sec) (Figures 6a through d). Eddy action below the existing dike was reduced during overtopping.

L-head dikes reduce both ambient velocities and tow-induced velocity changes depending on the size of the L-head dike. Average ambient velocities below the existing dike with addition of a 137-m-long by 3.5-m-high L-head dike were 0.12 m/sec compared to 0.17 m/sec for the existing dike alone. Average velocity changes induced by the tow for the 137-m-long by 3.5-m-high L-head dike were about 50 percent of the average velocity changes for the existing dike alone. Shorter and/or lower L-head dikes appeared to provide reductions based on the contour plots of velocity changes but were inconclusive when comparing average velocity change, maximum velocity change, or average ambient velocity.

The vertical velocity profile measured in the scour hole showed a similar peak velocity in the scour hole during tow passage for the four vertical positions. The peak velocity increase at the ADV meter position near the nose of the dike (but not in the shadow of the dike) was two to three times the return velocity computed

from NAVEFF for the upbound tow which reflects the concentrating effect of the dike on return flows.

Velocity patterns downstream of dikes with and without tow passage could also be evaluated using the numerical model HIVEL (Stockstill and Berger in preparation). Velocities presented herein or field data could be used to validate such a modeling effort.

References

- Copeland, R. R. (1981). "Bank protection using spur dikes," The Streambank Erosion Control Evaluation and Demonstration Act of 1974, Section 32, Public Law 93-251, Appendix B: Hydraulic Research, U.S. Army Corps of Engineers, Washington, DC.
- Gupta, V. P., and Raju, G. R. (1987). "Separated flow in lee of solid and porous fences," *ASCE J of Hydraulic Engineering* 113(10), 1264-1276.
- Krauss, N., Lohrmann, A., and Cabrera, R. (1994). "New acoustic meter for measuring 3D laboratory flows," *J of Hydraulic Engineering* 120(3), 406-412.
- Maynard, S. T. (1996). "Return velocity and drawdown in navigable waterways," Technical Report HL-96-7, U.S. Army Engineer Waterways Experiment Station, Vicksburg, MS.
- Maynard, S. T., and Martin, S. K. (1998). "Interim report for the Upper Mississippi River-Illinois Waterway System navigation study, physical forces study, Clark's Ferry, Mississippi River," ENV Report 5, U.S. Army Engineer Waterways Experiment Station, Vicksburg, MS.
- Pande, P. K., Prakash, R., and Agarwal, M. L. (1980). "Flow past fence in turbulent boundary layer," *ASCE J of Hydraulic Engineering* 106(1), 191-207.
- Pilarczyk, K. W., Klaassen, G. J., and Verhey, H. J. (1989). "Control of bank erosion in the Netherlands, state of the art." *ASCE, Proceeding of the 1989 National Conference on Hydraulic Engineering*. New Orleans, LA.
- Rajaratnam, N., and Nwachukwu, B. A. (1983). "Flow near groin-like structures," *ASCE J of Hydraulic Engineering* 109(3), 463-480.
- Raudkivi, A. J. (1967). *Loose boundary hydraulics*. Pergamon Press, Oxford.
- Simons, D. B., and Richardson, E. V. (1971). "Flow in alluvial sand channels." *River Mechanics*. H. W. Shen, Fort Collins, CO.
- Stockstill, R. L., and Berger, R. C. "A two-dimensional model for vessel-generated currents," Technical Report (in preparation), U.S. Army Engineer Waterways Experiment Station, Vicksburg, MS.

Tingsanchali, T., and Maheswaran, S. (1990). "2-D depth-averaged flow computation near groyne," *ASCE, J of Hydraulic Engineering* 116(1), 71-86.

U.S. Army Corps of Engineers. (1994). "Upper Mississippi River-Illinois Waterway System navigation study," Baseline Initial Project Management Plan, U.S. Army Engineer Districts, Rock Island, St Louis, and St Paul.

REPORT DOCUMENTATION PAGE

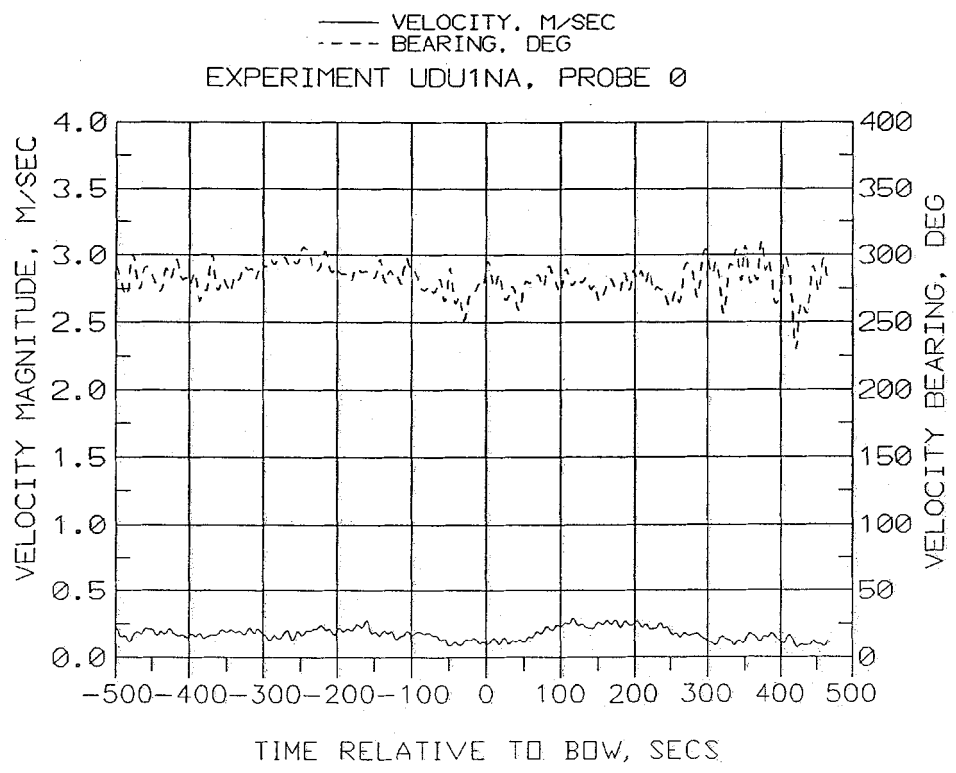
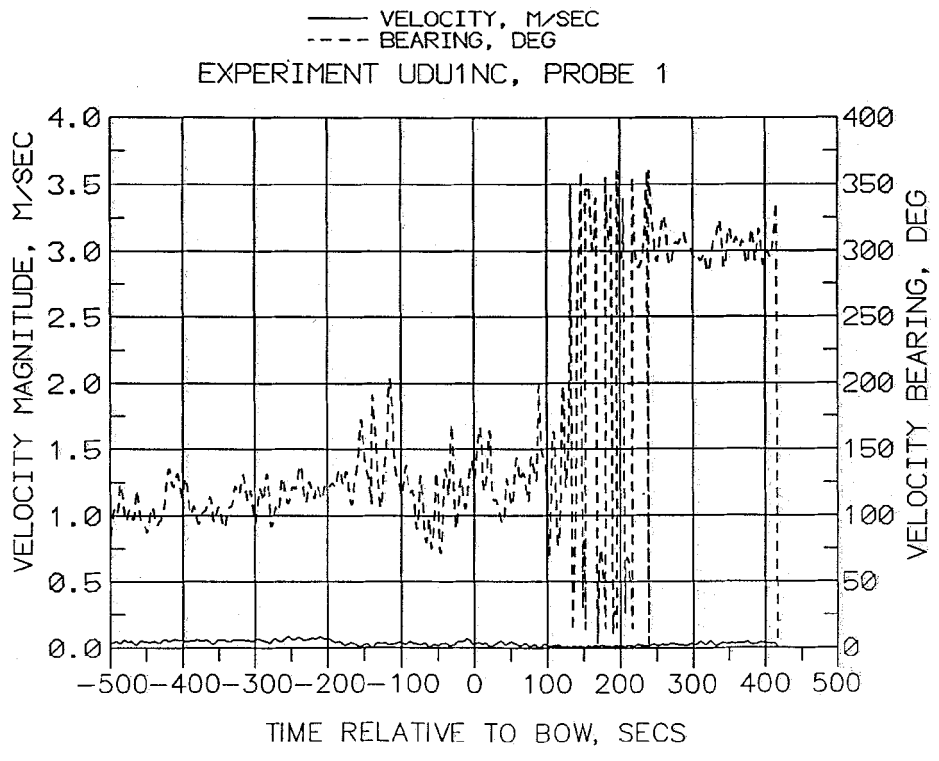
Form Approved
OMB No. 0704-0188

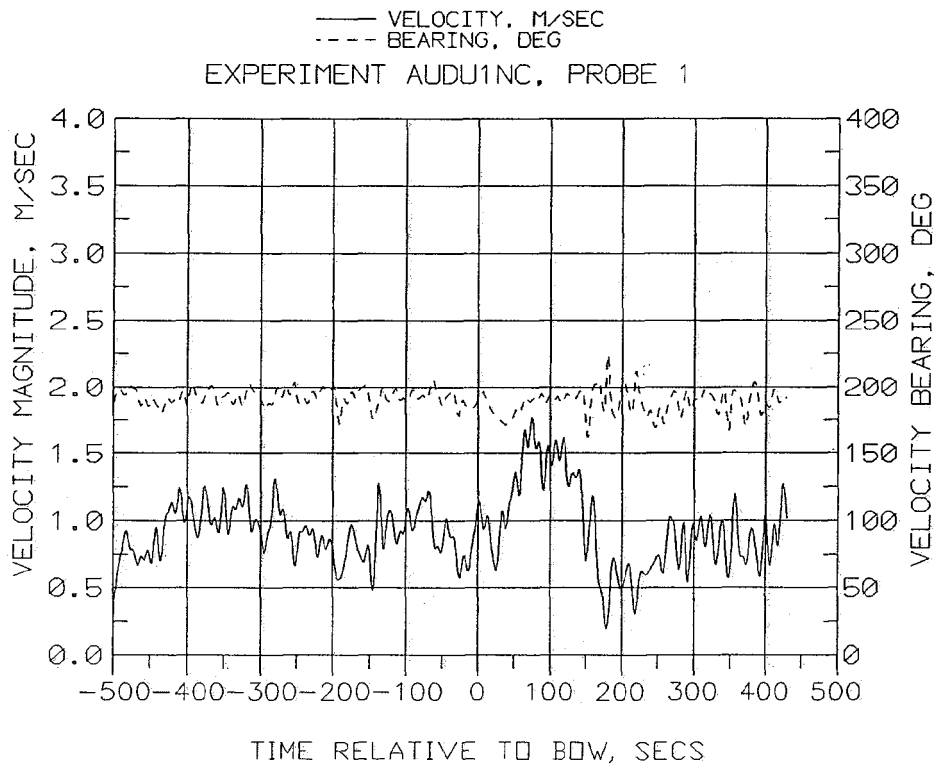
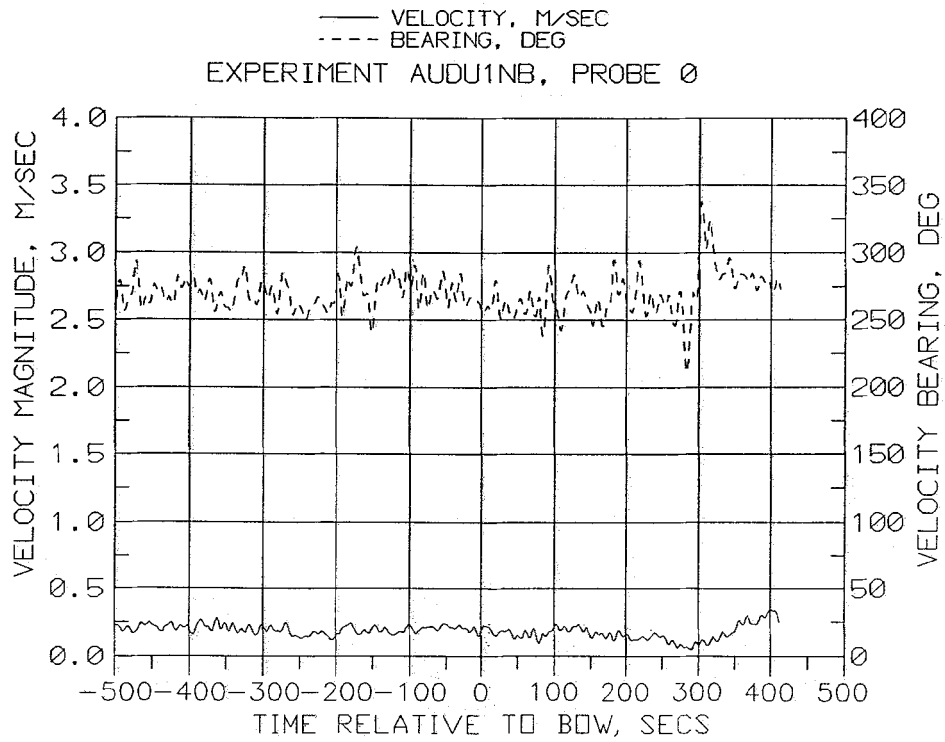
Public reporting burden for this collection of information is estimated to average 1 hour per response, including the time for reviewing instructions, searching existing data sources, gathering and maintaining the data needed, and completing and reviewing the collection of information. Send comments regarding this burden estimate or any other aspect of this collection of information, including suggestions for reducing this burden, to Washington Headquarters Services, Directorate for Information Operations and Reports, 1215 Jefferson Davis Highway, Suite 1204, Arlington, VA 22202-4302, and to the Office of Management and Budget, Paperwork Reduction Project (0704-0188), Washington, DC 20503.

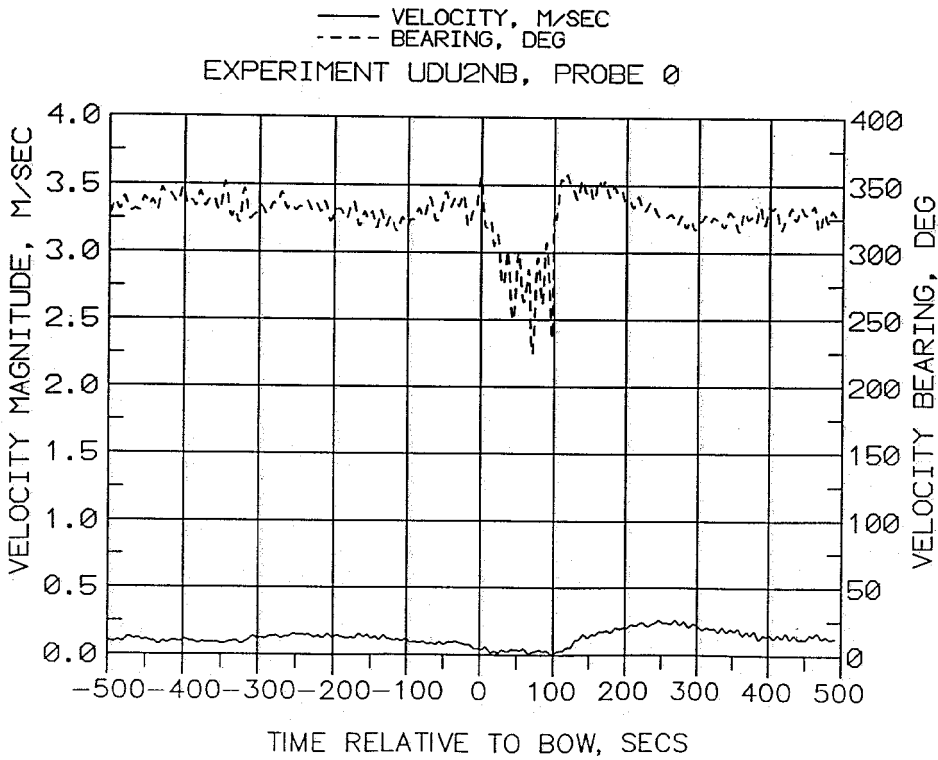
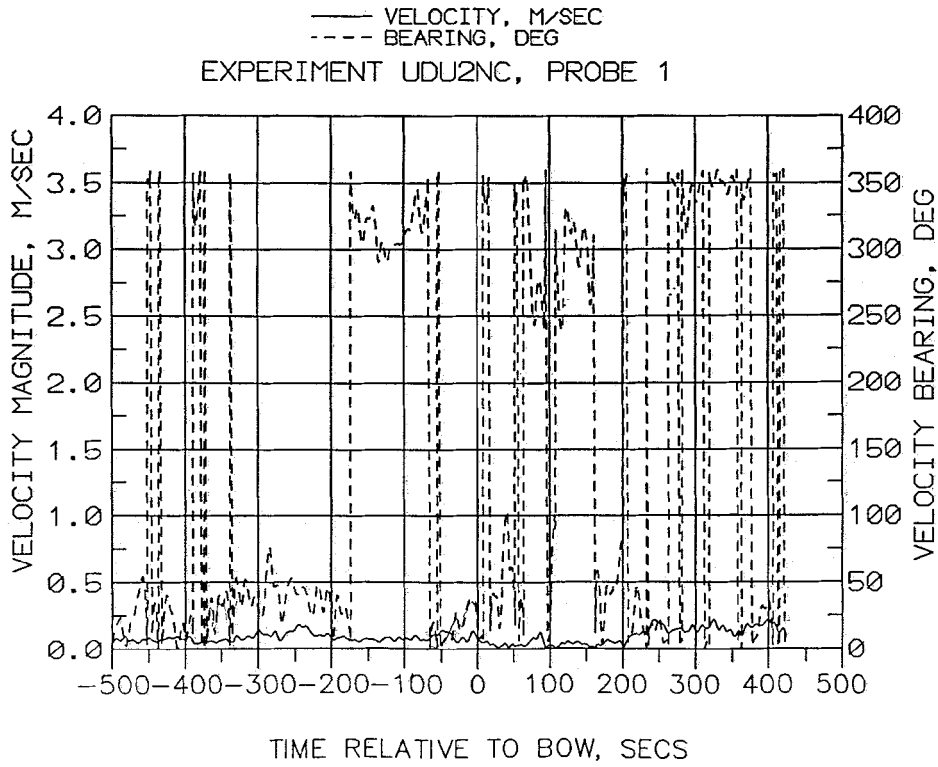
1. AGENCY USE ONLY (Leave blank)	2. REPORT DATE March 2000	3. REPORT TYPE AND DATES COVERED Interim report	
4. TITLE AND SUBTITLE Velocity Patterns Downstream of a Mississippi River Dike with and without Tow Traffic		5. FUNDING NUMBERS	
6. AUTHOR(S) Stephen T. Maynard			
7. PERFORMING ORGANIZATION NAME(S) AND ADDRESS(ES) U.S. Army Engineer Research and Development Center Coastal and Hydraulics Laboratory 3909 Halls Ferry Road Vicksburg, MS 39180-6199		8. PERFORMING ORGANIZATION REPORT NUMBER	
9. SPONSORING/MONITORING AGENCY NAME(S) AND ADDRESS(ES) See reverse.		10. SPONSORING/MONITORING AGENCY REPORT NUMBER ENV Report 21	
11. SUPPLEMENTARY NOTES			
12a. DISTRIBUTION/AVAILABILITY STATEMENT Approved for public release; distribution is unlimited.		12b. DISTRIBUTION CODE	
13. ABSTRACT (Maximum 200 words) <p>The Upper Mississippi River-Illinois Waterway System (UMR-IWWS) Navigation Feasibility Study will evaluate the justification of providing additional lockage capacity at sites on the UMR-IWWS while maintaining the social and environmental qualities of the river system. The system navigation feasibility study will be accomplished by executing the Initial Project Management Plan that outlines Engineering, Economic, Environmental, and Public Involvement Plans.</p> <p>The Environmental Plan identifies the significant environmental resources on the UMR-IWWS and probable impacts in terms of threatened and endangered species; water quality; recreational resources; fisheries; mussels and other macroinvertebrates; waterfowl; aquatic and terrestrial macrophytes; and historic properties. It considers system-wide impacts of navigation capacity increases, while also assessing in preliminary fashion potential construction effects of improvement projects.</p> <p>One element of the Environmental Plan addresses the impacts of navigation on larval and adult fish. Part of the fish study evaluates the impact of tow traffic on adult fish using the low-velocity habitat found during winter months downstream of dikes on the Mississippi River.</p> <p style="text-align: right;">(Continued)</p>			
14. SUBJECT TERMS Dike Fish Habitat		Mississippi River Navigation Velocity	Winter
			15. NUMBER OF PAGES 90
			16. PRICE CODE
17. SECURITY CLASSIFICATION OF REPORT UNCLASSIFIED	18. SECURITY CLASSIFICATION OF THIS PAGE UNCLASSIFIED	19. SECURITY CLASSIFICATION OF ABSTRACT	20. LIMITATION OF ABSTRACT

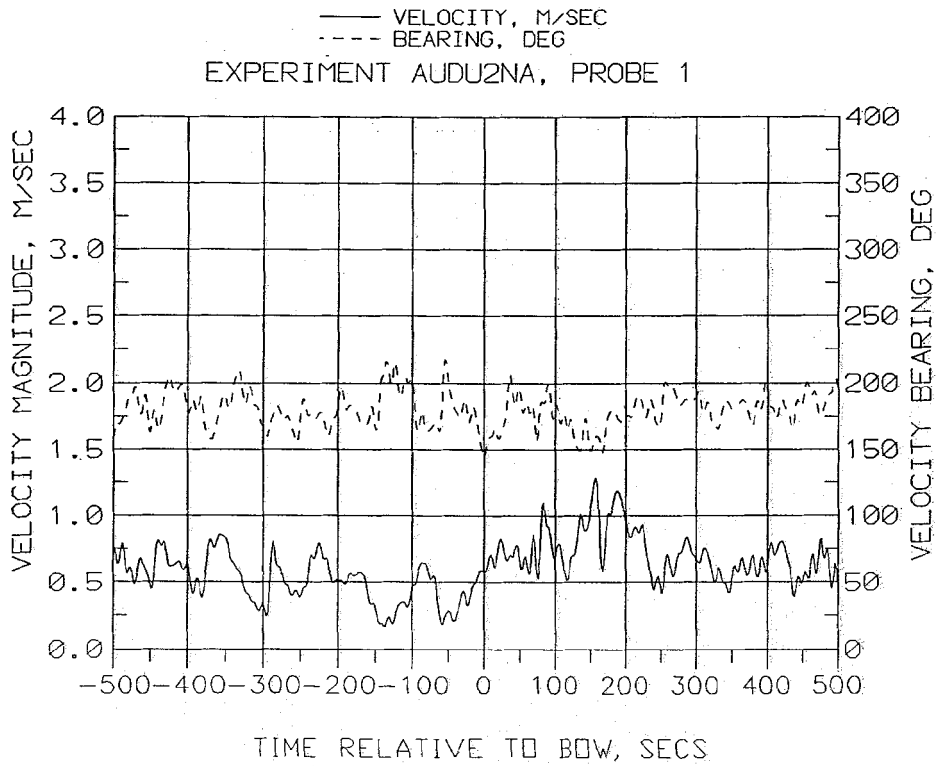
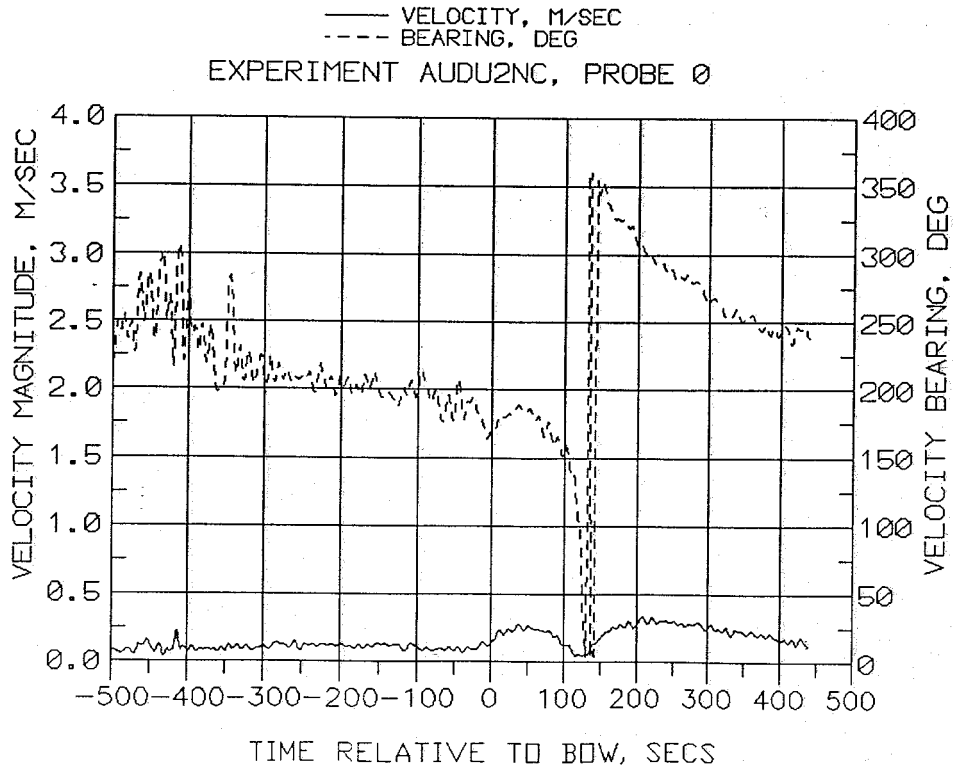
Appendix A

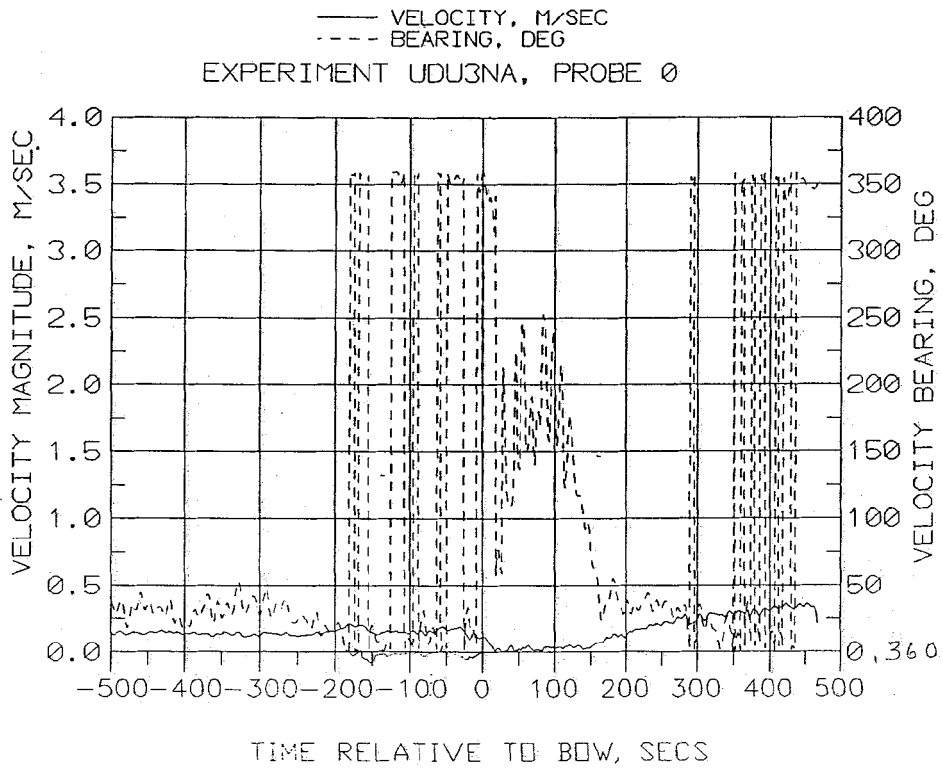
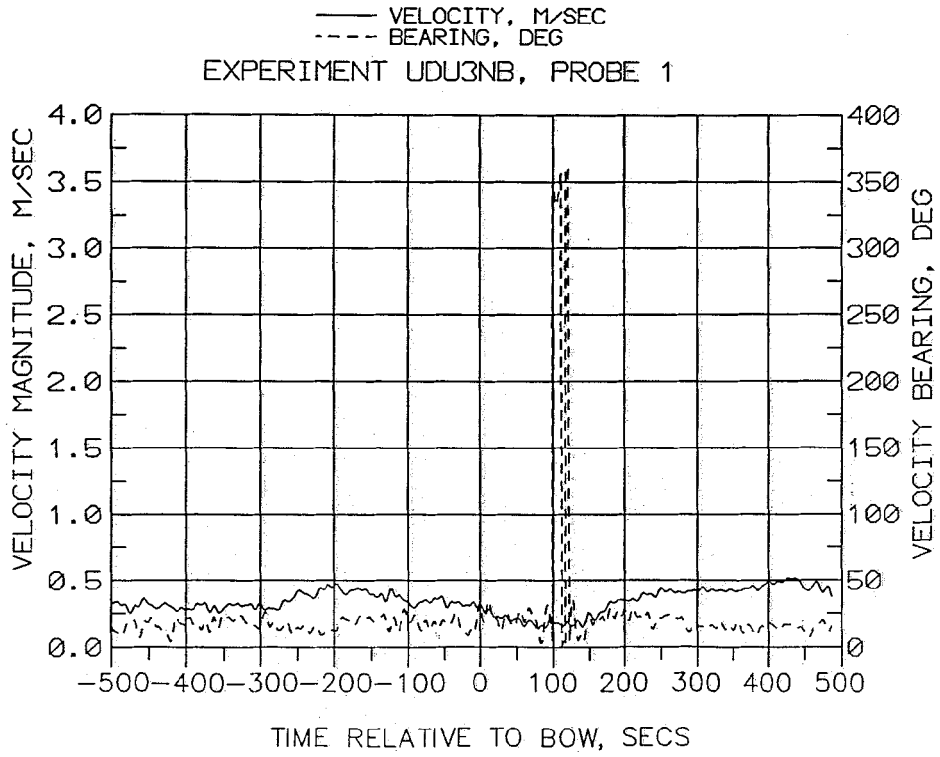
Time-Histories of Velocity for Existing Dike Experiments

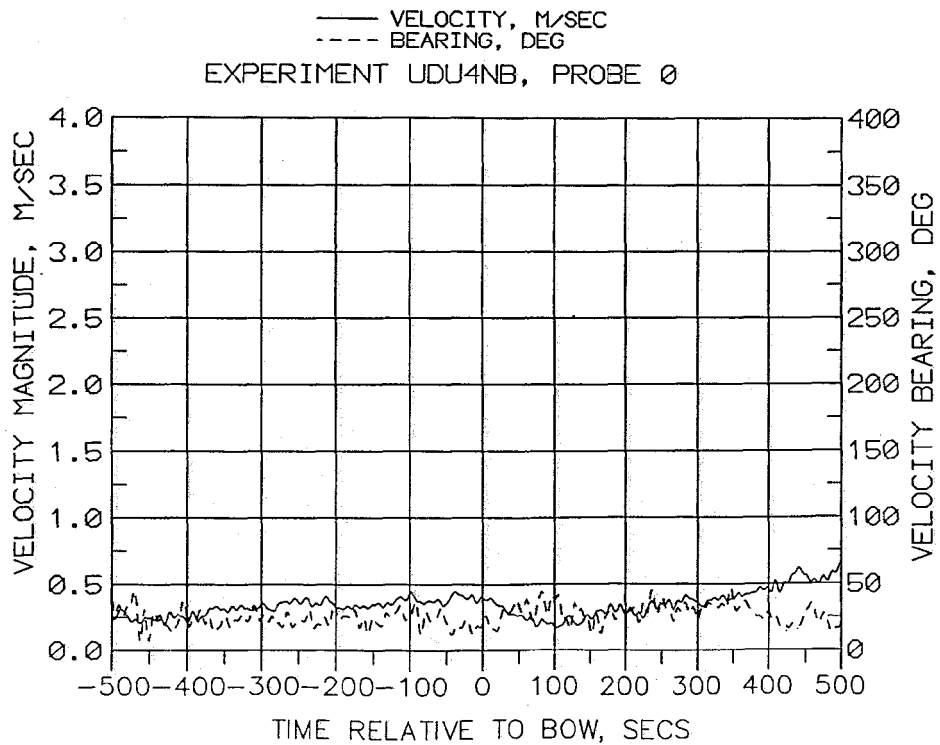
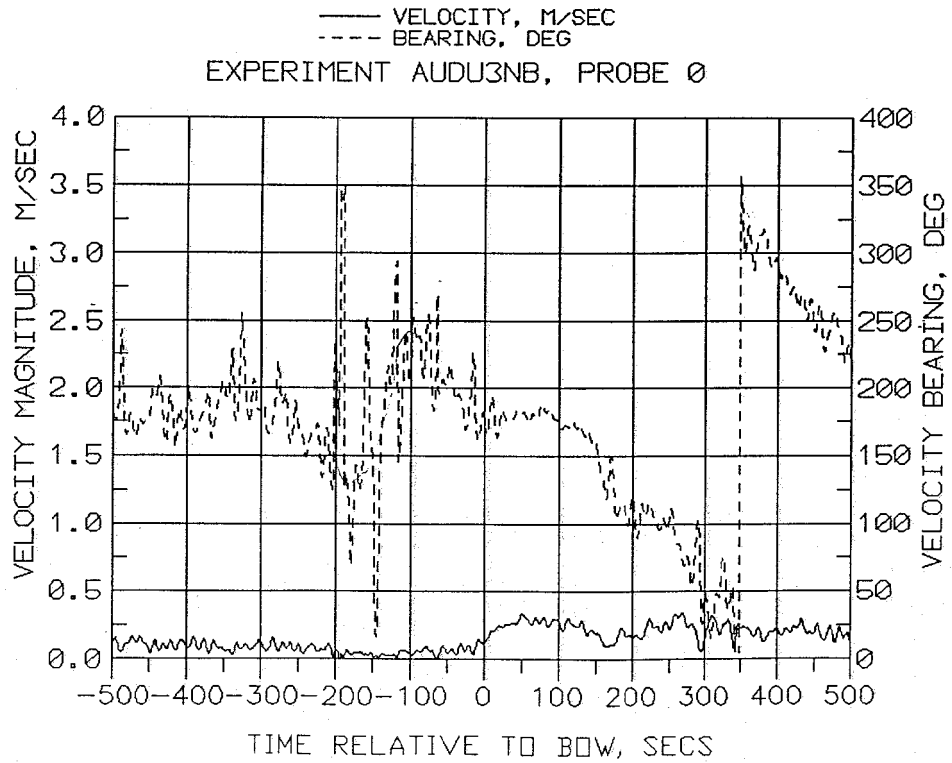


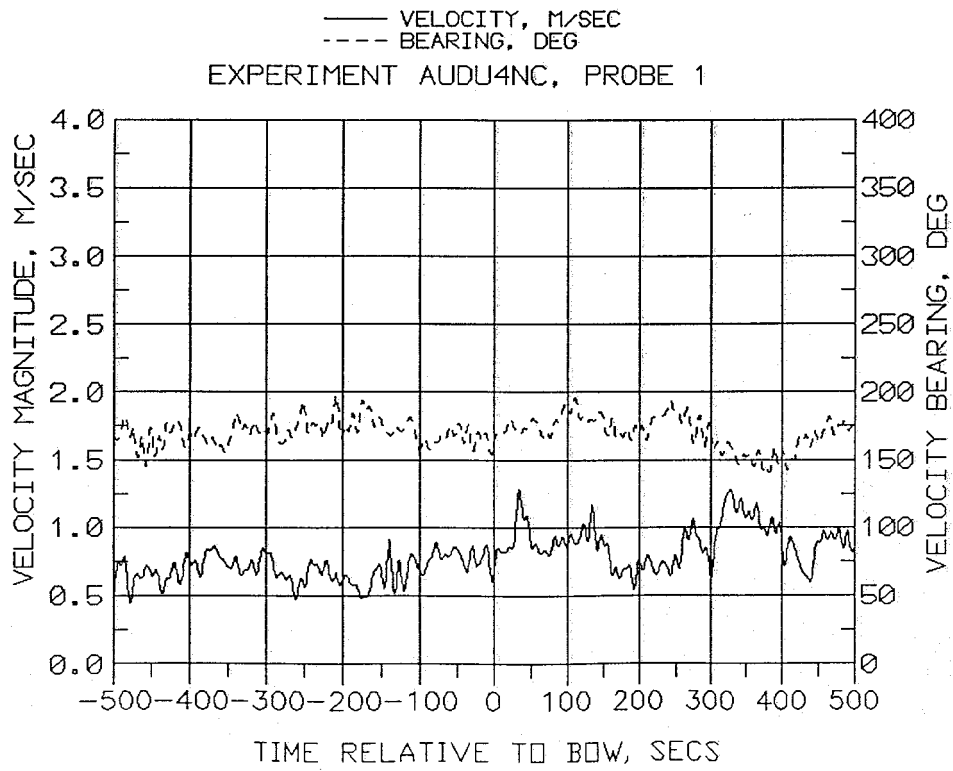
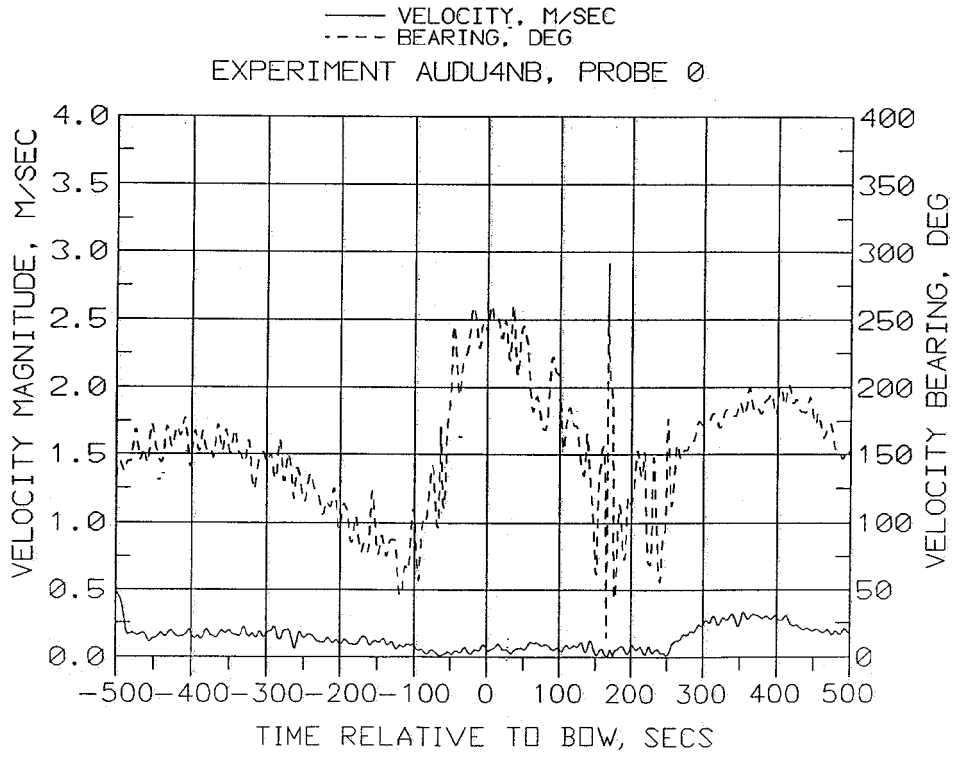


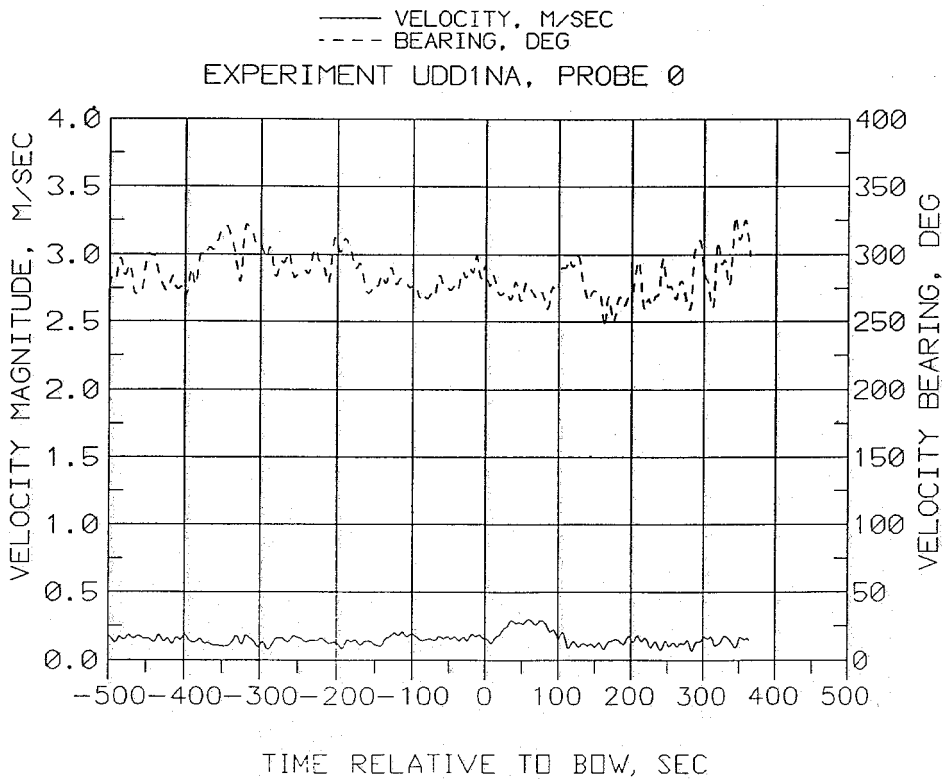
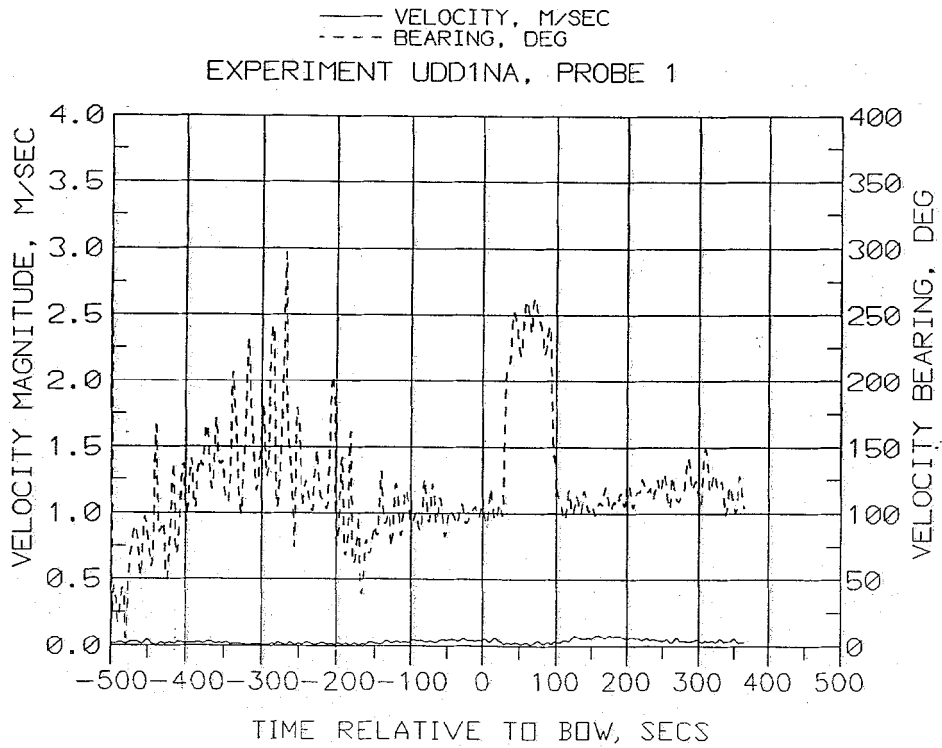


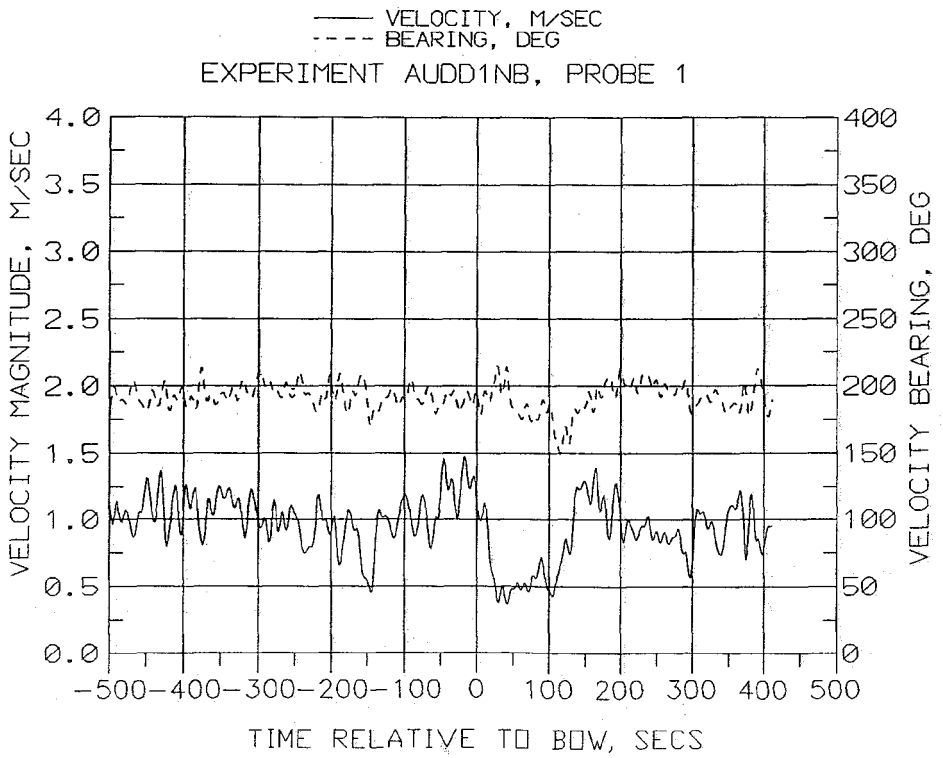
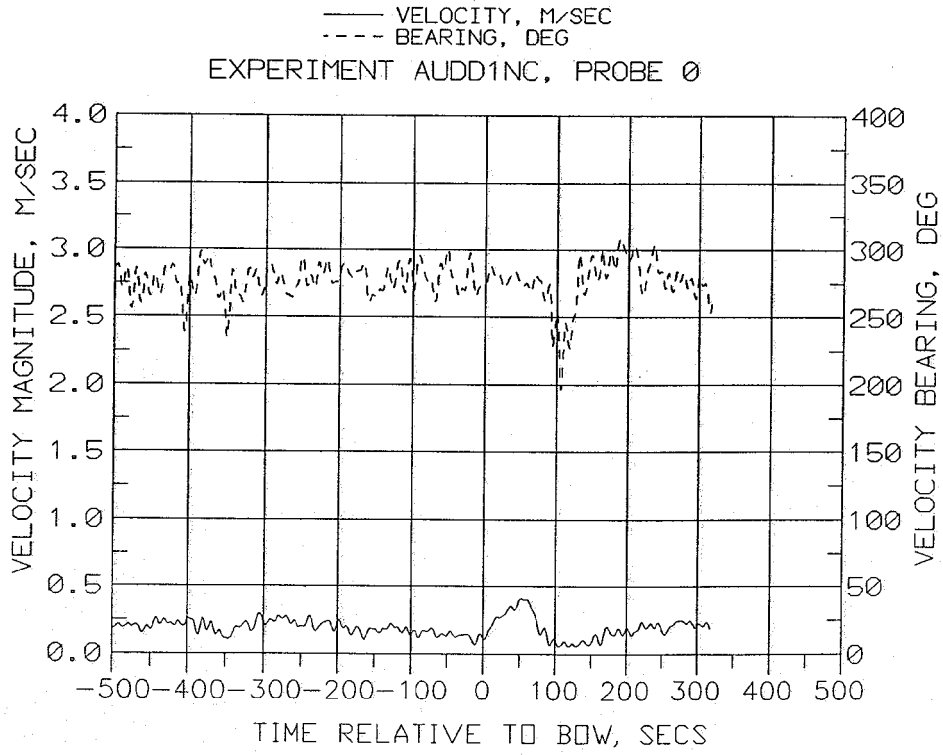


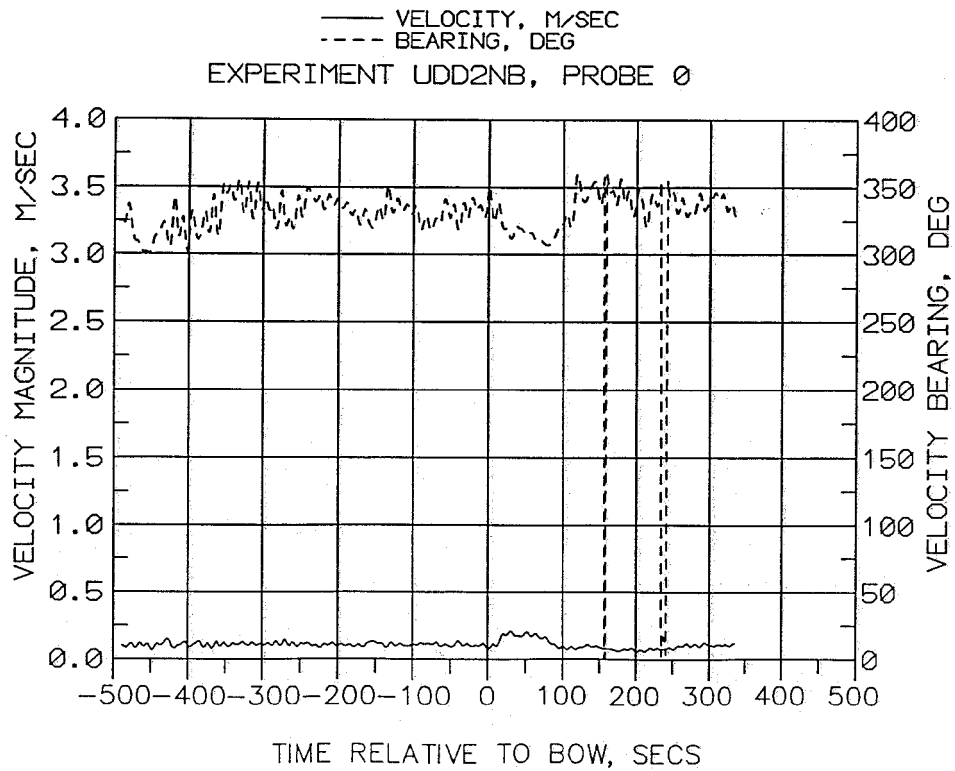
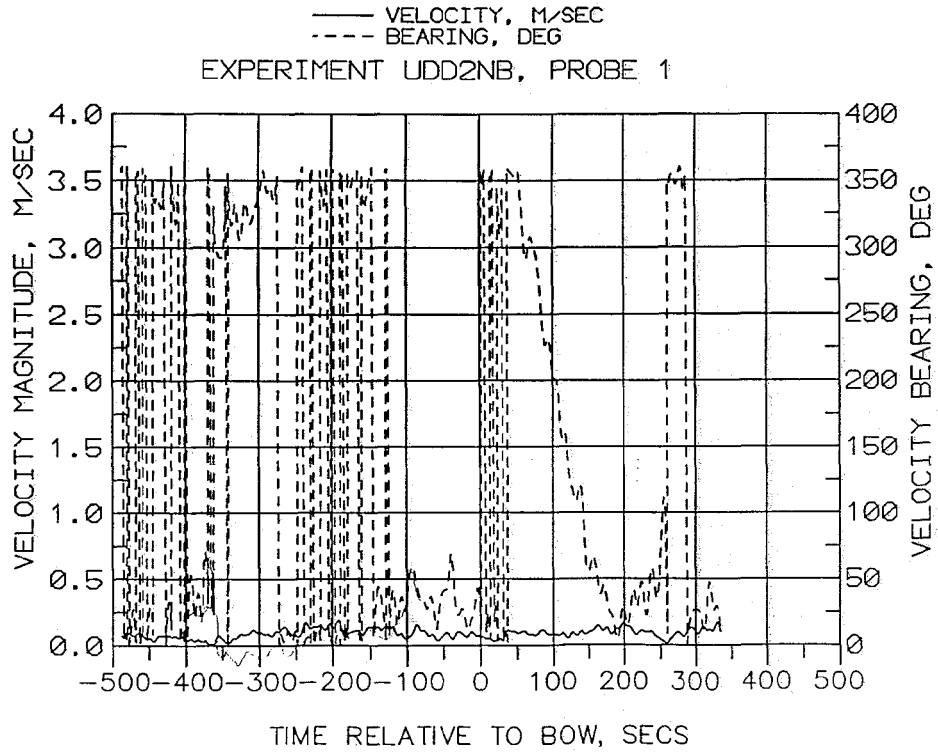


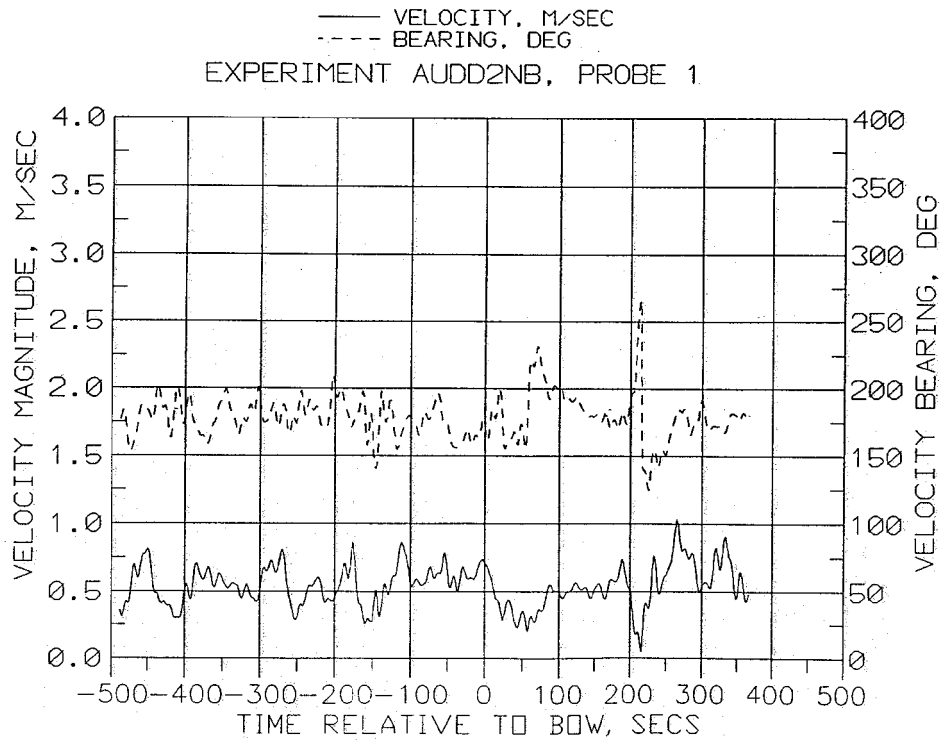
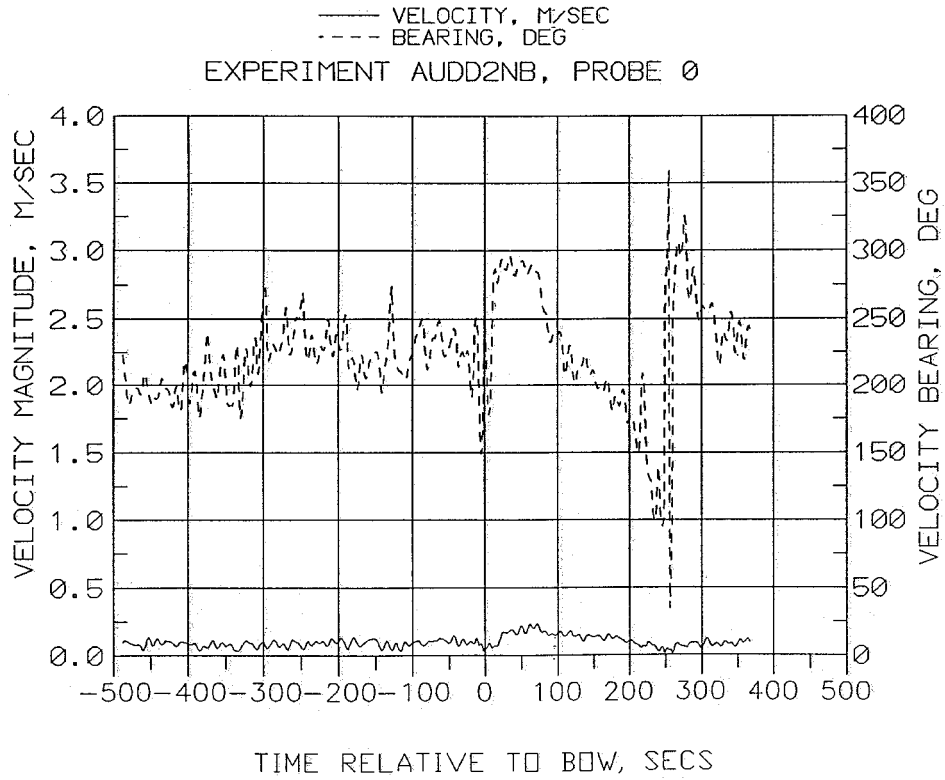


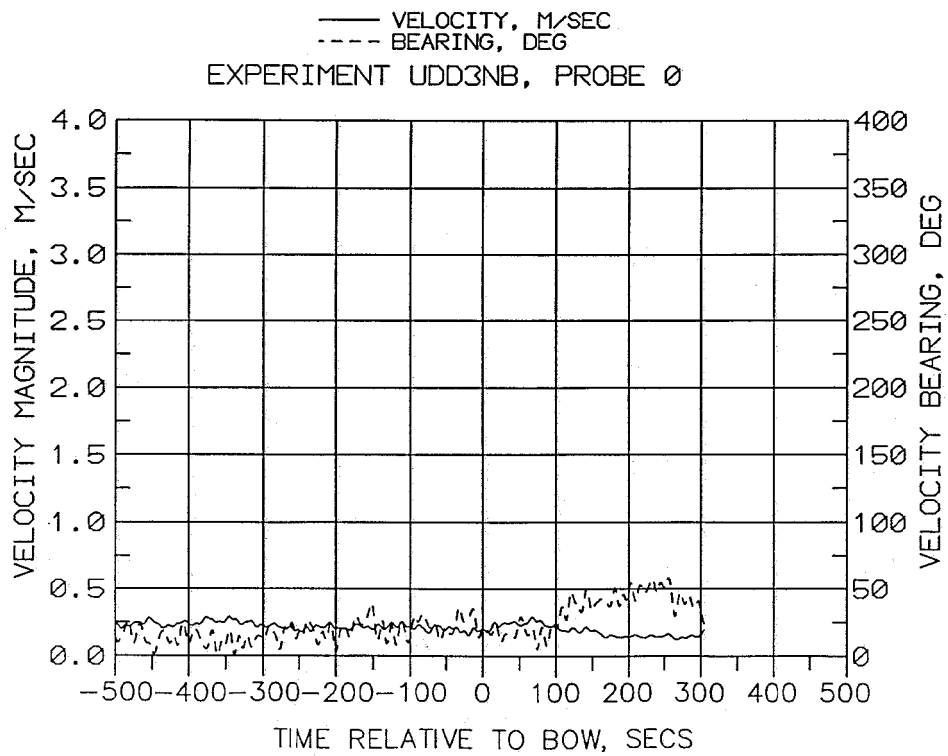
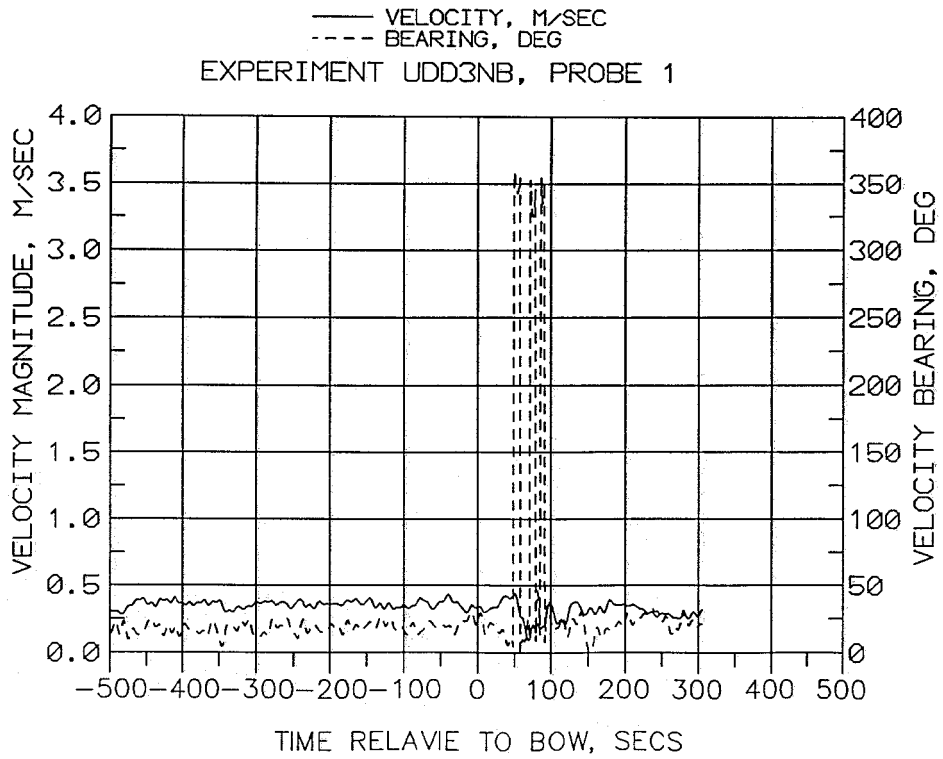


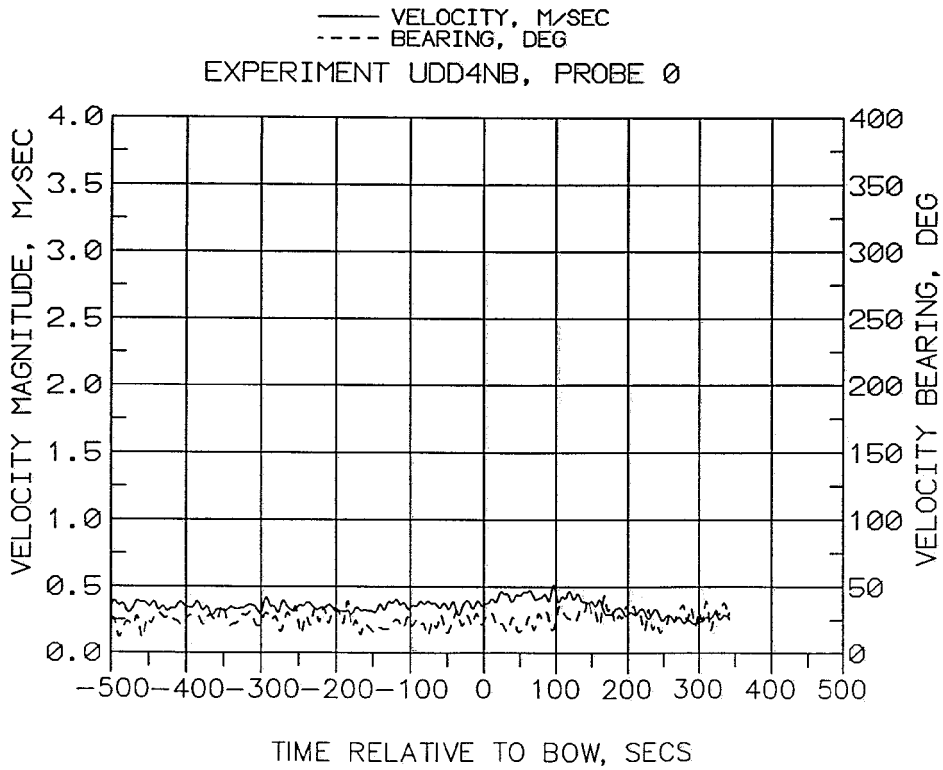
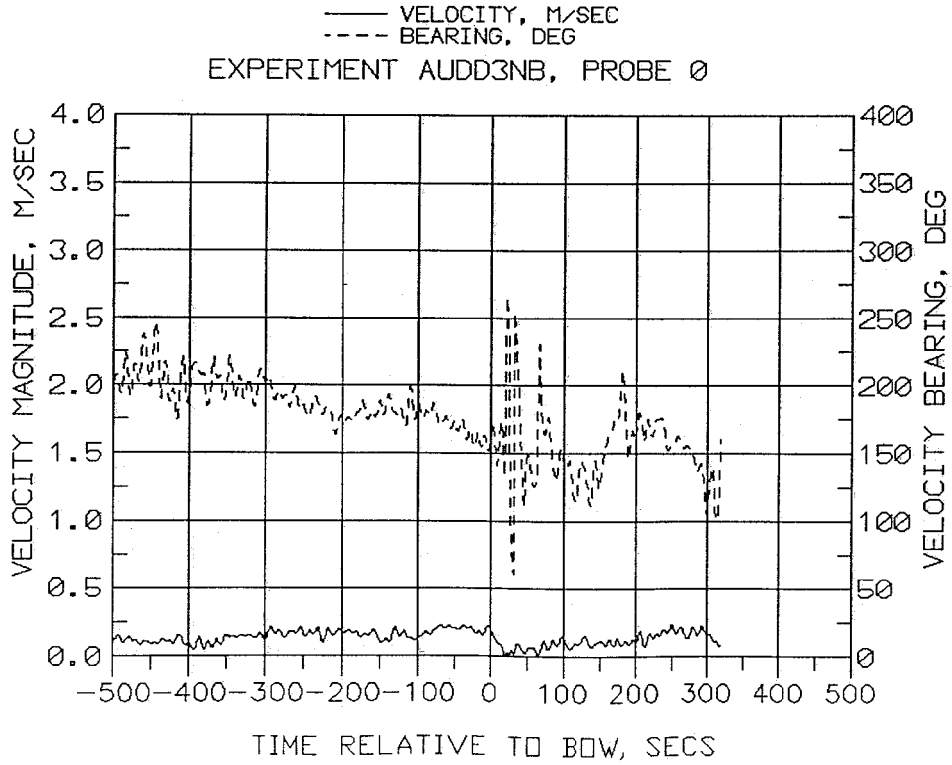




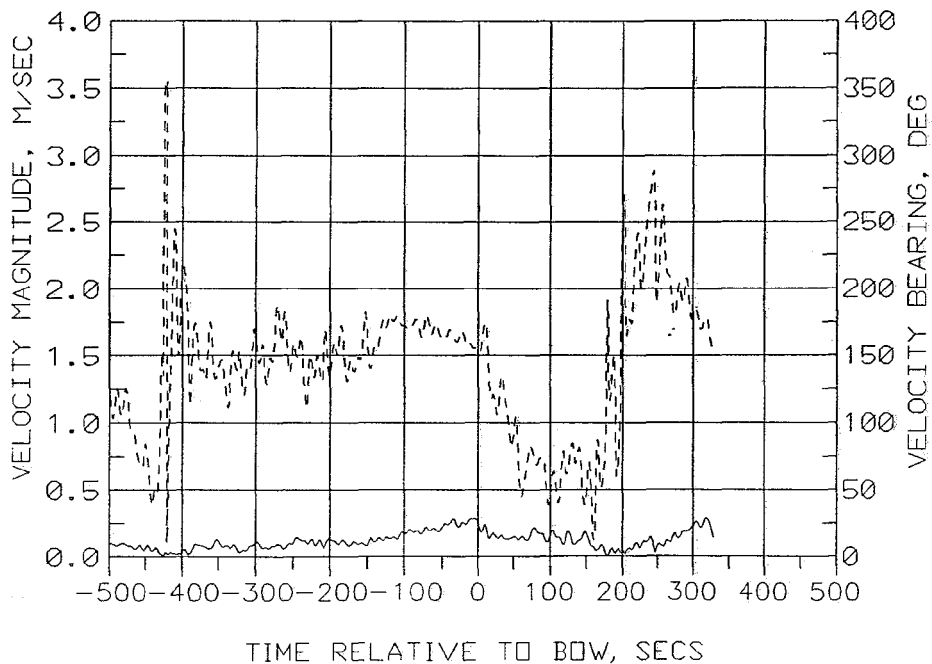




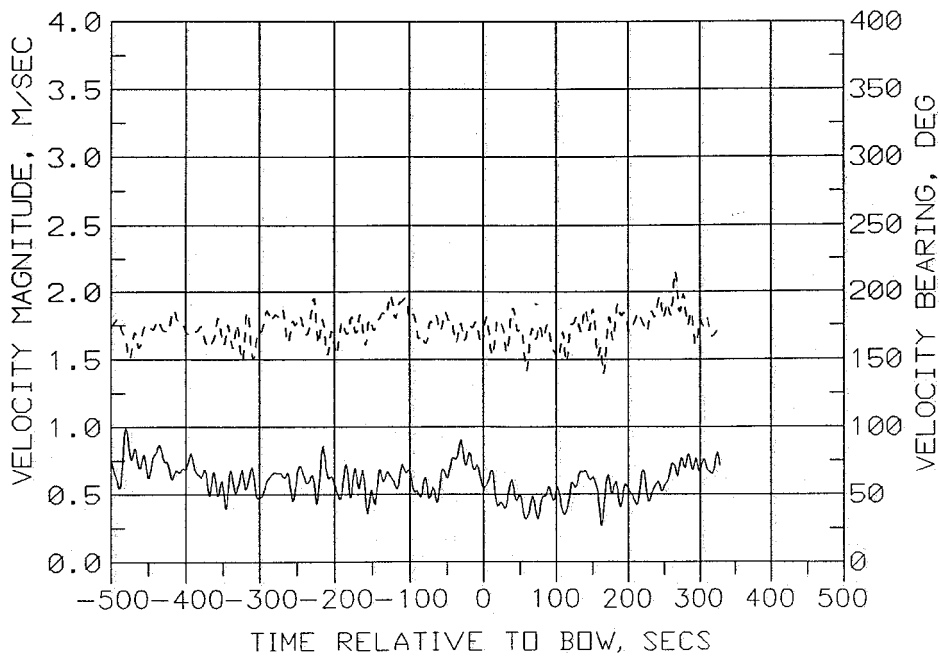


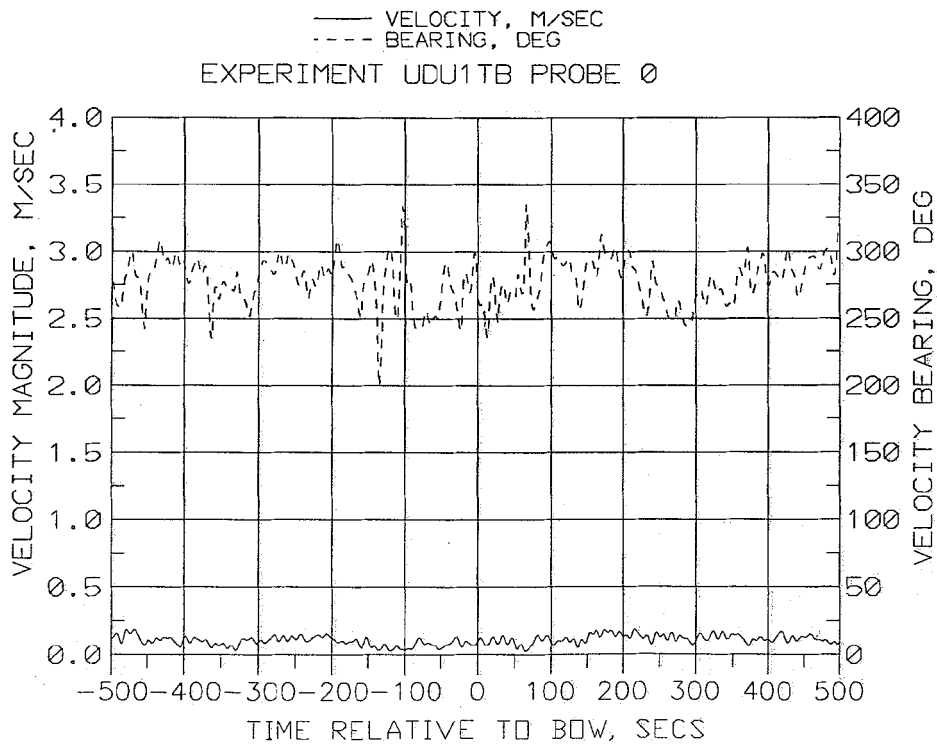
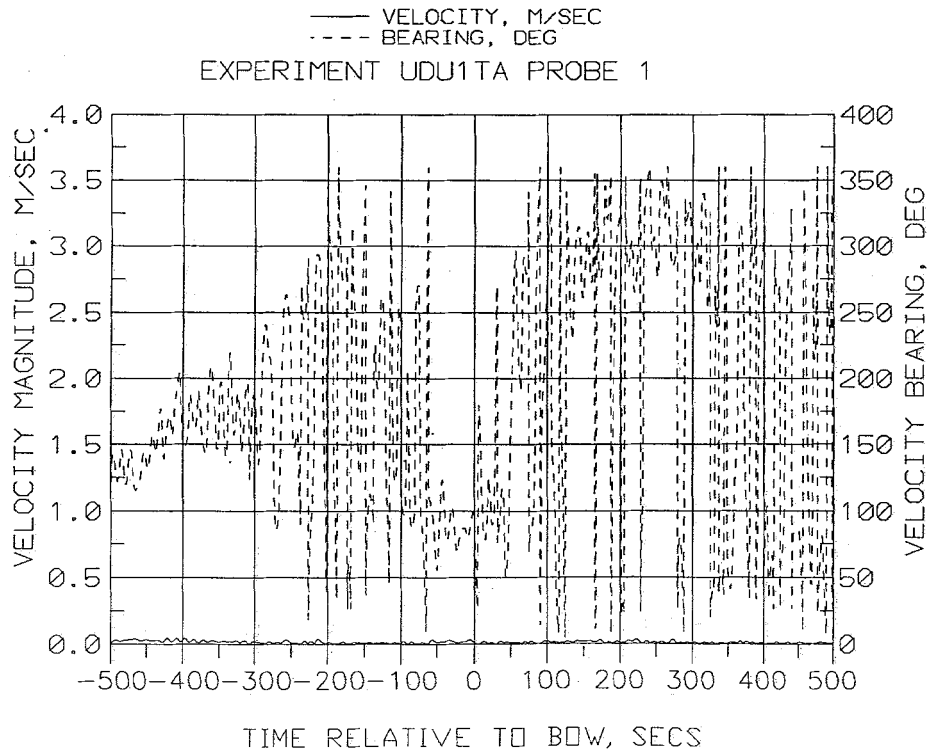


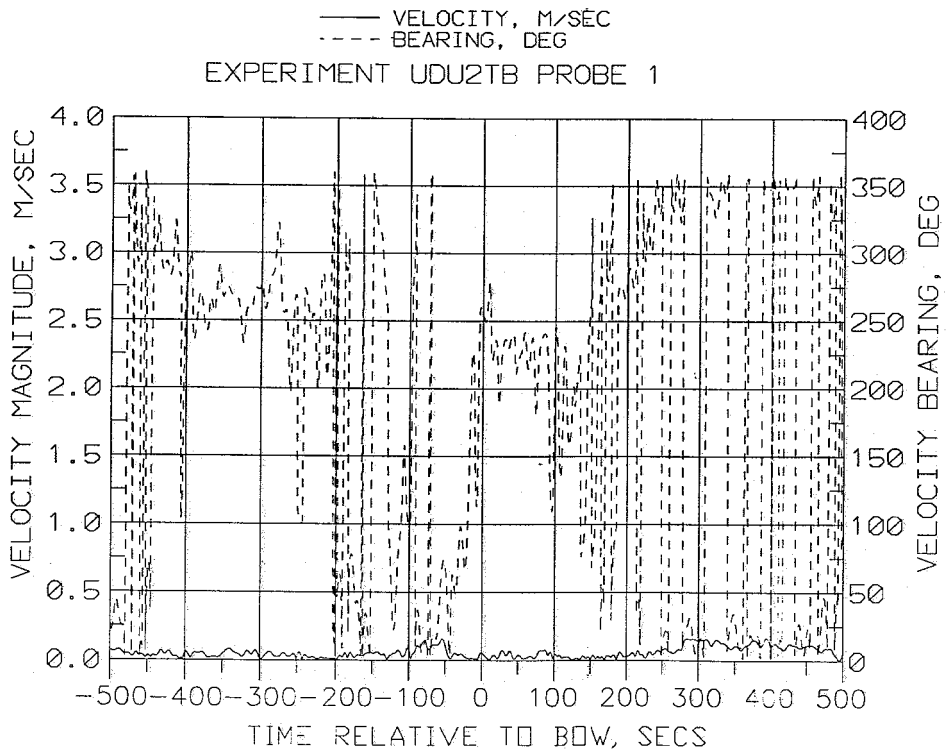
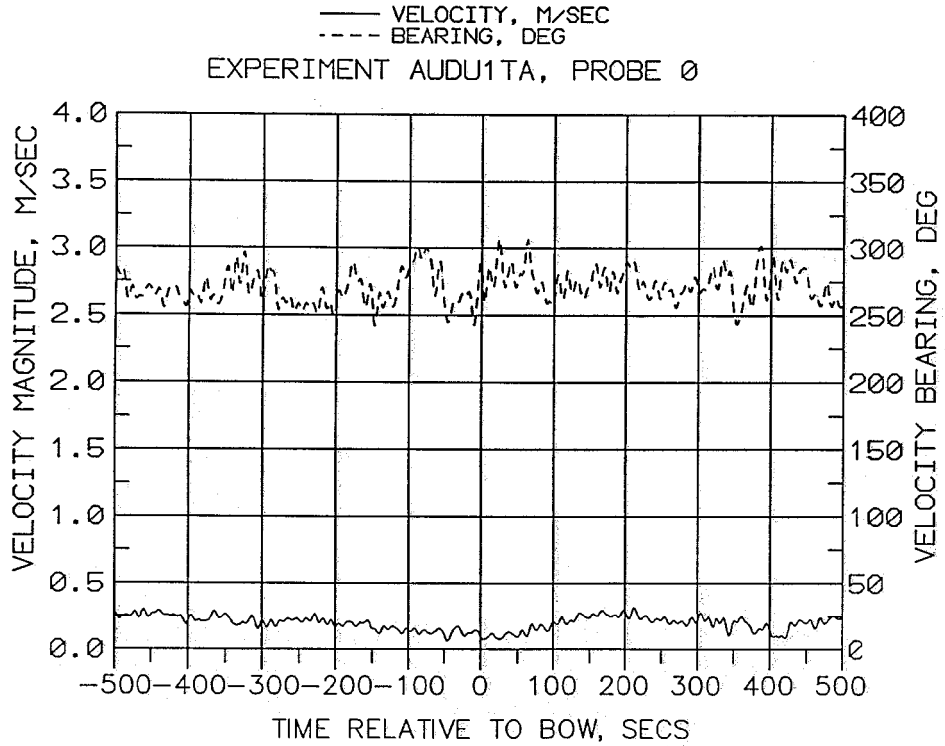
— VELOCITY, M/SEC
- - - BEARING, DEG
EXPERIMENT AUDD4NB, PROBE 0

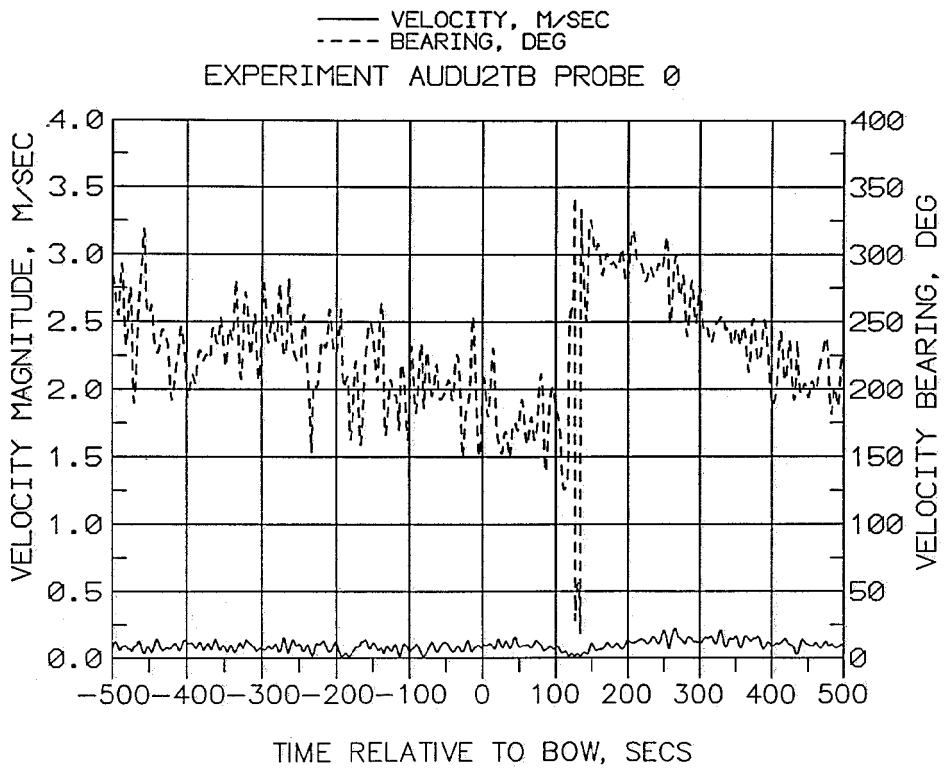
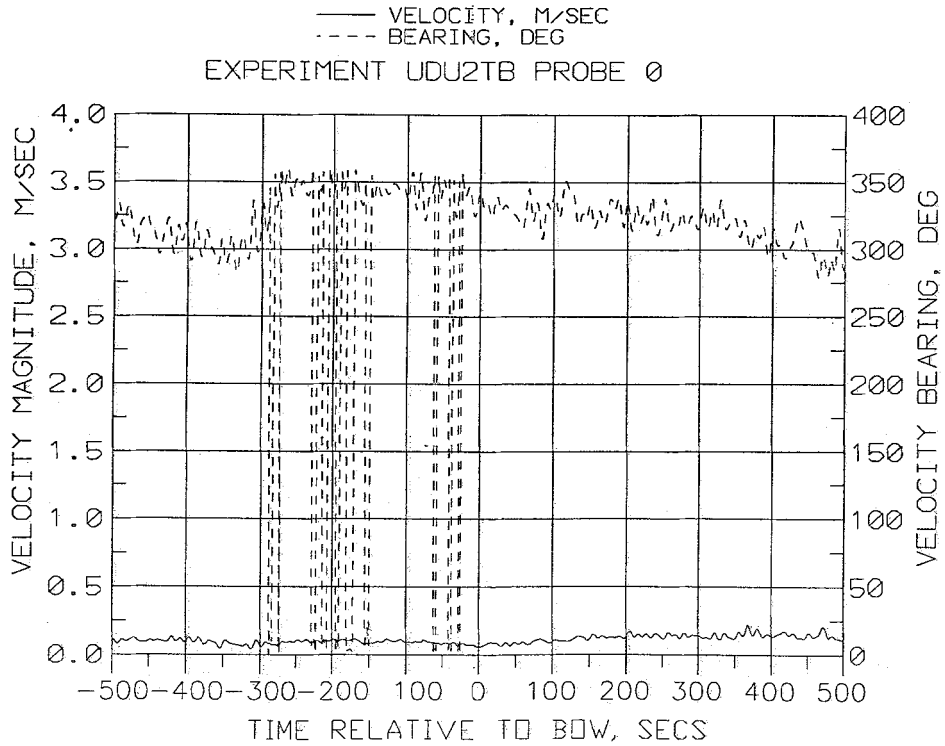


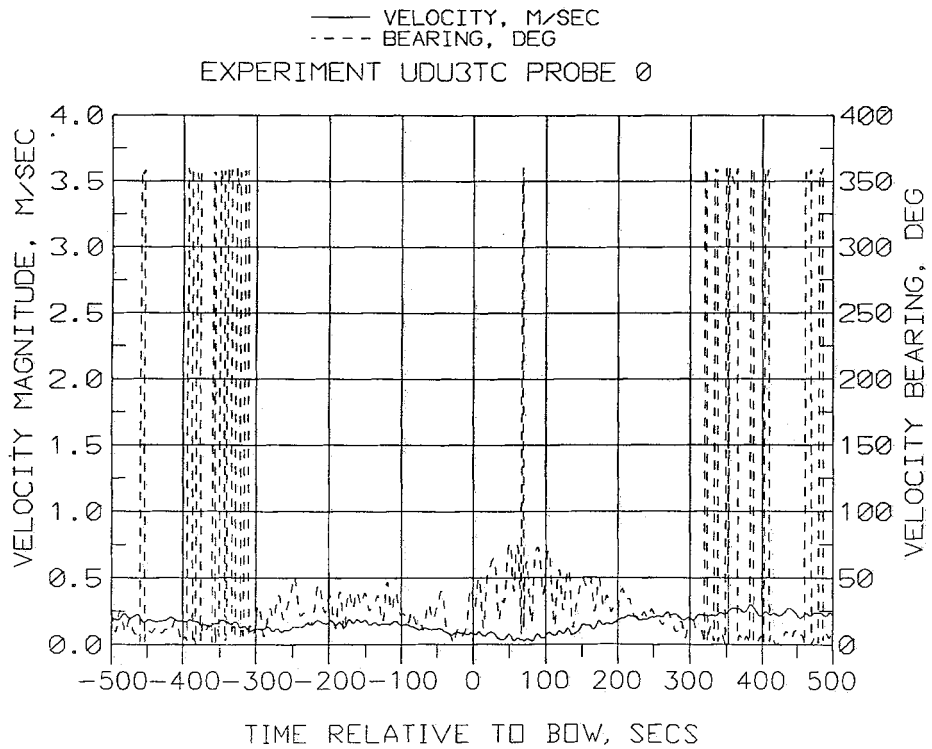
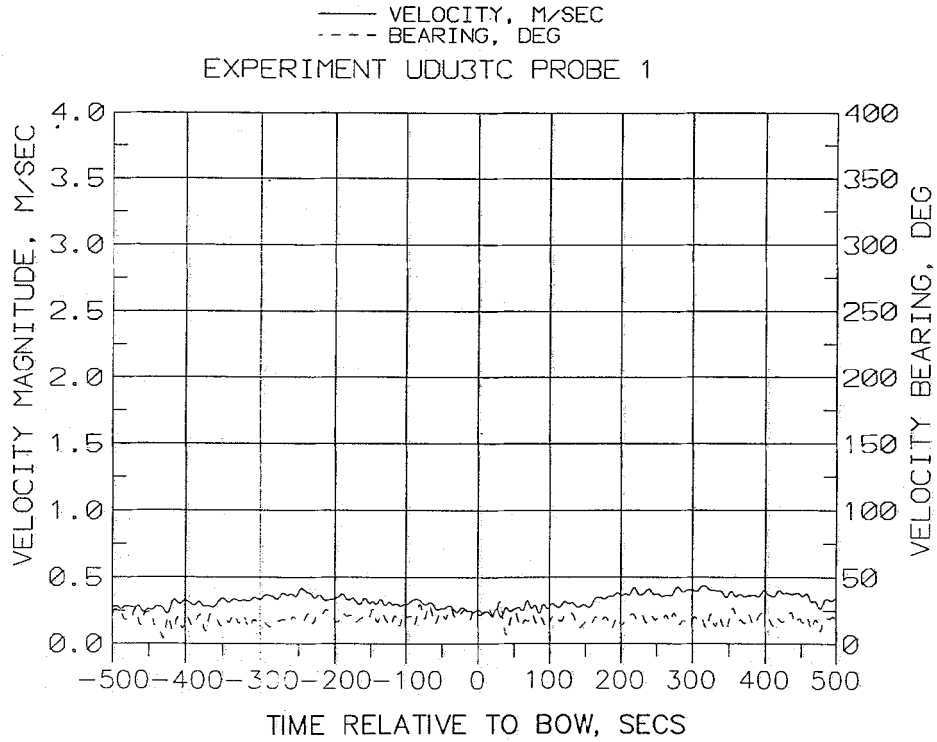
— VELOCITY, M/SEC
- - - BEARING, DEG
EXPERIMENT AUDD4NB, PROBE 1

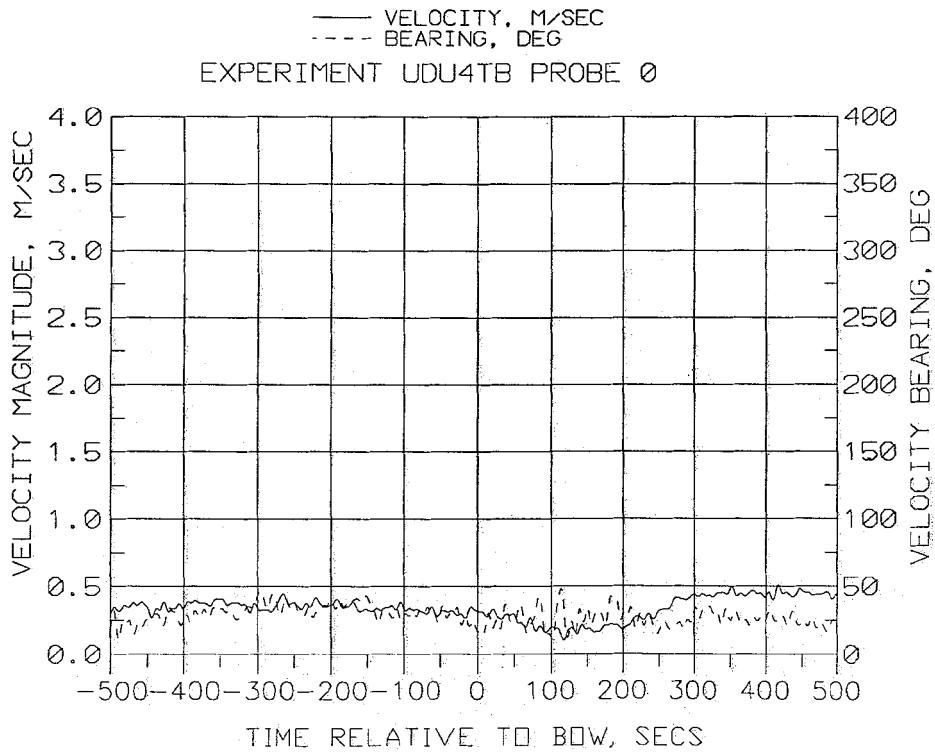
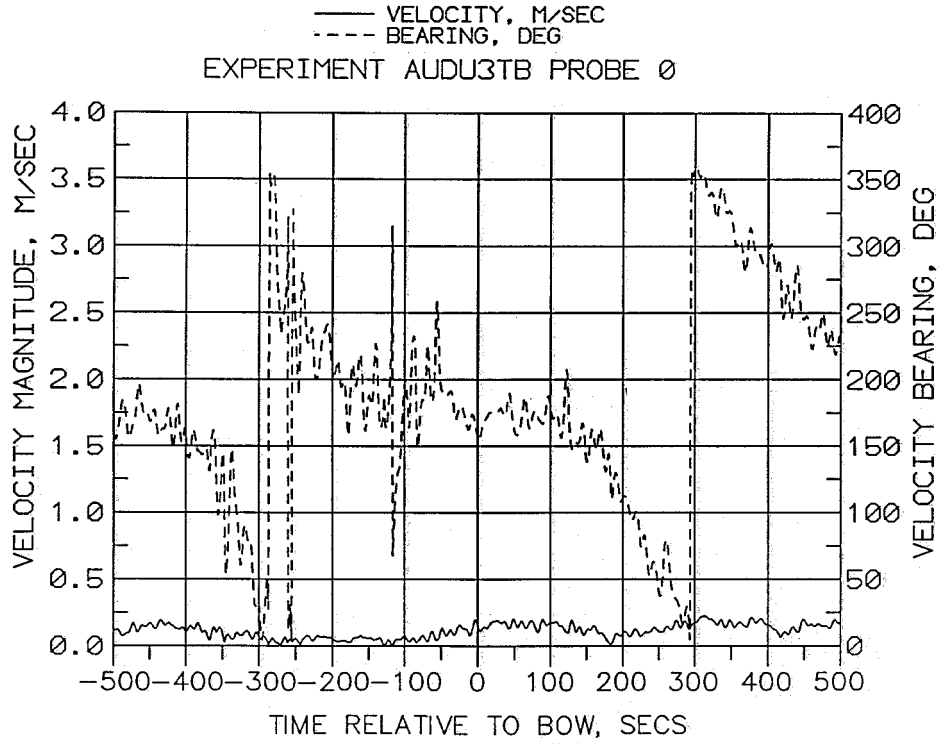


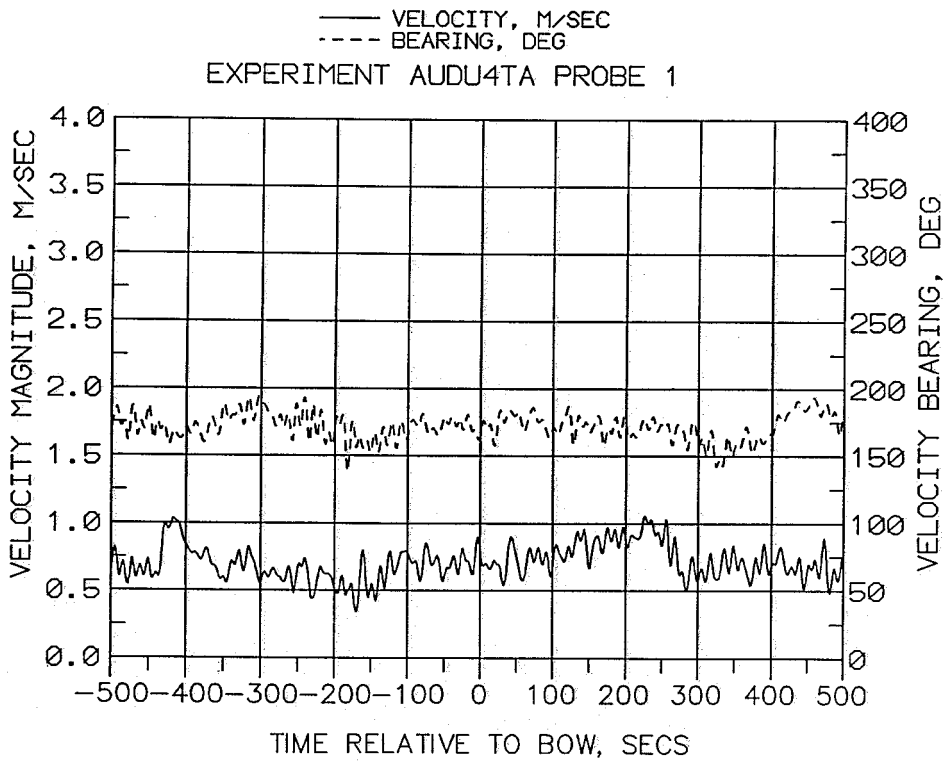
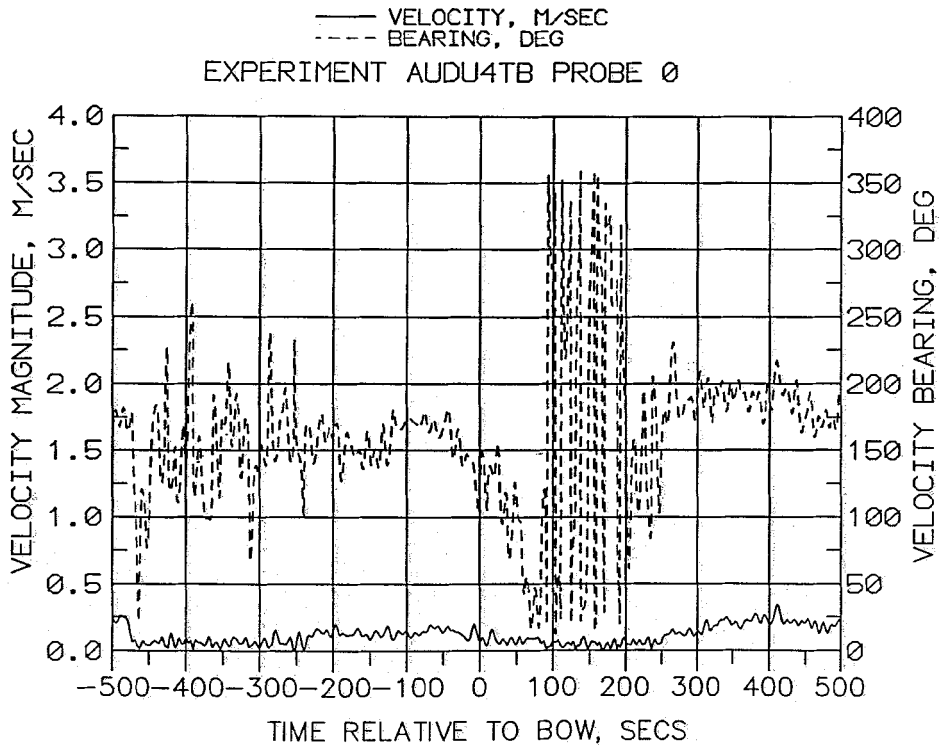


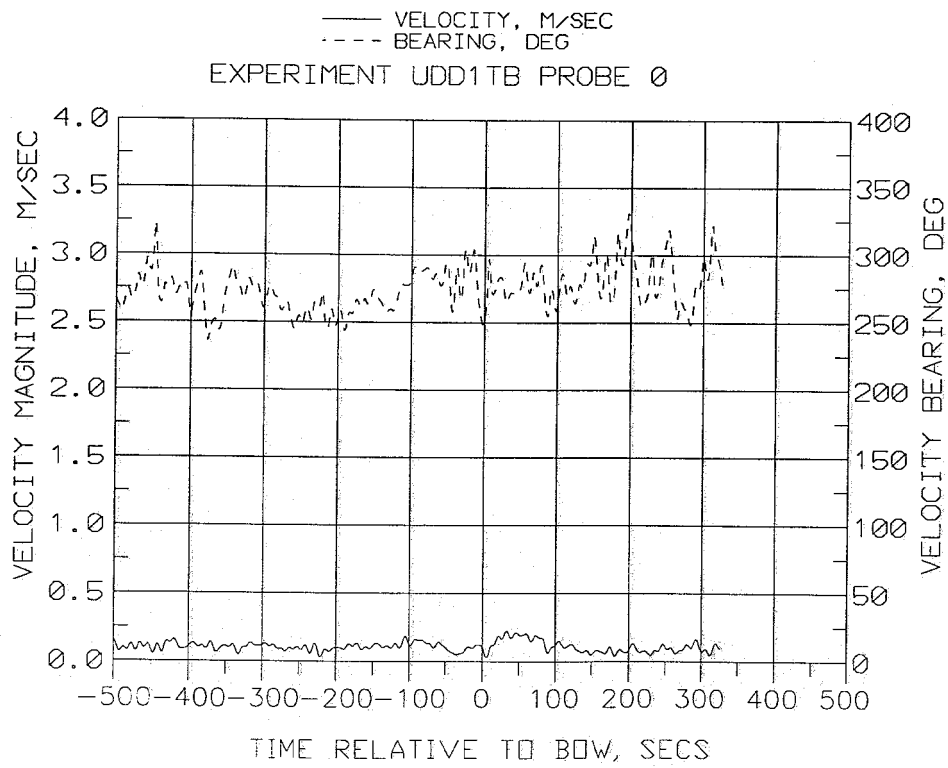
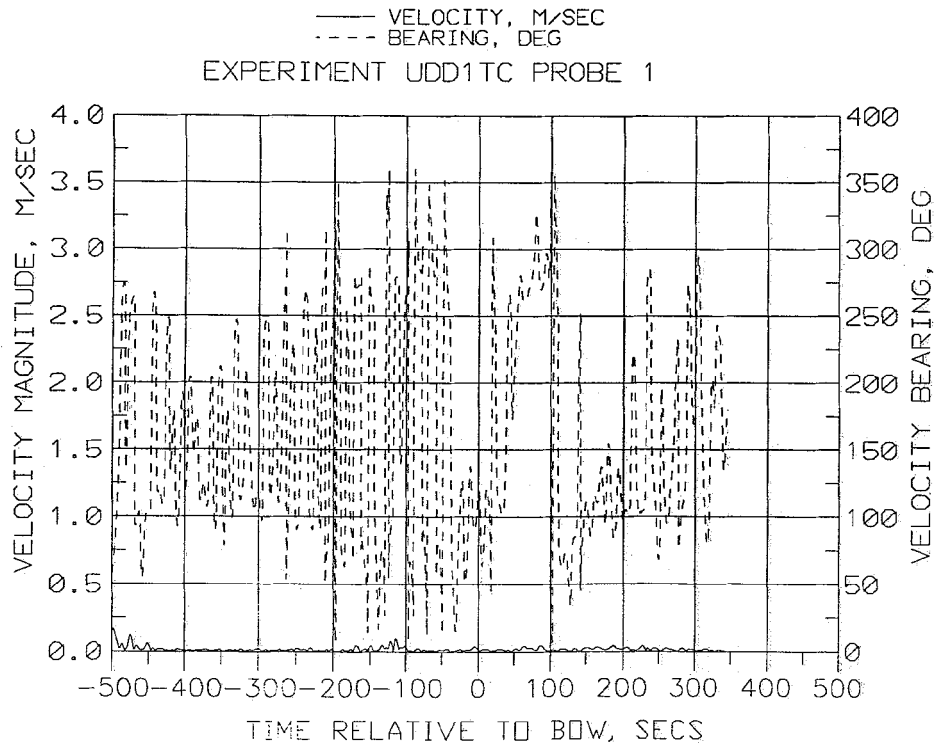


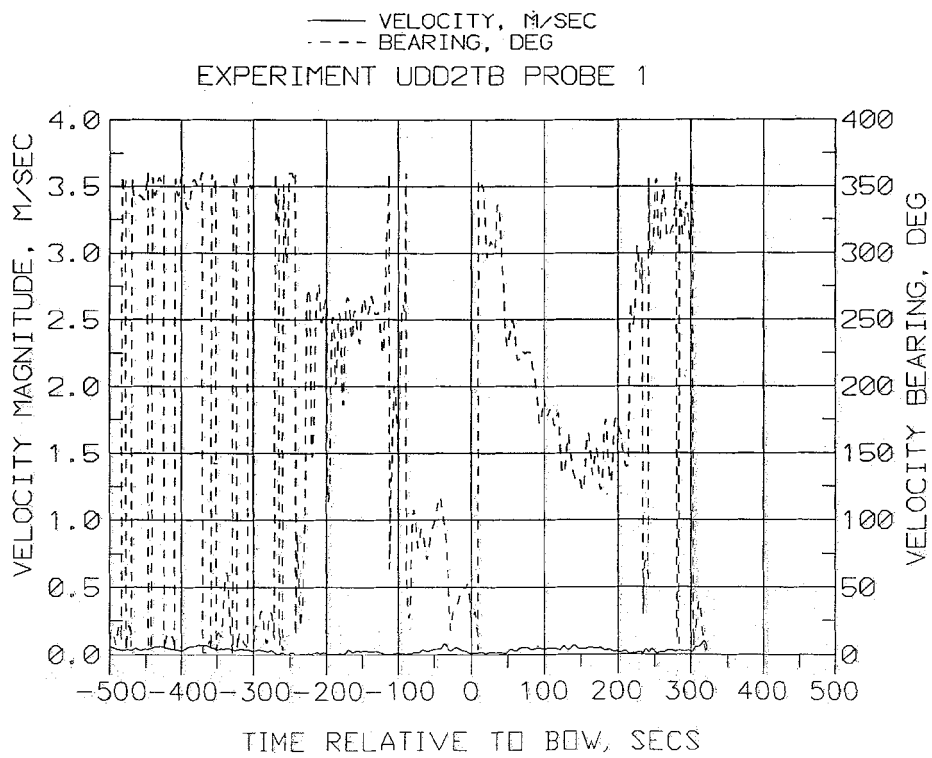
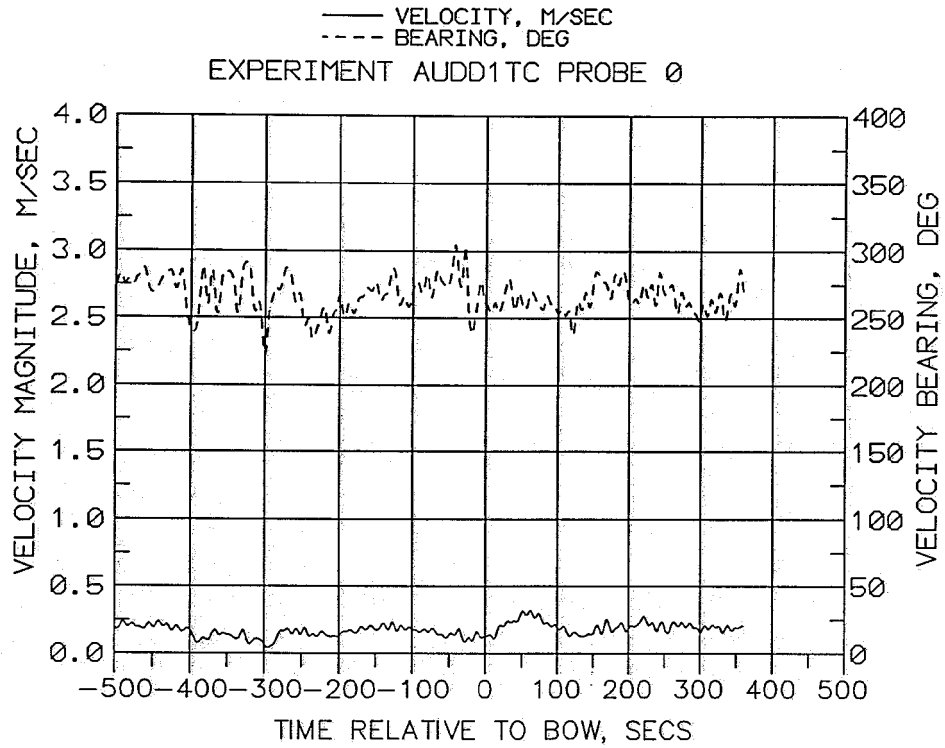


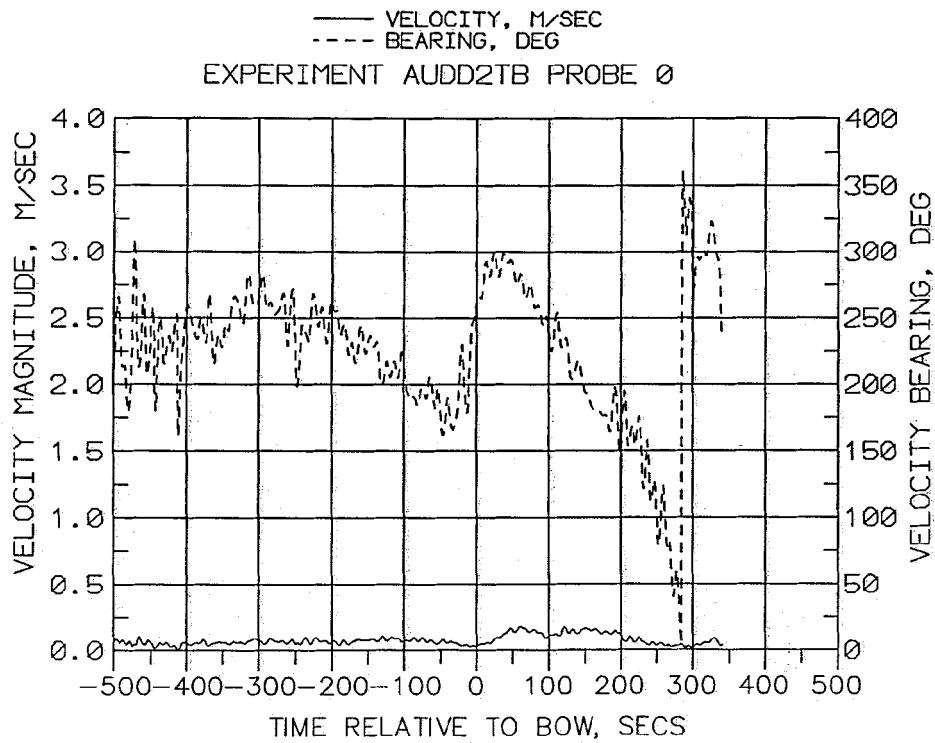
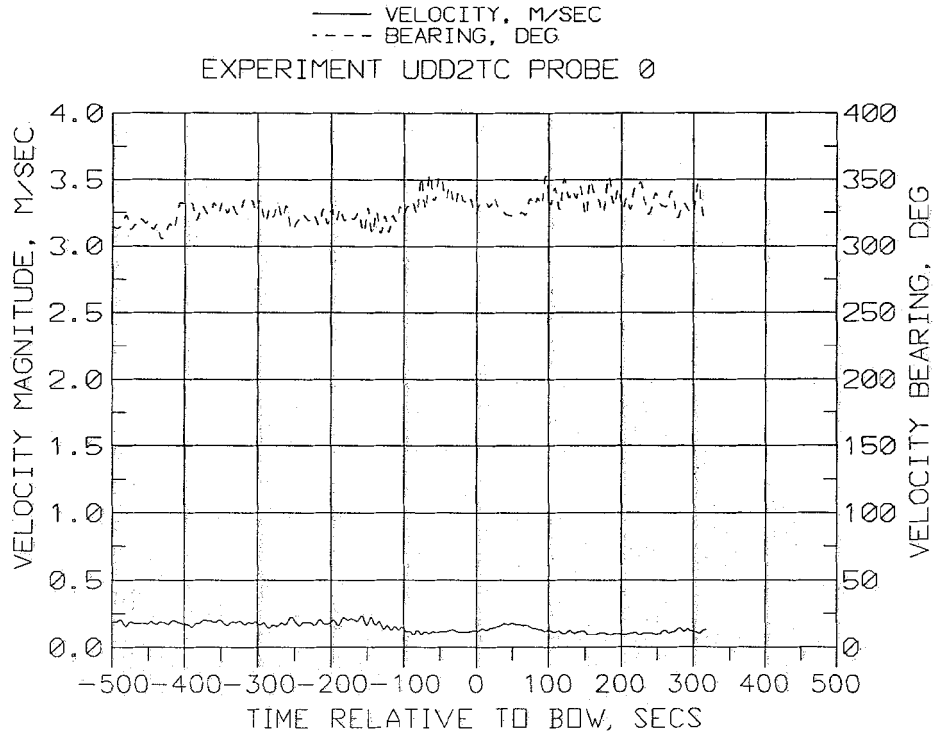


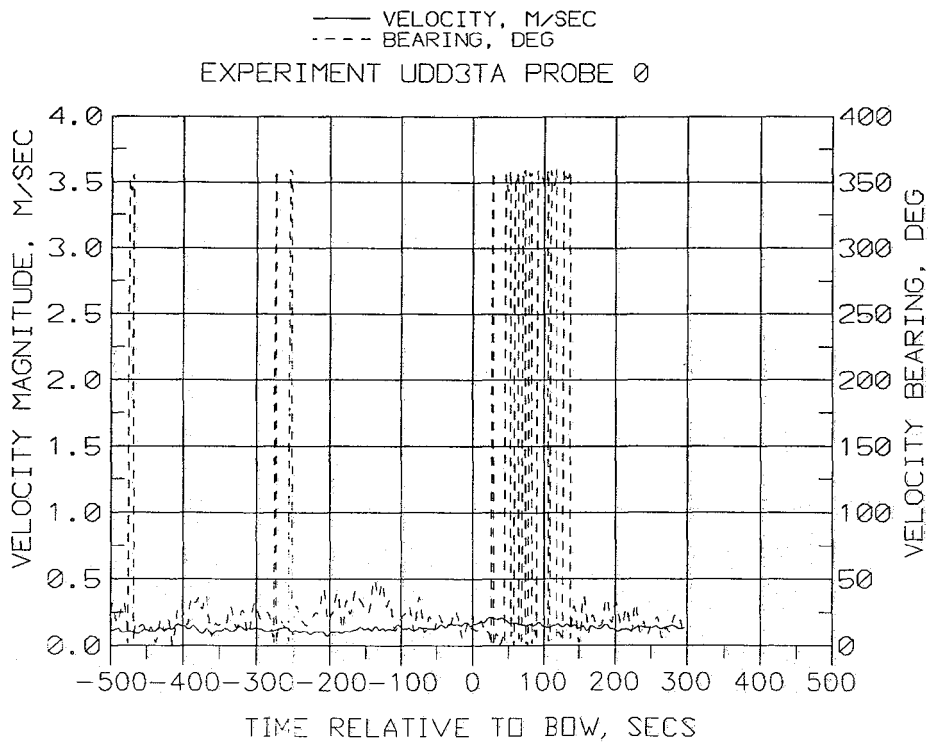
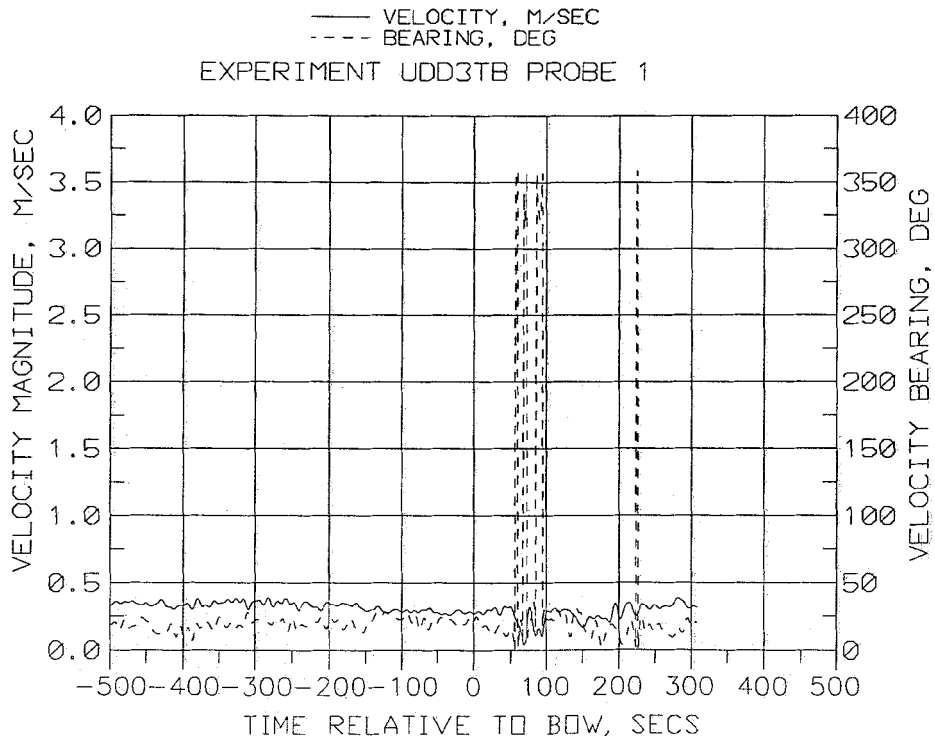


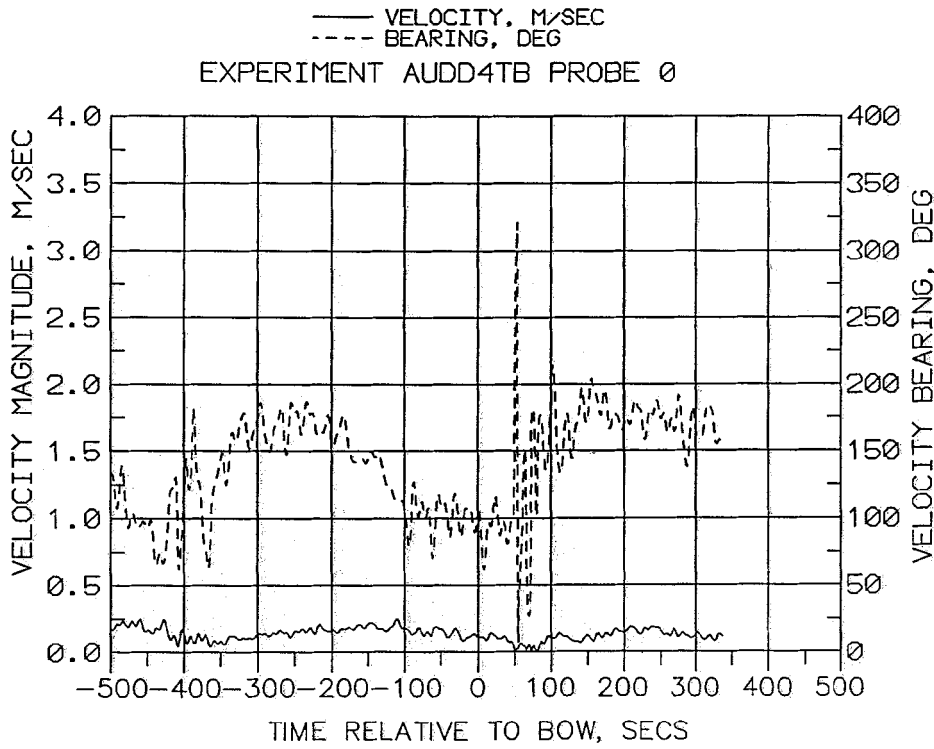
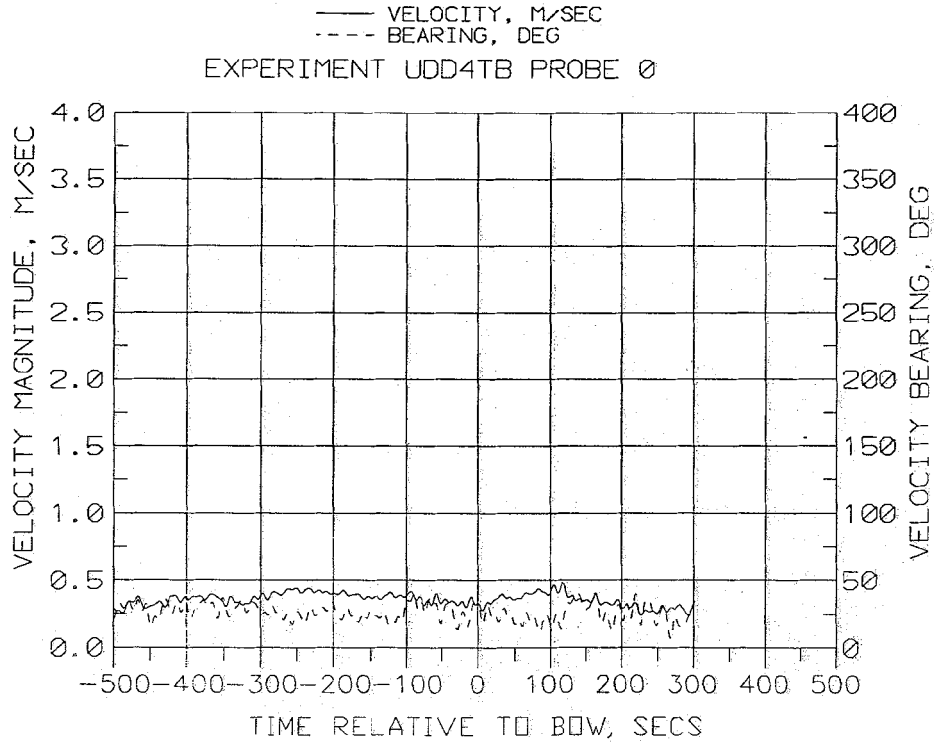




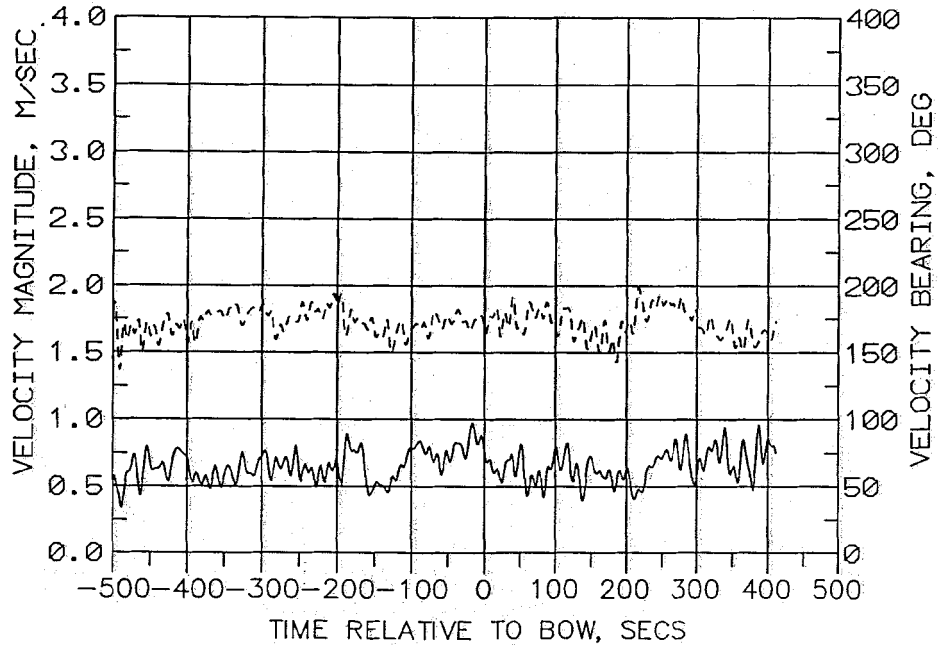






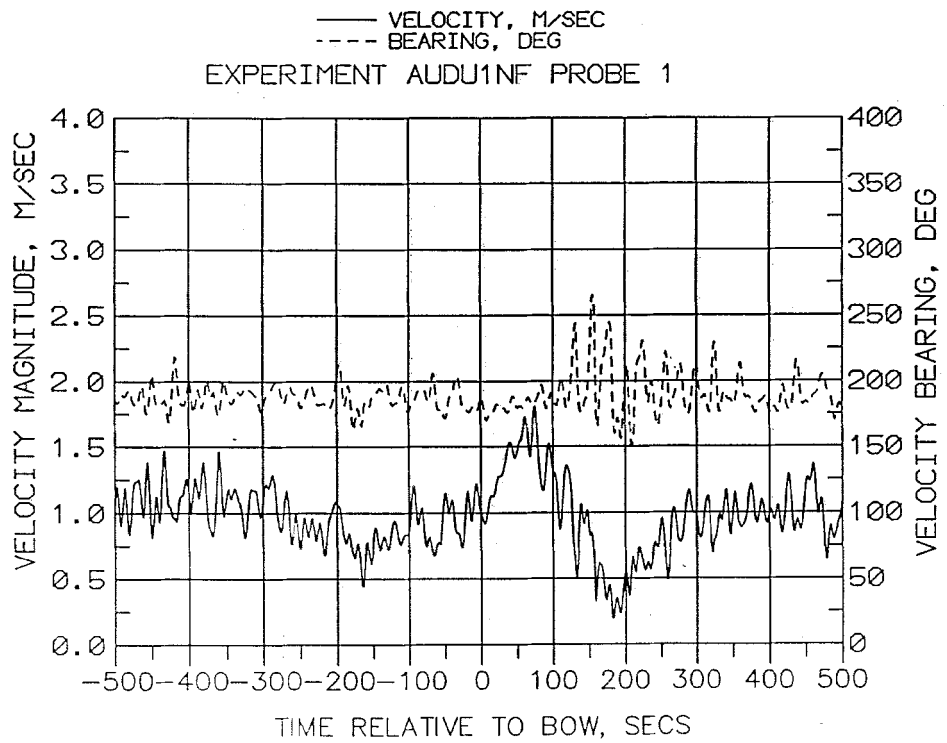
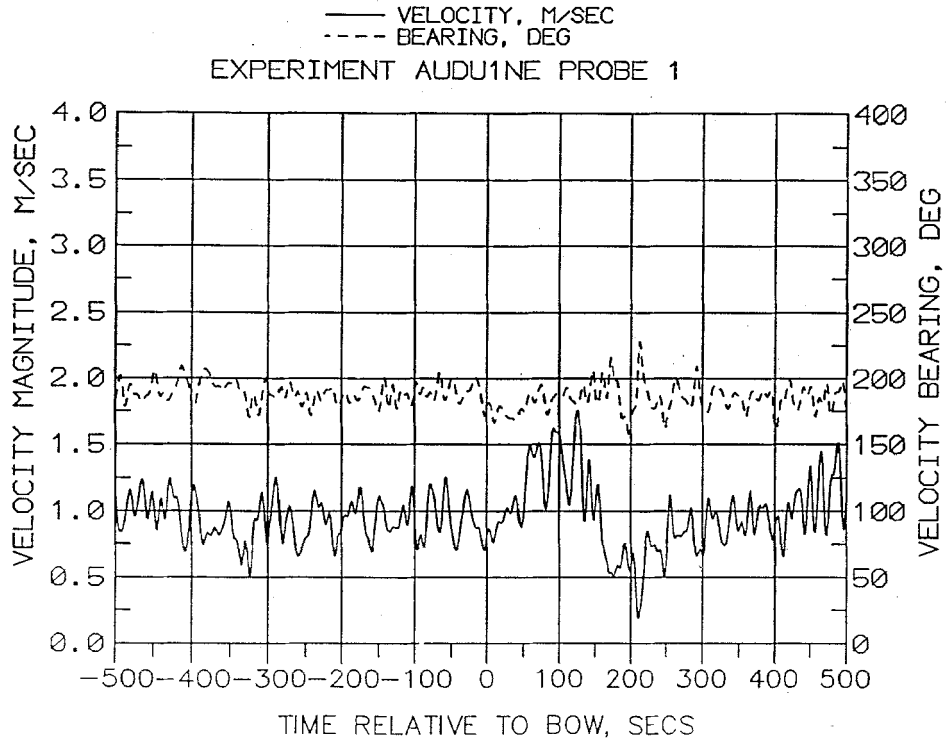


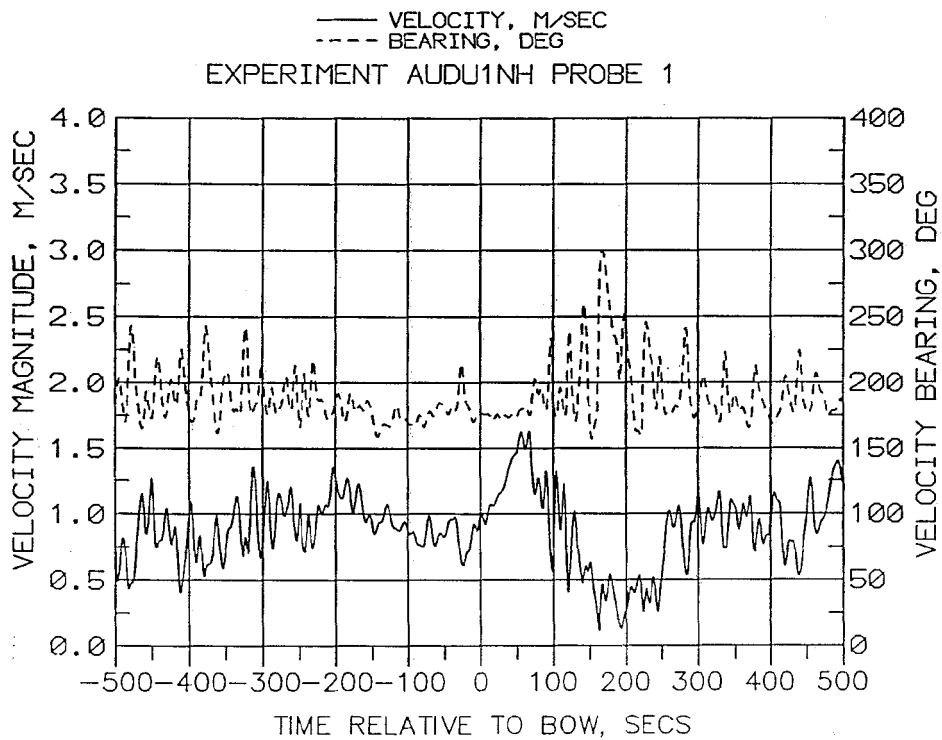
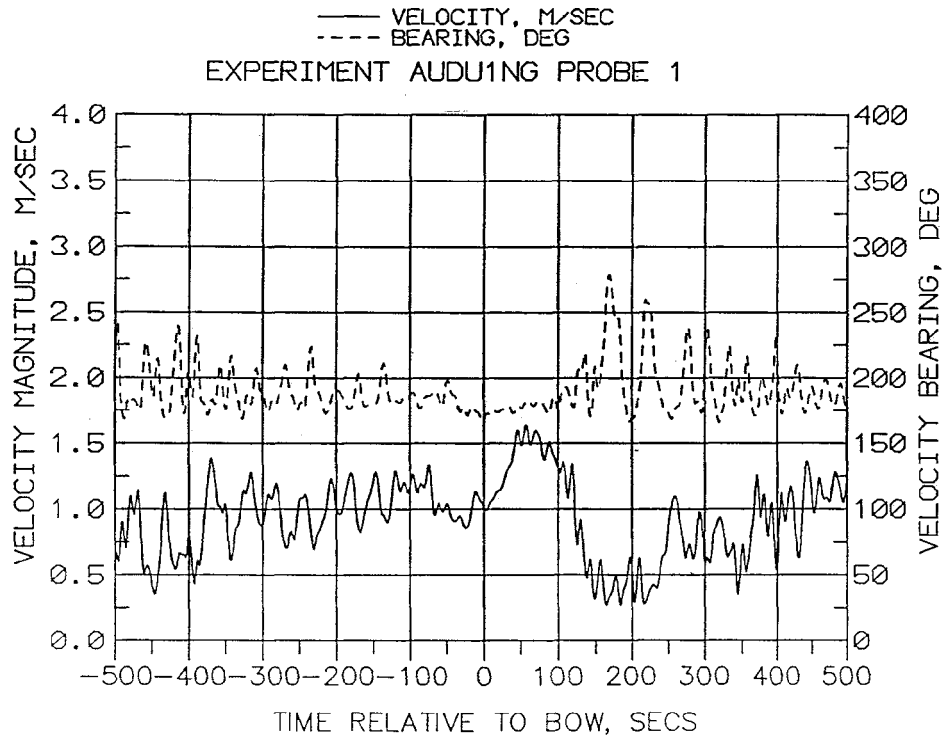
— VELOCITY, M/SEC
- - - BEARING, DEG
EXPERIMENT AUDD4TA PROBE 1



Appendix B

Time-Histories of Velocity for Vertical Velocity Profile Experiments

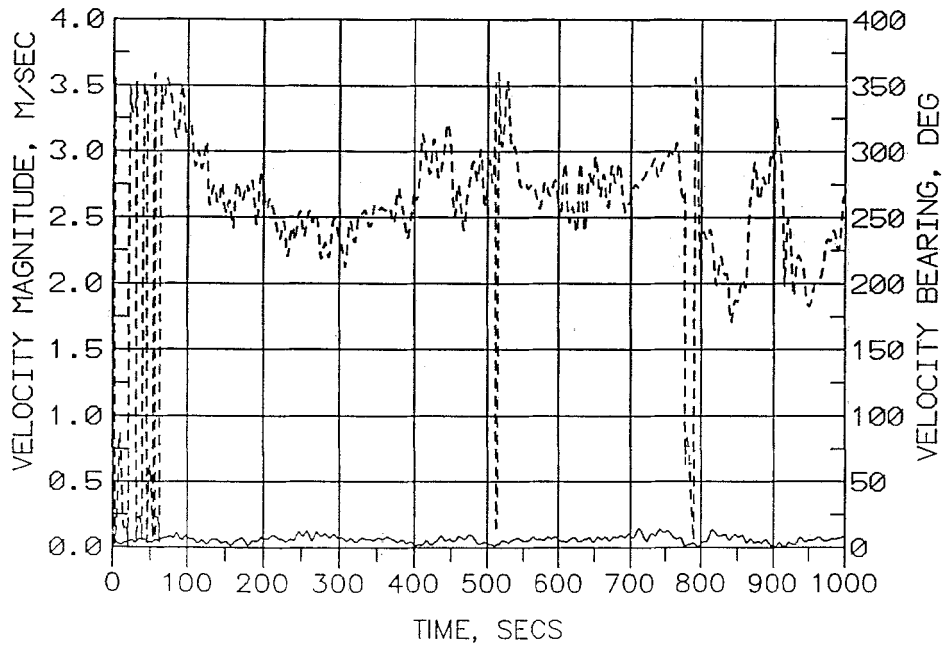




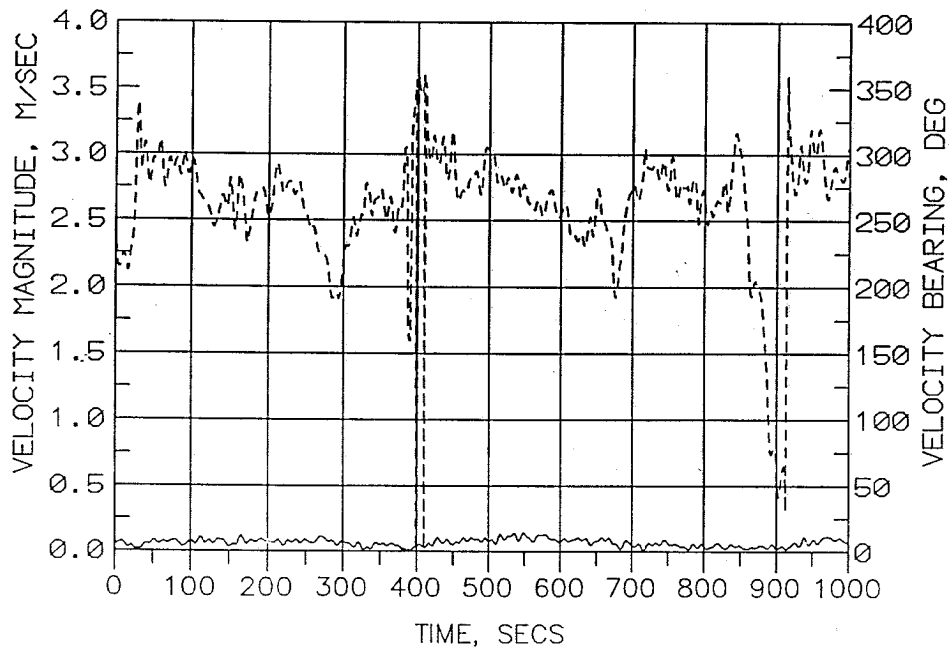
Appendix C

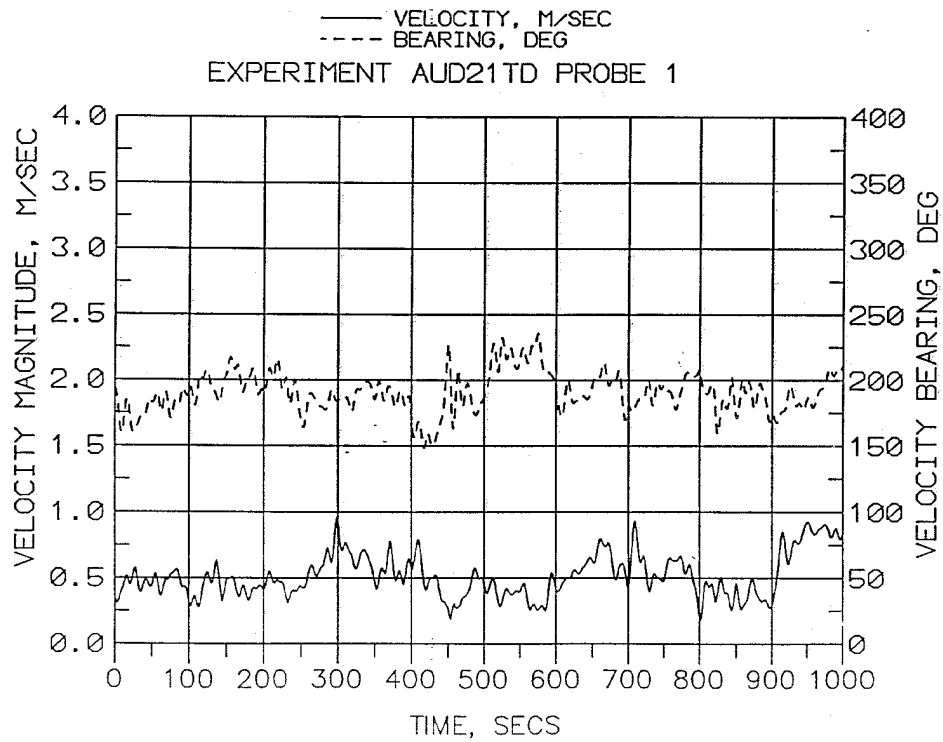
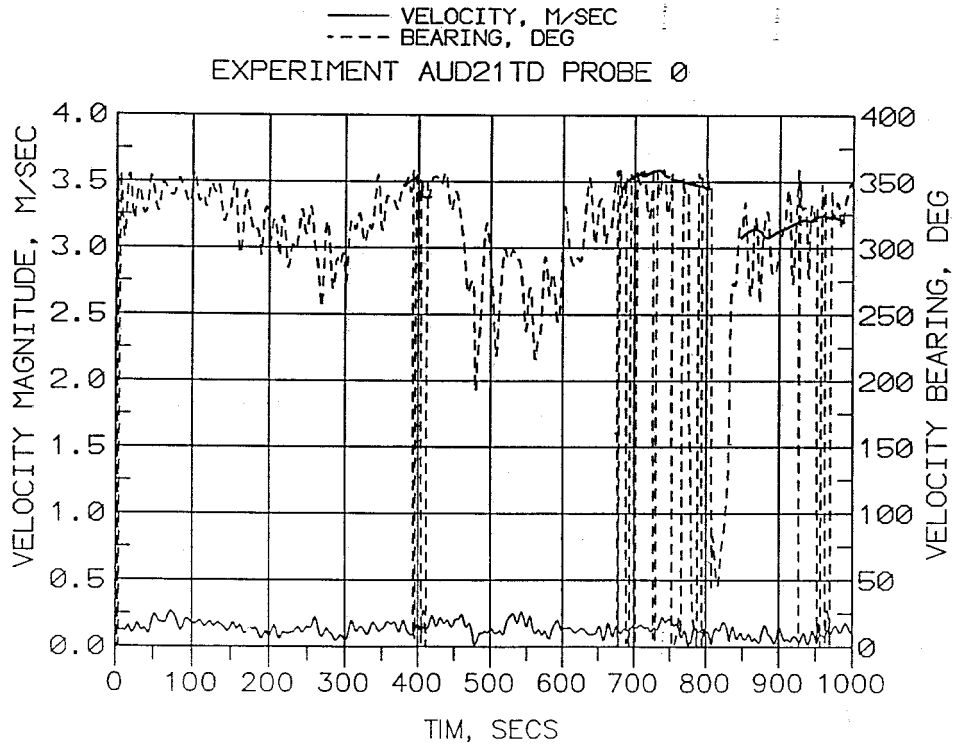
Time-History of Velocity for Overtopping Dike Experiments

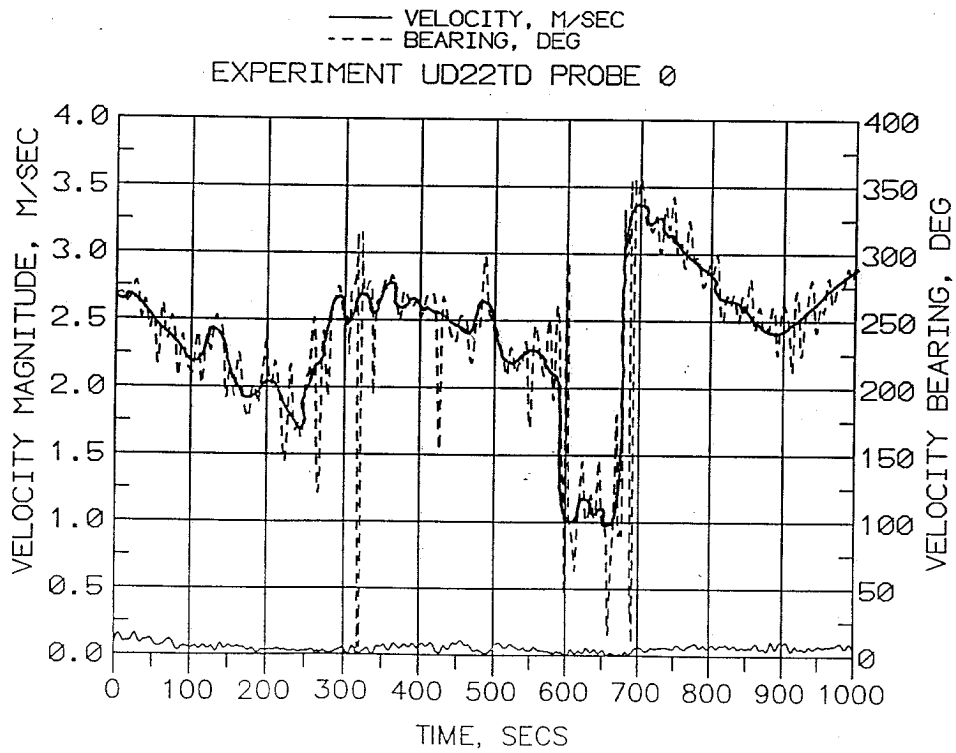
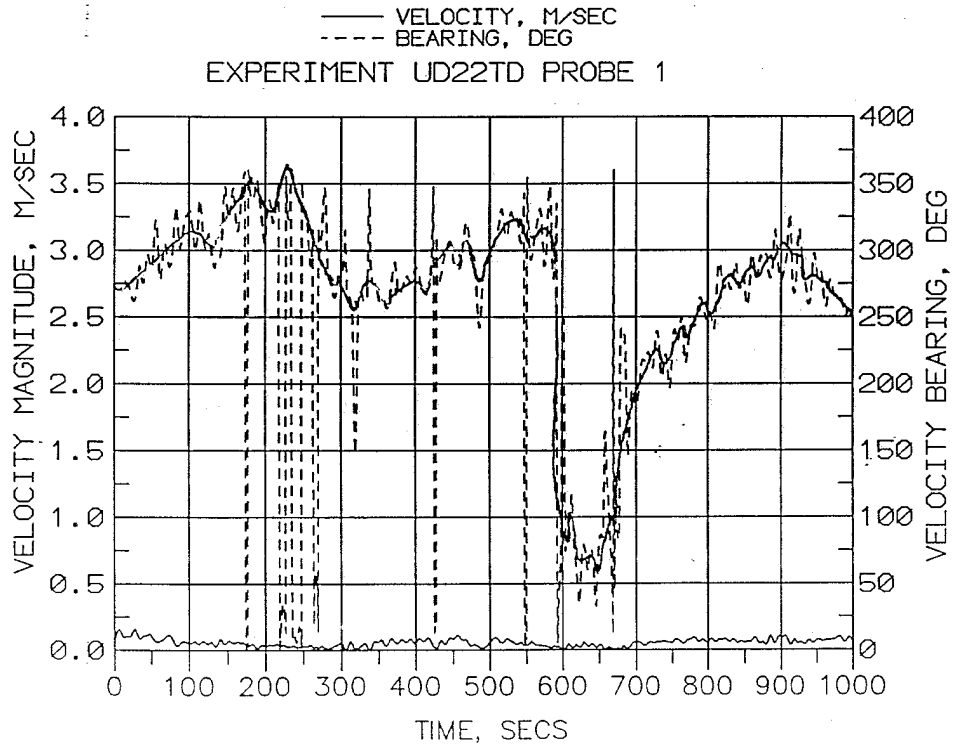
— VELOCITY, M/SEC
- - - BEARING, DEG
EXPERIMENT UD21TD PROBE 1

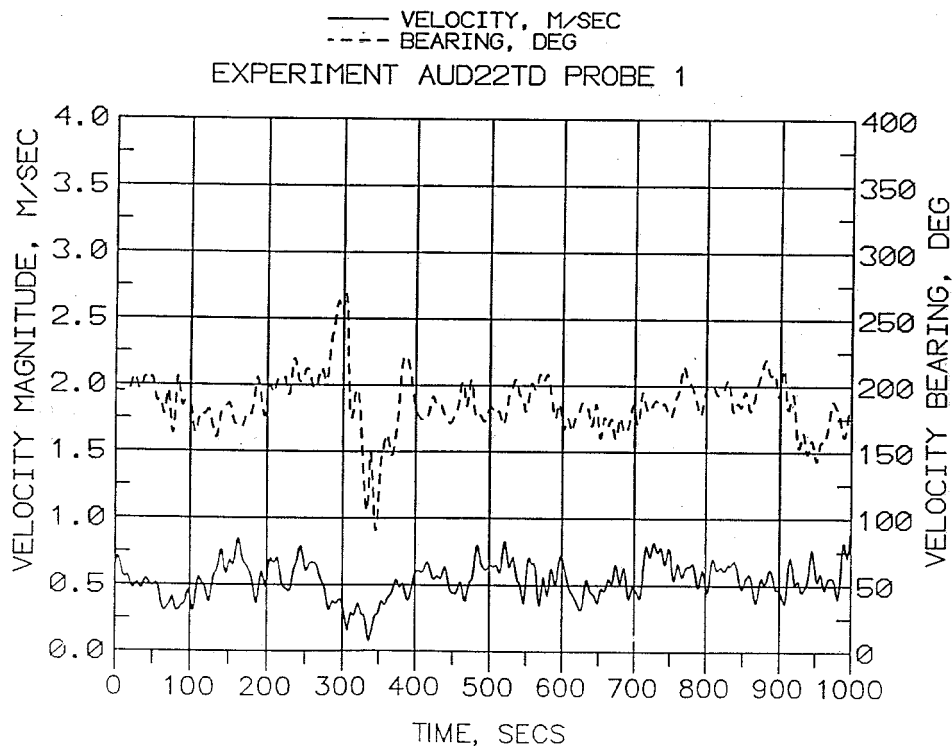
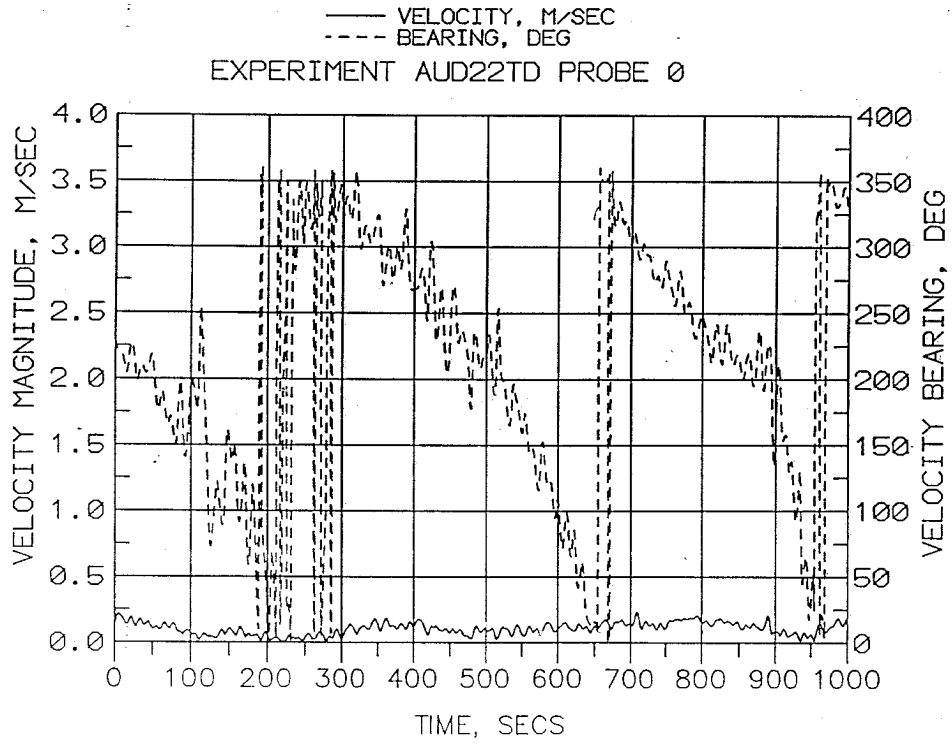


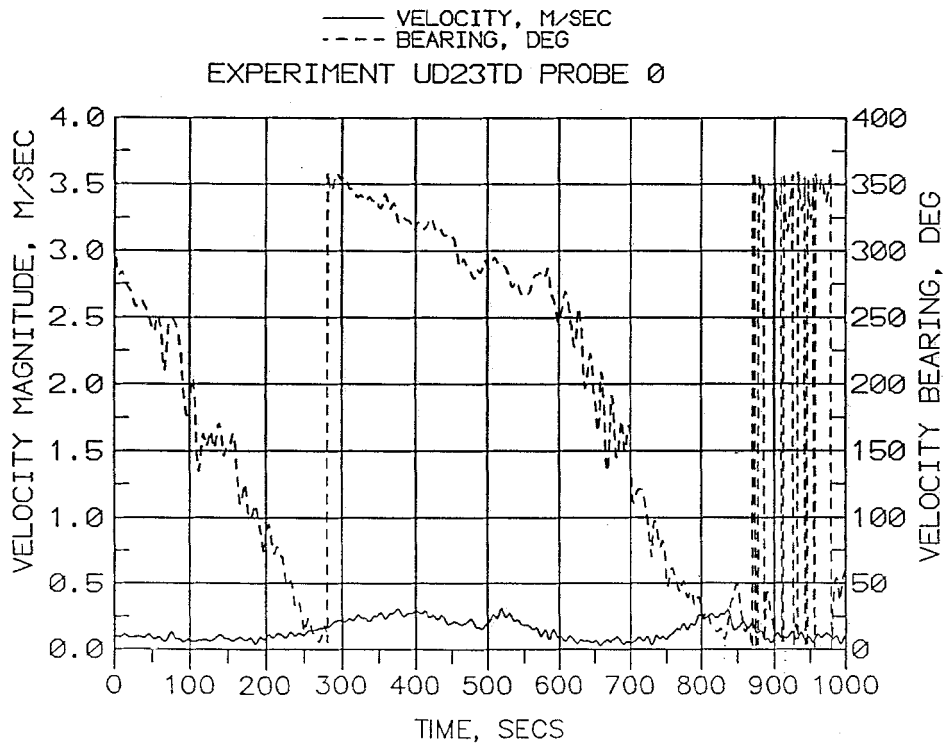
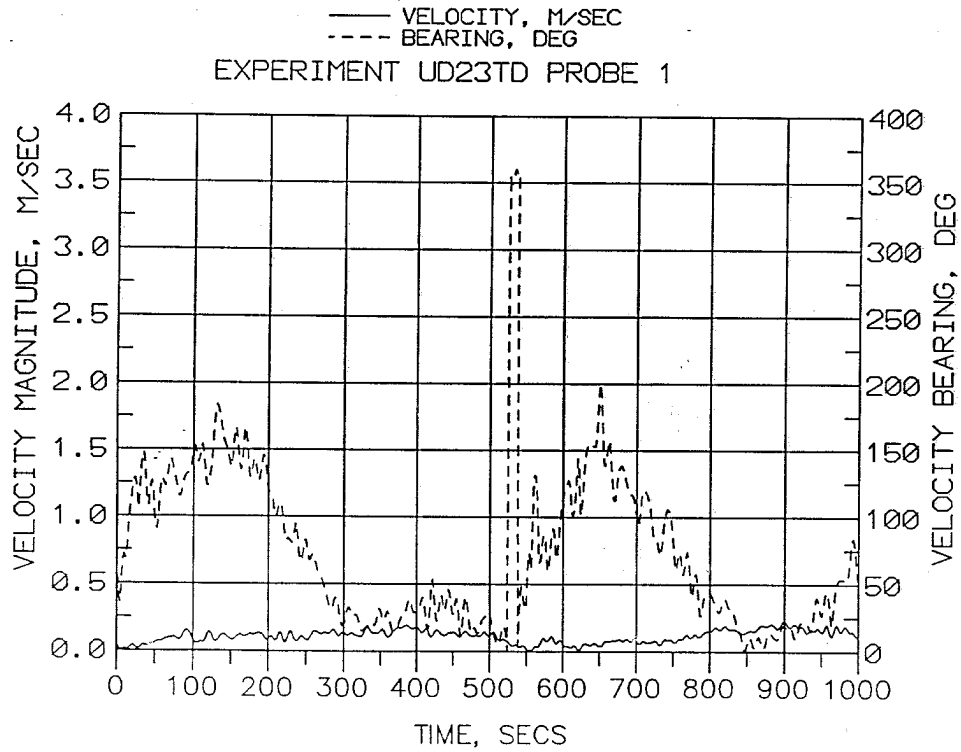
— VELOCITY, M/SEC
- - - BEARING, DEG
EXPERIMENT UD21TD PROBE 0

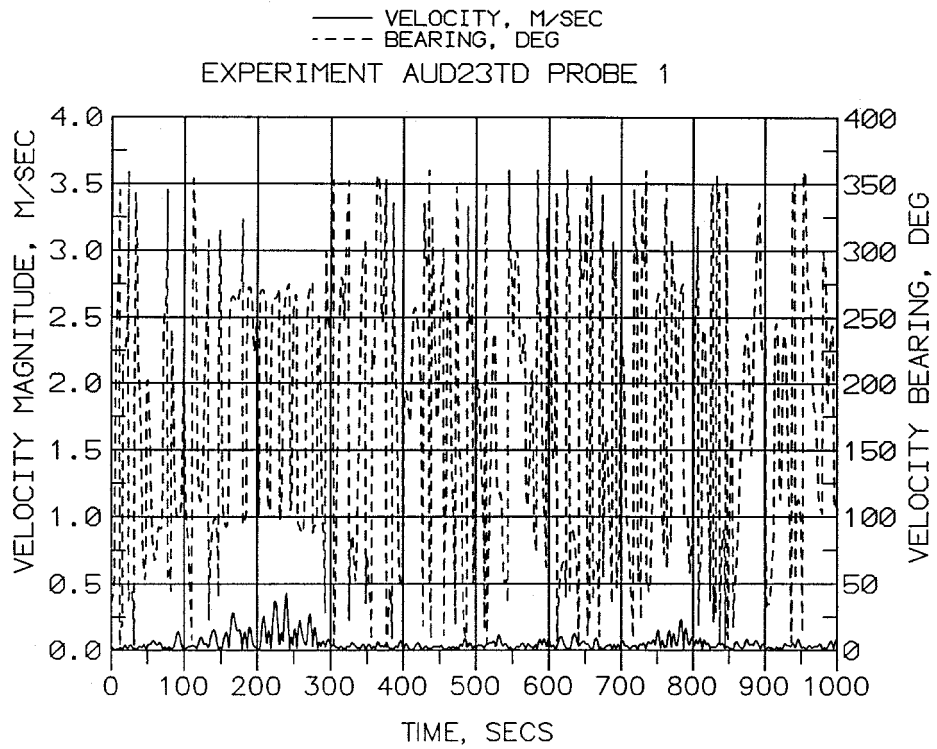
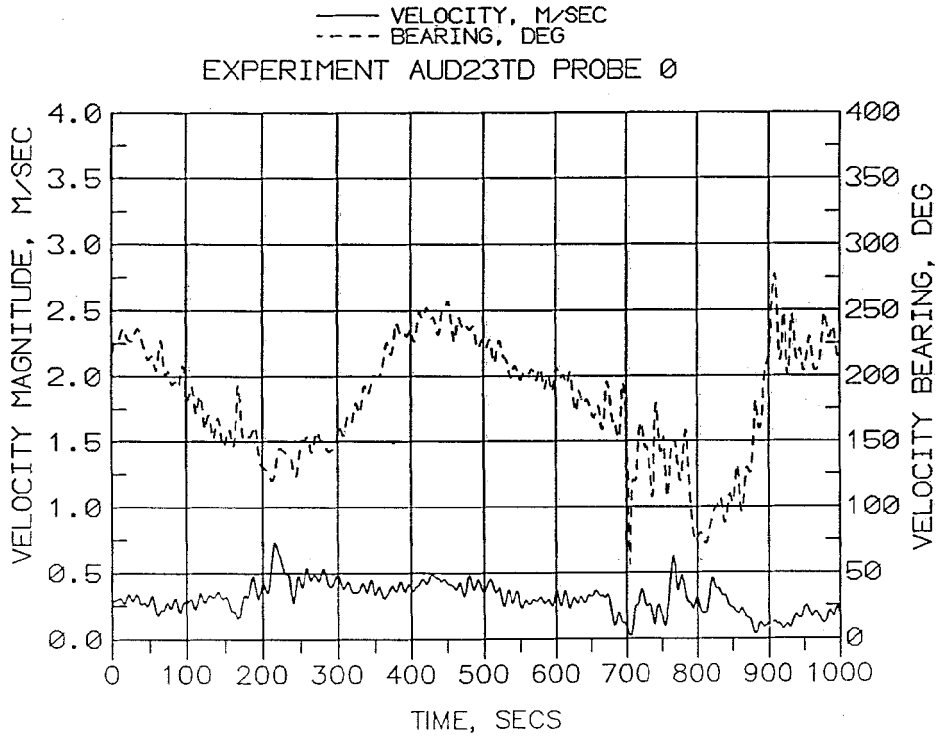


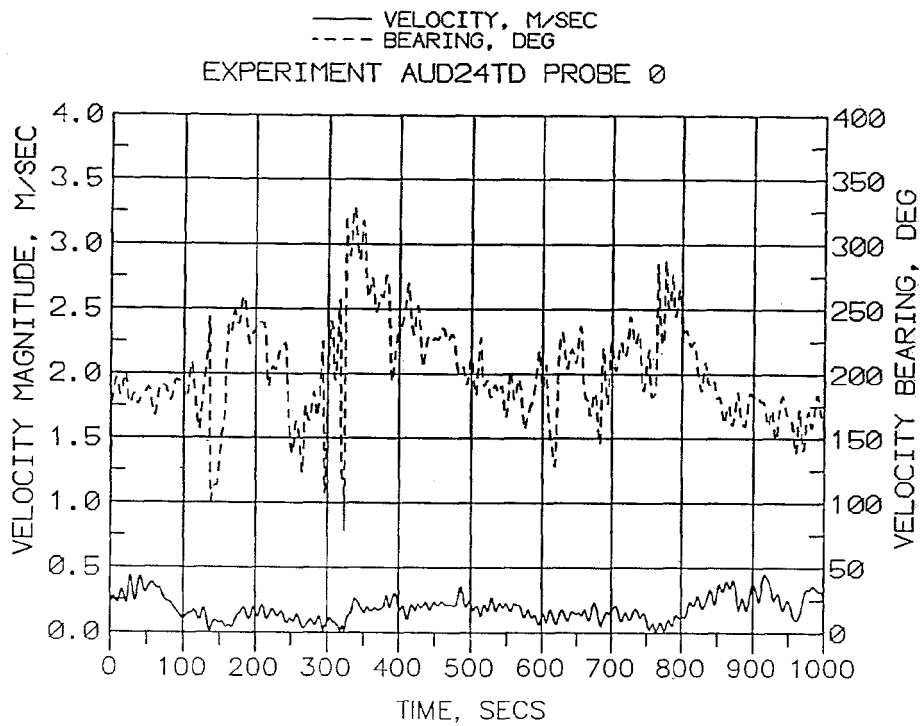
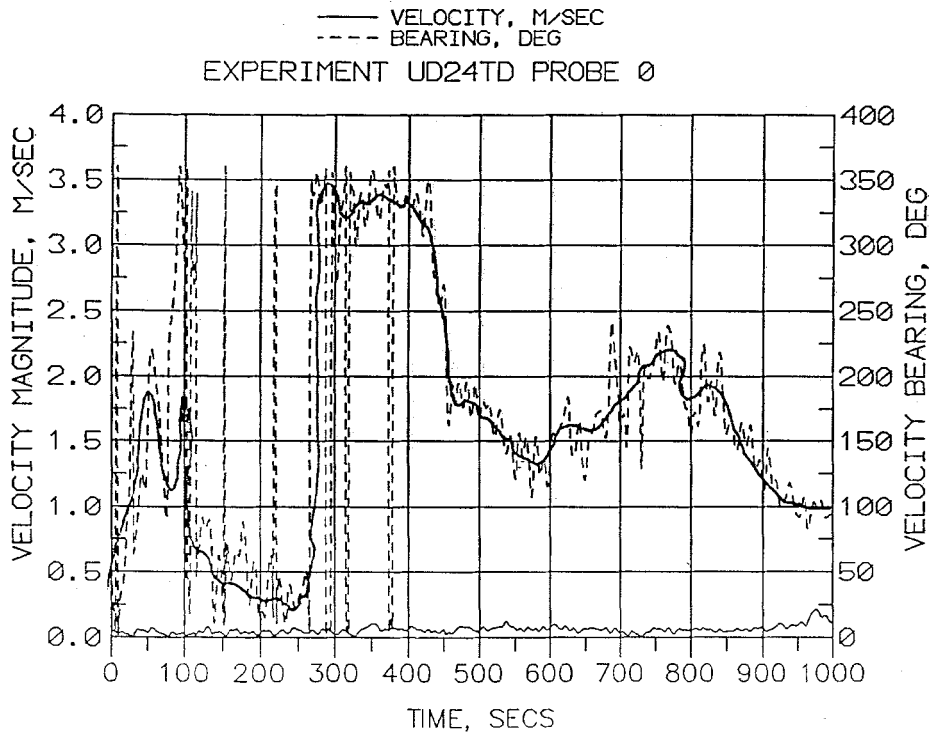


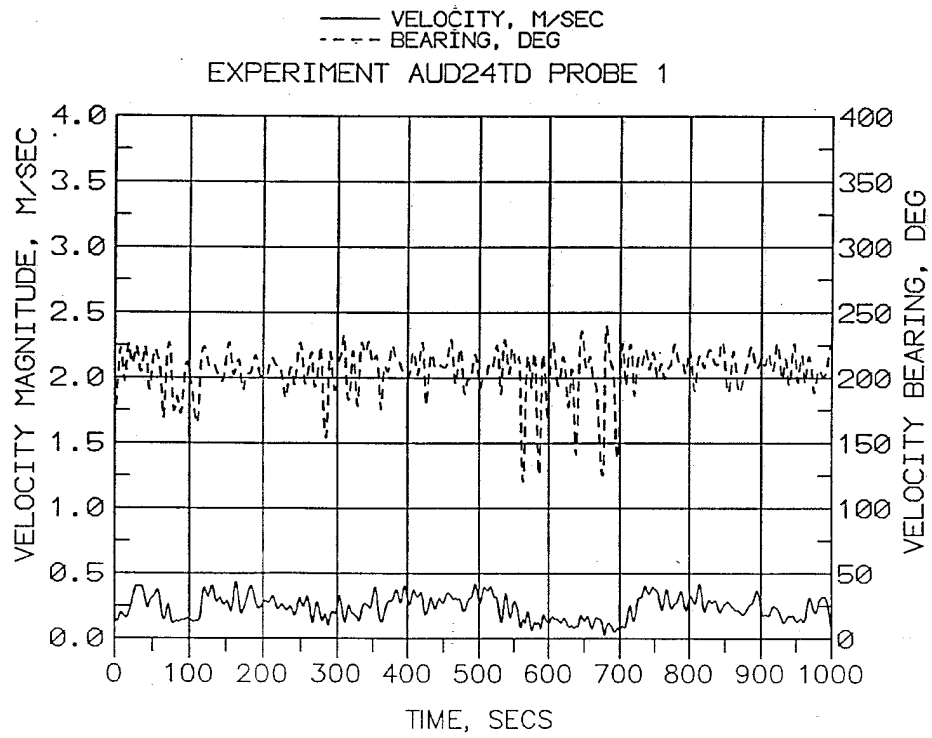






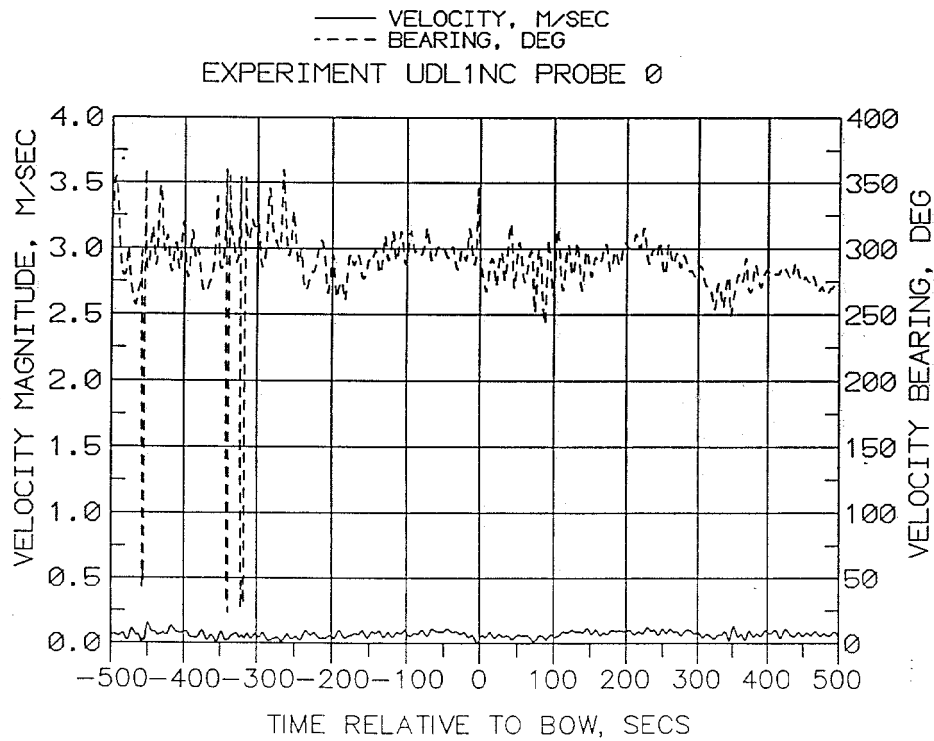
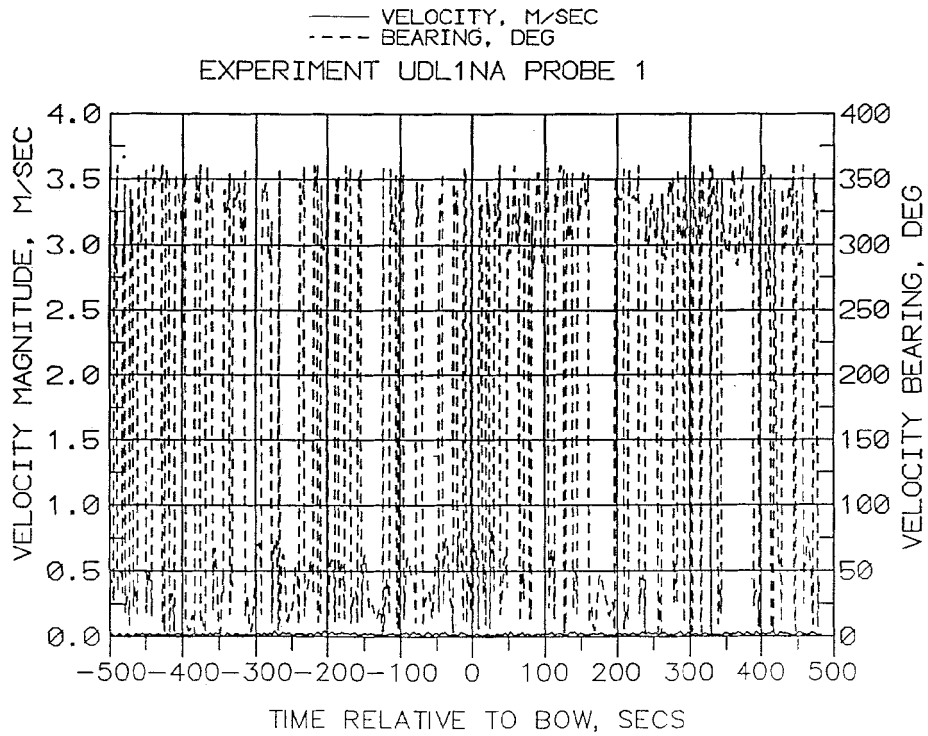


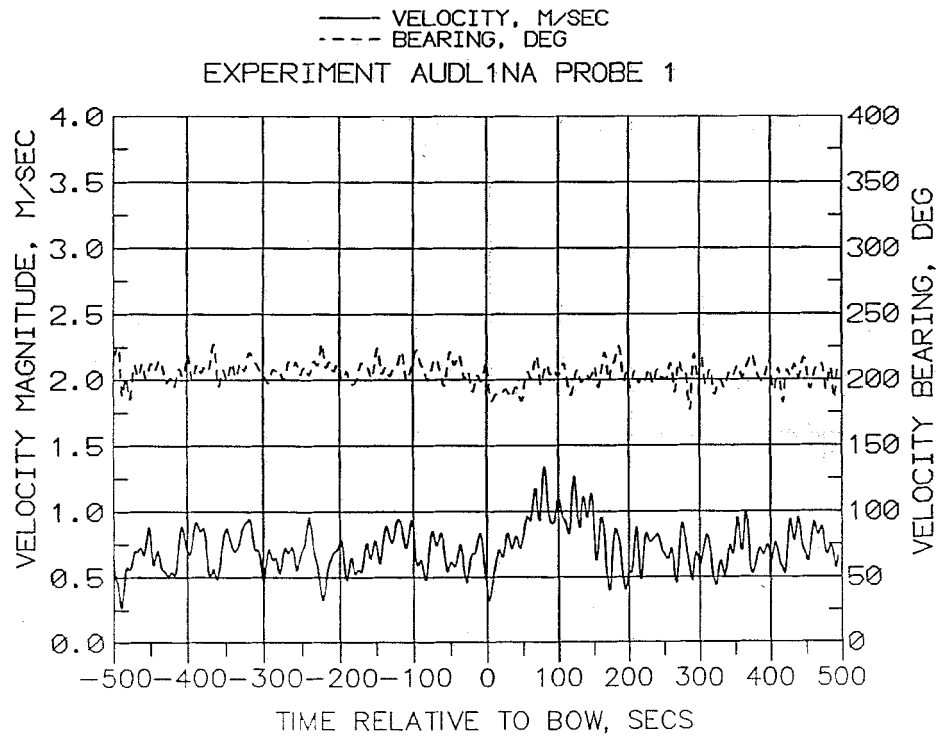
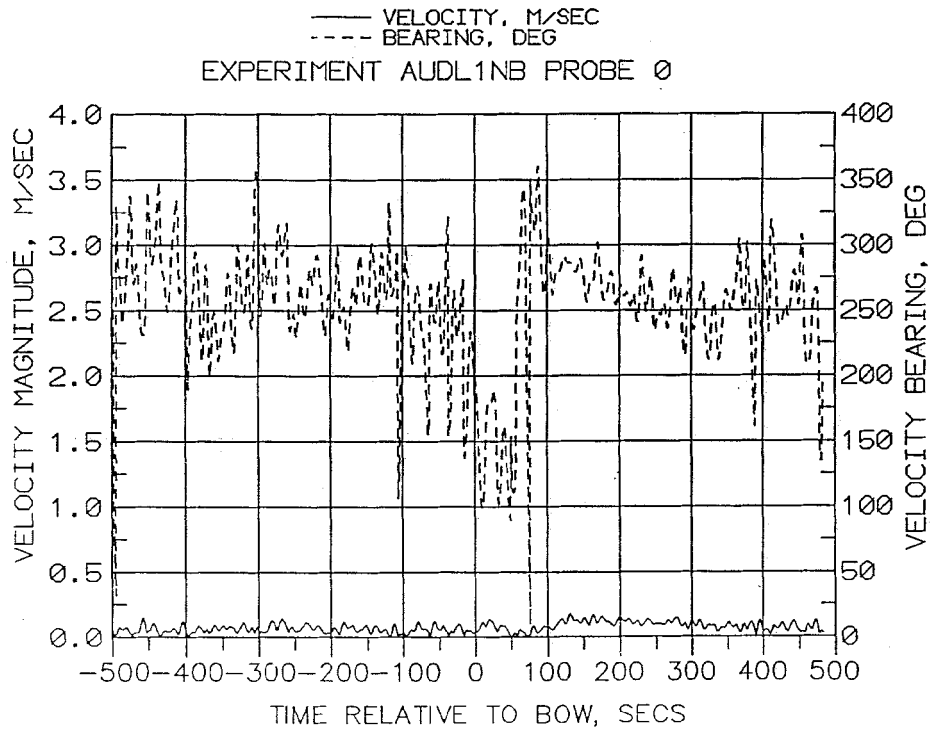


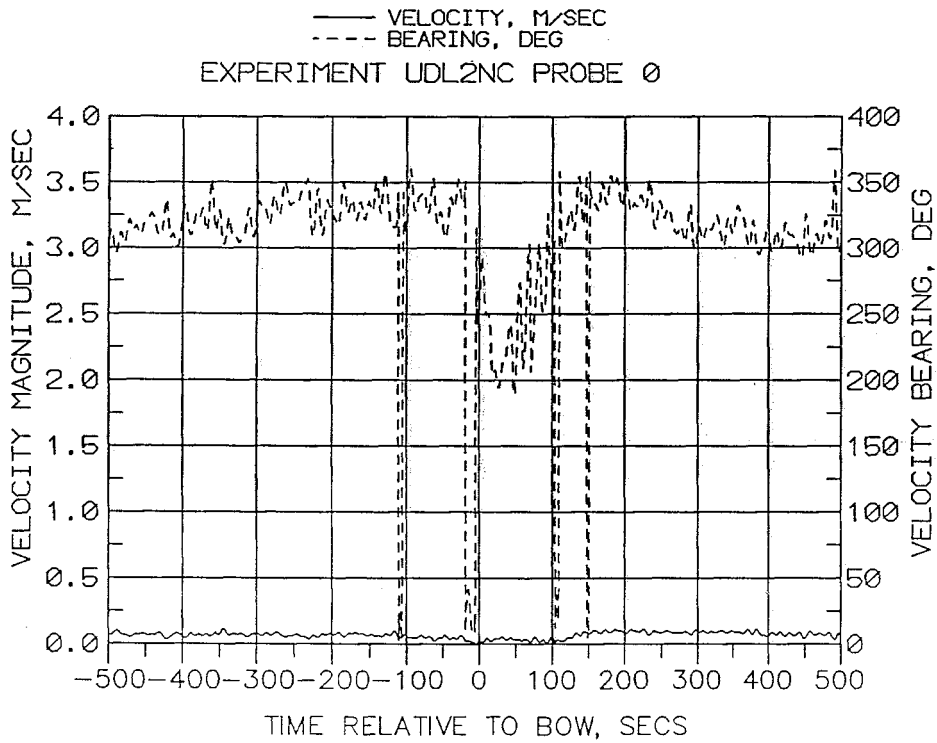
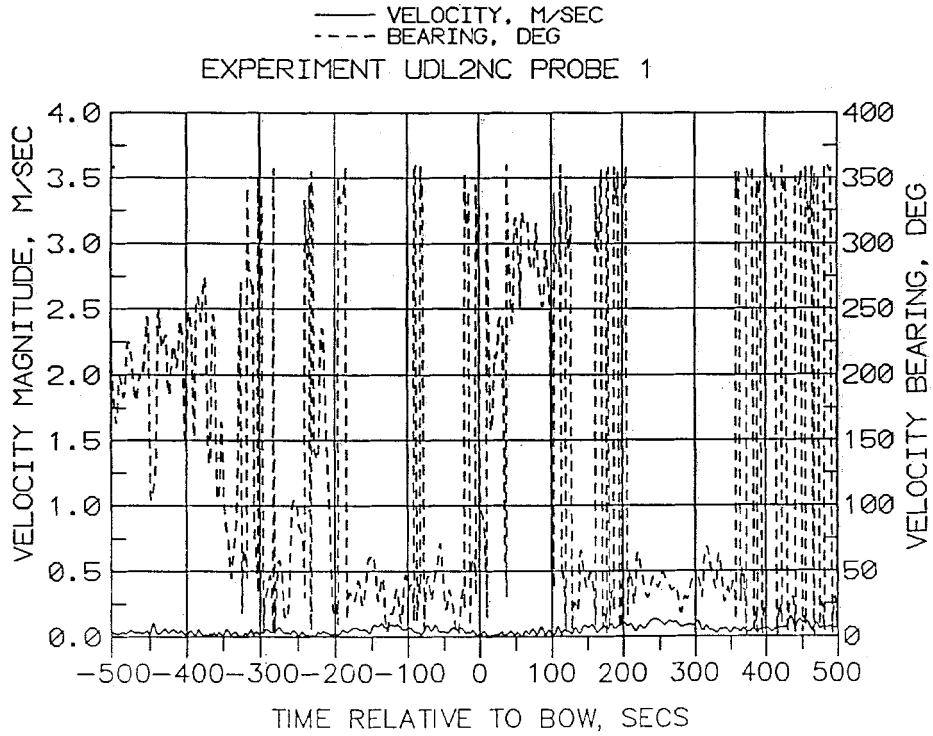


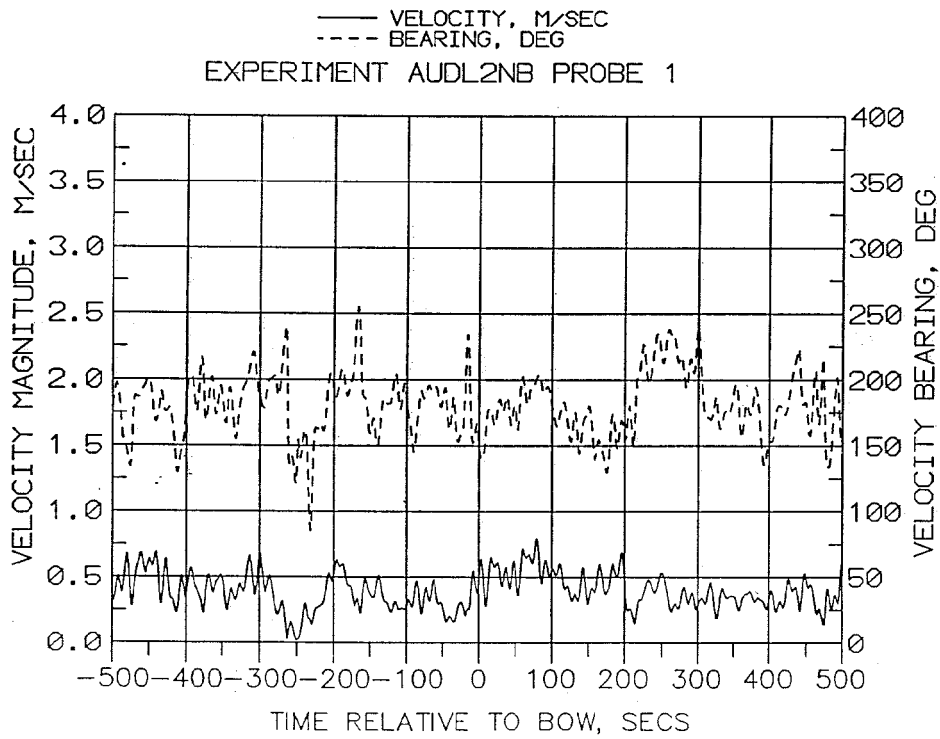
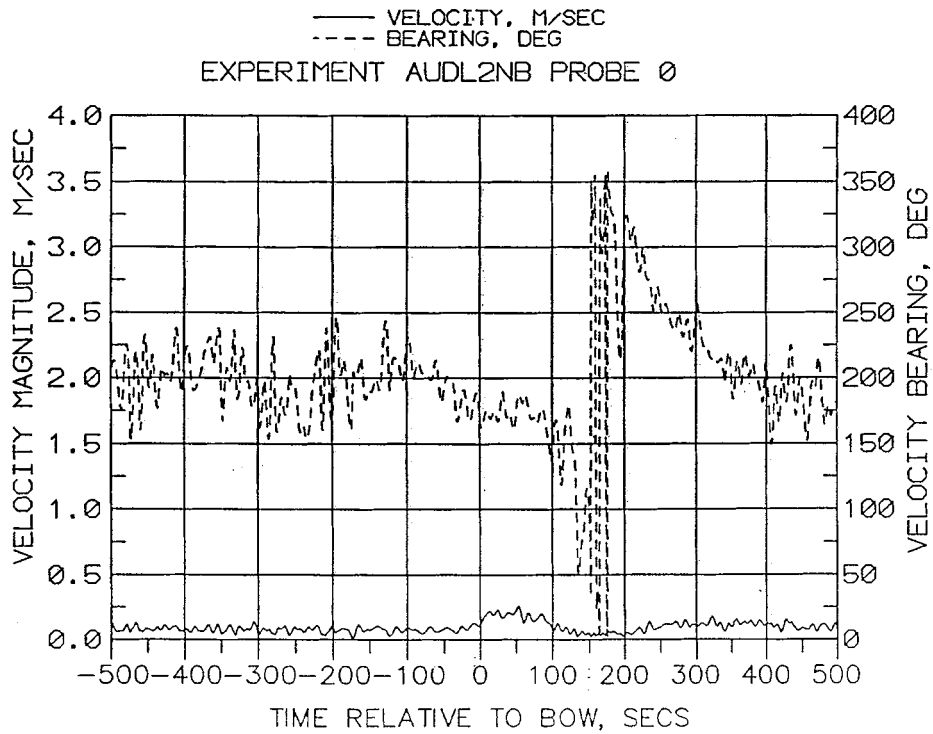
Appendix D

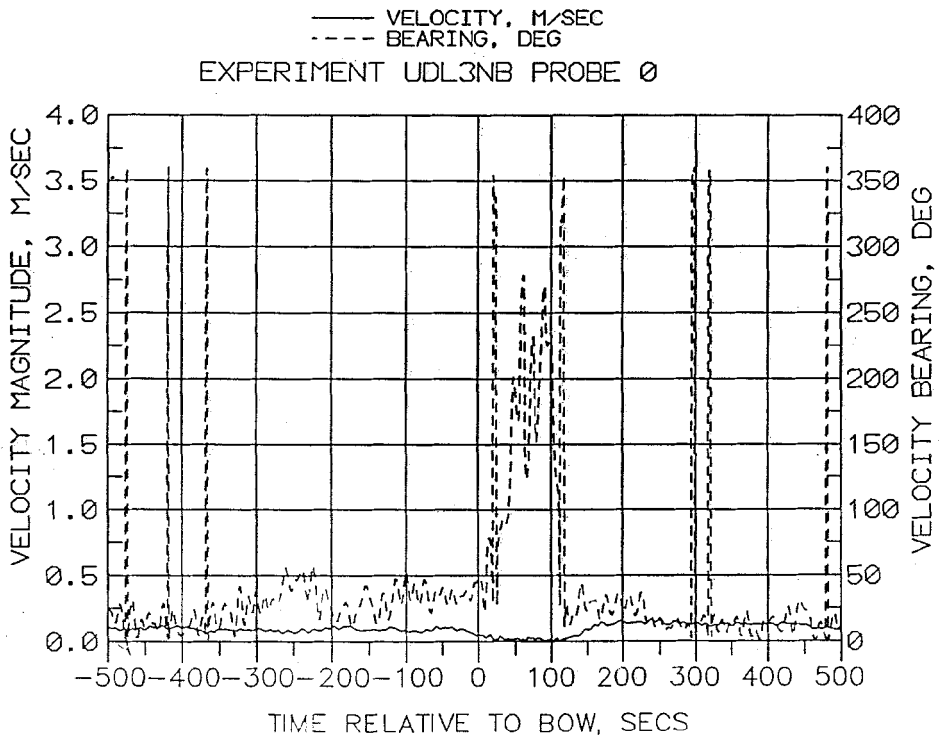
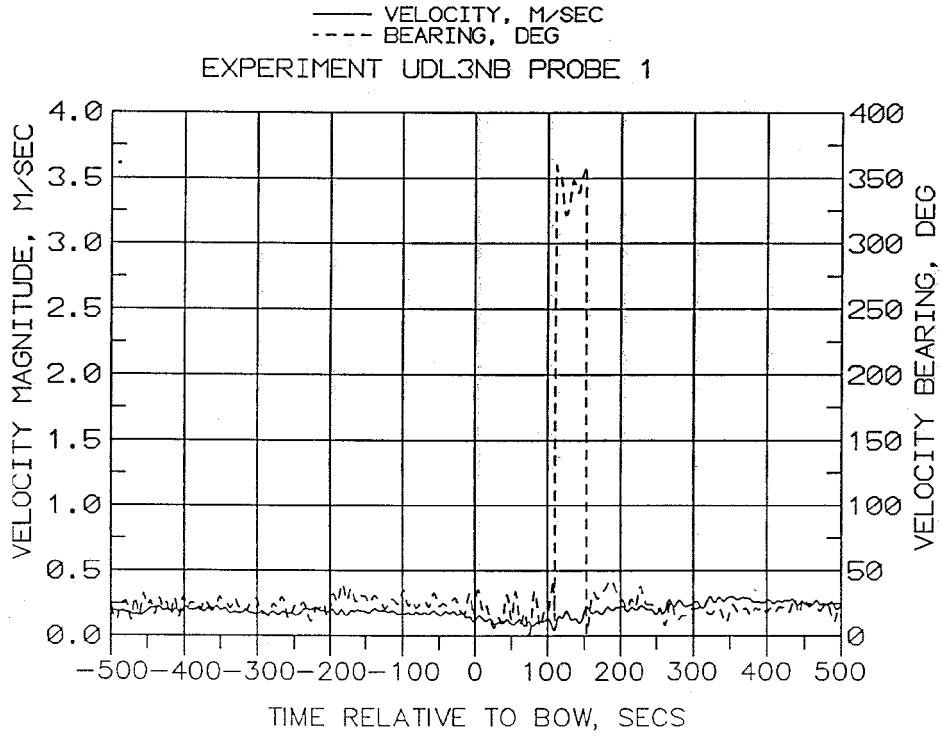
Time-History of Velocity for L-head Dike Experiments

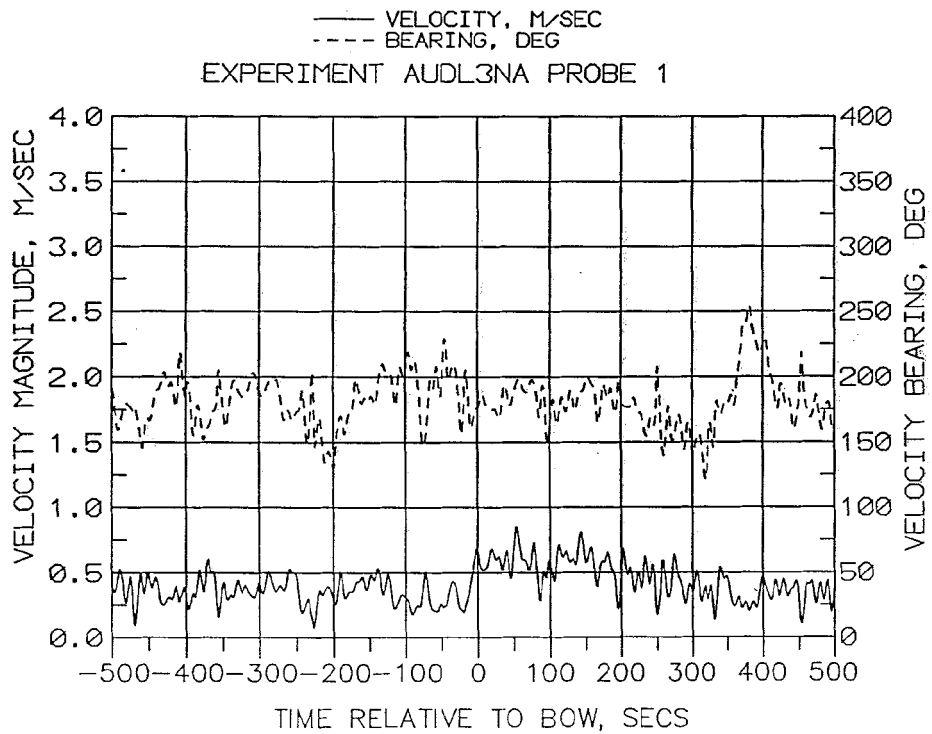
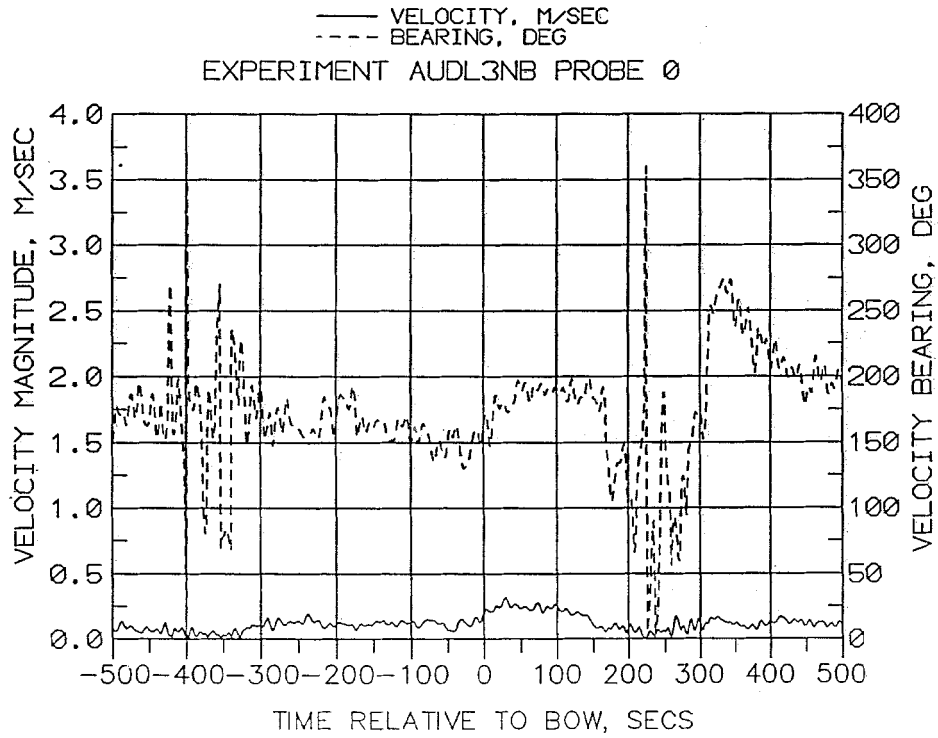


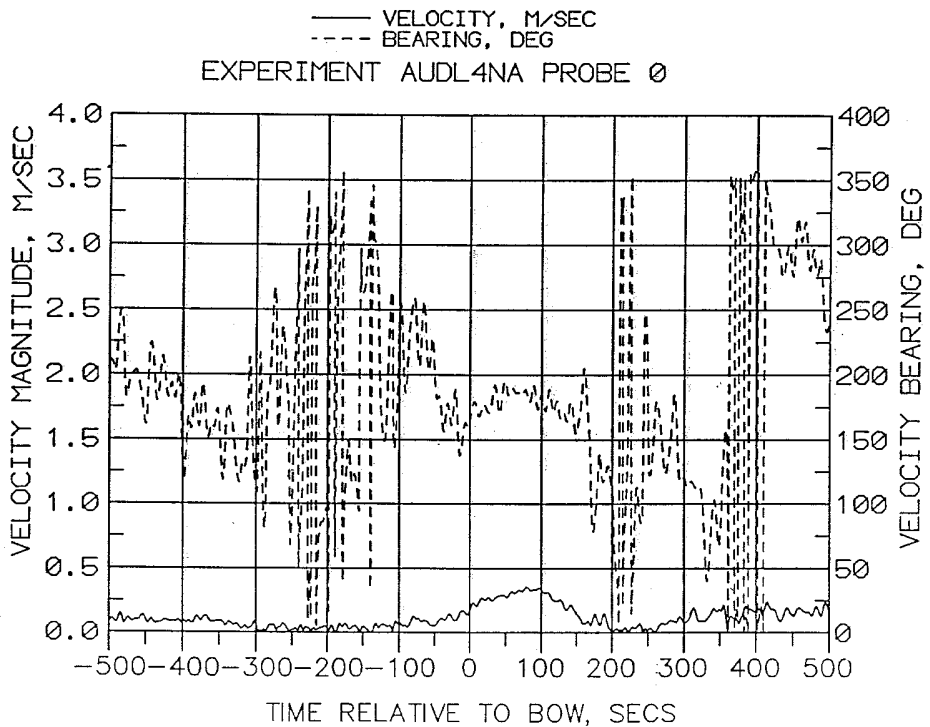
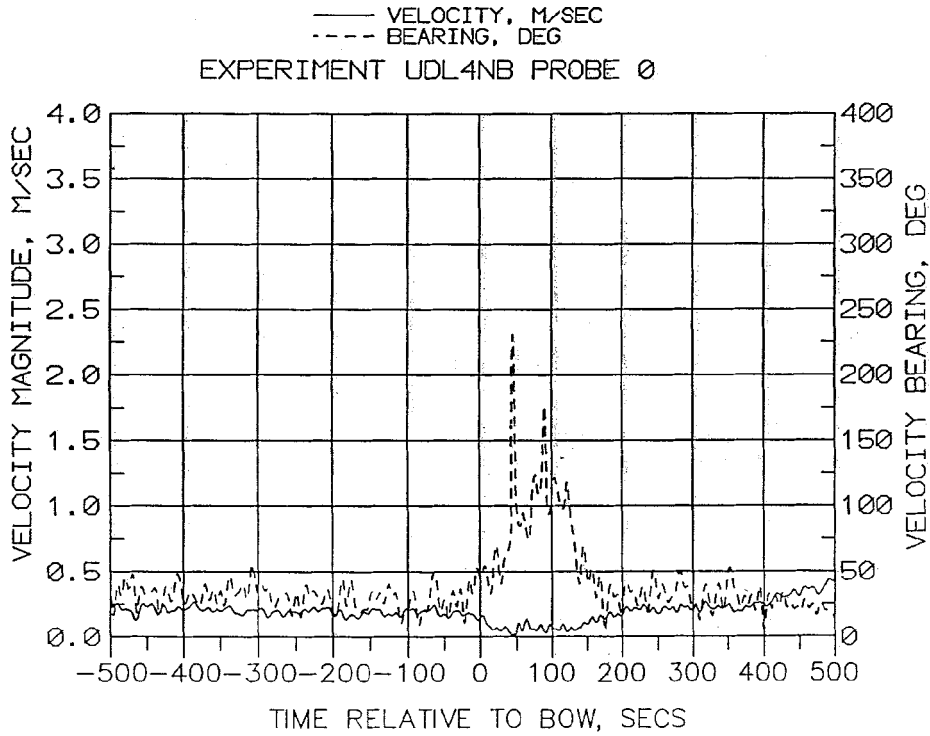












— VELOCITY, M/SEC
- - - BEARING, DEG
EXPERIMENT AUDL4NB PROBE 1

